DISSERTATION

Role of microglia in removal of autoantibody-bound NMDA receptors and post-synaptic proteins.

Rolle der Mikroglia bei der Entfernung von an Autoantikörper gebundenen NMDA-Rezeptoren und postsynaptischen Proteinen.

zur Erlangung des akademischen Grades
Doctor of Philosophy (PhD)

vorgelegt der Medizinischen Fakultät
Charité – Universitätsmedizin Berlin

von

Kazi Atikur Rahman

Erstbetreuung: Prof. Dr. Craig Curtis Garner

Datum der Promotion: 30.06.2024

Table of contents

List of figures

List of abbreviations

NMDAR – N-methyl-D-aspartate receptor

NMDARE - N-methyl-D-aspartate receptor encephalitis

CSF- Cerebrospinal fluid

hNR1-mAb – Patient derived monoclonal NR1 subunit autoantibody

$GABA_AR$ – Gamma-aminobutyric acid type A receptor

FcγR – Fc gamma receptors

TNFα – Tumor necrosis factor alpha

IL- Interleukin

AD – Alzheimer's Disease

PD – Parkinson's Disease

MS – Multiple Sclerosis

AQP4 – Aquaporin 4

CASPR2 - Contactin-associated protein-like 2

LTP – Long-term potentiation

ELISA – Enzyme-linked immunosorbent assay

PE - Phycoerythrin

NBA – Neurobasal-A

MAP2 – Microtubule-associated protein 2

CD11b – Integrin alpha M

Iba1 – Ionized calcium binding adaptor molecule 1

ROI – Region of interest

ANOVA – Analysis of variance

Lamp2a – Lysosome-associated membrane protein 2a

DAB - 3,3´-diaminobenzidine tetrahydrochloride

ROS – Reactive oxygen species

List of abbreviations

ATP – Adenosine triphosphate

EM – Electron microscopy

DIC – Differential Interference Contrast microscopy

EGFP – Enhanced green fluorescent protein

mCh – m-Cherry

PSD95 – Postsynaptic protein 95

vGLUT1 – Vesicular glutamate transporter 1

LALA - Leucine234Alanine/Leucine235Alanine

PA – Proline329Alanine

LALA-PG - Leucine234Alanine/Leucine235Alanine/Proline329Glycine

RA - Rheumatoid Arthritis

C1q – Complement component 1q

Abstract

Prominent microgliosis was reported as a common feature in autopsied brain samples of patients with NMDA receptor encephalitis (NMDARE). Pathogenic autoantibodies from patient cerebrospinal fluid (CSF) have been shown to cause cross-linking and internalization of bound NMDARs via their Fc region leading to disease phenotypes. However, the link between the presence of receptor-bound autoantibodies and microglia activation remains largely unexplored. To study this, we developed an *in-vitro* co-culture model with mouse primary hippocampal neurons, astrocytes, and microglia. We used this co-culture system together with fluorescence imaging, electron microscopy, and molecular biology techniques to show that NMDARs with bound patient-derived monoclonal autoantibodies against its NR1 subunit (hNR1-mAb) caused a specific removal of NMDAR and hNR1-mAb complexes by microglia. Microglia-mediated specific removal of autoantibody-bound neuronal receptors was also observed for either patient-derived monoclonal autoantibody against $GABA_A$ receptors (α1-$GABA_A$-mAb) alone or in combination with hNR1-mAb. Furthermore, we found that engagement of microglia by hNR1-mAb bound to NMDARs also led to microglial activation and secretion of pro-inflammatory cytokines IL6 and TNFα. Microglia activation by hNR1-mAb bound to NMDARs also resulted in a decrease in synapse number with a specific removal of post-synaptic proteins like PSD95 and Homer 1 by microglia. We also introduced mutations in the Fc region of hNR1-mAb that blocks its interaction with Fc gamma receptor (FcγR) and complement proteins. Mutant hNR1-mAbs prevented the removal of hNR1-mAb-bound NMDARs and synapses by microglia. Hence, we report a direct role of microglia-mediated innate immune response to the presence of hNR1-mAb which could further trigger infiltration and maturation of adaptive immune cells like B-cells and T-cells via secretion of inflammatory cytokines like IL6 worsening disease pathology in patients with NMDARE. Taken together, this study highlights that receptor removal and inflammation caused by microglia in the presence of patient-derived autoantibodies might be a common mechanism across different autoimmune encephalitis providing a promising target for developing future therapeutics.

Zusammenfassung

Eine ausgeprägte Mikrogliose wurde als gemeinsames Merkmal in autopsierten Gehirnproben von Patienten mit NMDA-Rezeptor-Enzephalitis (NMDARE) festgestellt. Es hat sich gezeigt, dass pathogene Autoantikörper aus der Liquorflüssigkeit (CSF) von Patienten eine Vernetzung und Internalisierung von gebundenen NMDARs über deren Fc-Region verursachen, was zu den Krankheitsphänotypen führt. Der Zusammenhang zwischen dem Vorhandensein von rezeptorgebundenen Autoantikörpern und der Aktivierung der Mikroglia ist jedoch noch weitgehend unerforscht. Um dies zu untersuchen, haben wir ein In-vitro-Kokulturmodell mit primären Hippocampus-Neuronen, Astrozyten und Mikroglia der Maus entwickelt. Mit Hilfe dieses Co-Kultursystems, Fluoreszenzbildgebung, Elektronenmikroskopie und molekularbiologischen Techniken konnten wir zeigen, dass NMDARs mit gebundenen monoklonalen Autoantikörpern gegen die NR1-Untereinheit (hNR1-mAb) von Patienten eine spezifische Entfernung von NMDAR- und hNR1-mAb-Komplexen durch Mikroglia bewirken. Die Mikroglia-vermittelte spezifische Entfernung von Autoantikörper-gebundenen neuronalen Rezeptoren wurde auch für einen vom Patienten stammenden monoklonalen Autoantikörper gegen GABAA-Rezeptoren (α1-GABAA-mAb) allein oder in Kombination mit hNR1-mAb beobachtet. Darüber hinaus stellten wir fest, dass die Aktivierung von Mikroglia durch an NMDARs gebundenes hNR1-mAb auch zu mikroglialer Aktivität und Sekretion der pro-inflammatorischen Zytokine IL6 und TNFα führte. Die Aktivierung der Mikroglia durch an NMDARs gebundenes hNR1-mAb führte auch zu einer Abnahme der Synapsenanzahl mit einer spezifischen Entfernung von postsynaptischen Proteinen wie PSD95 und Homer 1 durch die Mikroglia. Wir führten auch Mutationen in der Fc-Region von hNR1-mAb ein, die seine Interaktion mit dem Fc-Gamma-Rezeptor (FcγR) und Komplementproteinen blockiert. Mutierte hNR1-mAbs verhinderten die Entfernung von hNR1-mAb-gebundenen NMDARs und Synapsen durch Mikroglia. Daher weisen wir auf eine direkte Rolle der Mikroglia-vermittelten angeborenen Immunantwort auf die Anwesenheit von hNR1-mAb hin, die die Infiltration und Reifung von adaptiven Immunzellen wie B- und T-Zellen über die Sekretion von Entzündungszytokinen wie IL6 auslösen könnte, was die Krankheitspathologie bei Patienten mit NMDARE verschlimmert. Insgesamt unterstreicht diese Studie, dass die Entfernung von Rezeptoren und die durch Mikroglia verursachte Entzündung in Gegenwart von Autoantikörpern des Patienten ein gemeinsamer Mechanismus bei verschiedenen

Autoimmunenzephalitiden sein könnte, der ein vielversprechendes Ziel für die Entwicklung künftiger Therapeutika darstellt.

1 Introduction

1.1 Microglia in health and diseases

Microglia are specialized macrophages originating from the fetal yolk sac and taking residence in the brain during the early stages of development (Saijo & Glass, 2011). They perform several vital functions including complement-dependent pruning of unwanted synapses during development (Paolicelli et al., 2011; Schafer et al., 2012; Stevens et al., 2007), maintaining synaptic plasticity (Monje, Toda, & Palmer, 2003; Sierra et al., 2010) and regulation of neuronal activity together with astrocytes via their close interactions with synapses (Ben Achour & Pascual, 2010; Tremblay et al., 2011). They also play an essential role in controlling inflammation by secretion of pro and anti-inflammatory cytokines like IL6, TNFα, and IL-1β (Smith, Das, Ray, & Banik, 2012) and IL-10, and IL-4 (Pozzo et al., 2019) respectively. In addition to their functions during development and in homeostasis, microglia-mediated phagocytosis and secretion of pro-inflammatory cytokines have also been implicated in different disorders of the central nervous system (CNS). For example, complement-tagged removal of synapses by microglia has been shown to be activated in pre-plaque brains of mouse models of Alzheimer's disease (AD) (Hong et al., 2016). Microglial NLRP3 inflammasome pathway and subsequent IL-1β secretion was found to be upregulated both in patients and mouse models of various neurodegenerative diseases like AD (Heneka et al., 2013), Parkinson's Disease (PD) (Pike et al., 2022), and Multiple Sclerosis (MS) (Malhotra et al., 2020). Activation of microglia and microgliosis has also been reported in biopsied brain of patients with MS (Kamma, Lasisi, Libner, Ng, & Plemel, 2022; Locatelli et al., 2018) as well as antibody-mediated anti-NMDA receptor encephalitis (NMDARE) (Dalmau et al., 2007; Tüzün et al., 2009).

1.2 NMDA receptor Encephalitis

Autoantibody-mediated autoimmune encephalitis of the CNS are disorders wherein patients develop pathogenic autoantibodies against different synaptic and/or extra-synaptic receptors. In NMDARE, pathogenic autoantibodies arise against different subunits of the NMDA receptor (NMDAR) most commonly against its NR1 subunit (Dalmau et al., 2007; Kreye et al., 2016). Anti-NR1 autoantibodies were reported to cause crosslinking of bound NMDARs via its Fc region, ultimately driving the internalization of the bound NMDARs

from the surface of neurons and reduced NMDAR signalling (Hughes et al., 2010; Moscato et al., 2014). Such an internalization was not observed when NMDARs were bound with Fab fragments of anti-NR1 autoantibody, lacking its Fc region (Moscato et al., 2014). This internalization driven loss of NMDARs has been shown to cause reduction in NMDA and calcium currents (Andrzejak et al., 2022; Kreye et al., 2016), disruption of long-term potentiation (LTP) (Jézéquel et al., 2017; Moscato et al., 2014) and changes in excitatory-inhibitory balance (Andrzejak et al., 2022) that could contribute to pathogenic outcomes.

1.3 Activation of immune responses by Fc region of bound autoantibodies

The Fc region of bound autoantibodies has also been shown to trigger a downstream activation of immune response. For example, anti-Aquaporin-4 (AQP4) autoantibodies, implicated in Neuromyelitis Optica (NMO), were observed to provide a scaffold for complement deposition ultimately leading to cell death (Soltys et al., 2019). Patient derived anti-AQP4 autoantibody also led to a decrease in AQP4 receptors from astrocytes via internalization of bound receptors, which was found to be dependent on the interaction between the Fc region of autoantibody and astrocytic Fc receptors (Hinson, Clift, Luo, Kryzer, & Lennon, 2017).Interestingly, anti-Tau antibodies, designed to prevent cell to cell spread of Tau aggregates in AD, were reported to engage microglia by their Fc region, triggering microglial phagocytosis of Tau while secreting pro-inflammatory cytokines, detrimental to neuronal health (S. H. Lee et al., 2016). Maternal transfer of anti-NMDAR autoantibodies to foetuses led to long-term behavioural deficits, reduction in synapse number and microglial activation in brains of progenies (García-Serra et al., 2021). Similar results were also seen in gestational transfer models of anti-Contactin-associated protein-like 2 (CASPR2) antibodies, wherein prolonged activation of microglia along with synapse loss was reported in brains of mouse after birth (Coutinho et al., 2017). Together these studies illustrate a potential fundamental role for microglia in the pathology and response of the immune system that could contribute to the etiology of a number of neurological diseases.

1.4 Aim of the study

These studies along with observed microgliosis in post-mortem brain sections of patients with NMDARE (Bien et al., 2012; Dalmau et al., 2008) makes it imperative to study the role of microglia in pathophysiology of NMDARE and related diseases. To understand this, several questions need to be answered - Is the presence of bound NMDAR autoantibodies and microglia activation causally linked? Do bound anti-NMDAR autoantibodies engage microglia and what are the downstream effects? Is such an engagement Fc region driven and can it be dampened?

This thesis explores these concepts, by utilising patient derived monoclonal autoantibody against the NR1 subunit of NMDARs (hNR1-mAb) as well as $GABA_A$Rs autoantibodies (α1-$GABA_A$R-mAb) in a co-culture assay of primary microglia and hippocampal neurons. Our results show that bound hNR1-mAb triggers microglia engagement leading to removal of NMDAR/hNR1-mAb complexes and post-synaptic proteins like PSD95 and Homer1 by microglia along with an increase in secretion of pro-inflammatory cytokines like IL6 and TNFα. This removal was found to be Fc region dependent as mutations within the Fc region of hNR1-mAb, blocking its interaction with microglia, via either preventing complement deposition or direct Fc receptor interaction, prevented such a loss of NMDARs. Furthermore, we saw similar decrease in $GABA_A$ receptors ($GABA_A$Rs) in the presence of patient derived autoantibody against the α1 subunit of $GABA_A$Rs (α1-$GABA_A$R-mAb) on addition of microglia. Interestingly, such a decrease was found to be specific to the autoantibody tagged receptors as no changes were observed in the number of NMDARs when neurons bound with α1-$GABA_A$R-mAb were co-cultured with microglia and vice-versa. Taken together, this study argues for a prominent role of microglia in the removal of autoantibody-bound neuronal receptors like NMDARs and $GABA_A$Rs, which could dramatically contribute to adverse disease outcomes in patients with autoimmune encephalitis.

2 Methods

All methods have been described in detail in the material and method section of the published manuscript (Rahman et al., 2023). This section only contains the methodology of unpublished data.

Cytokine measurement by Luminex Multiplex ELISA

Supernatants from co-culture experiments after 1, 3 and 6 hr were collected before fixing the cells with 4% PFA. The supernatants were stored in ice followed by centrifugation at 2000 rpm for 10 minutes (min) at 4°C. The cleared supernatants were transferred to fresh tubes, snap frozen in liquid nitrogen and stored at -83°C until cytokine measurements. The amounts of different cytokines like TNFα, IL6, IL1β, IL4 and IL10, were measured using a custom-made multiplex ELISA kit (ProcartaPlex™ Multiplex Immunoassay, Invitrogen, ThermoFischer) using the manufacturer's protocol. Briefly, 12.5 µl of magnetic beads mixture, provided in the kit, was added to each well (384 well plate) and washed twice with 1x wash buffer (provided in the kit) for 1 min. Note, washing of the magnetic beads were done by placing the plates on top of a magnetic plate to prevent the beads from being washed off. Immediately after the last washing step, 12.5 µl of cell culture supernatant from different experimental conditions, were added to the wells containing beads, preventing the beads from drying. The plates were then shaken at 1700 rpm for 30 min followed by incubation at 4°C overnight without agitation. Following the incubation, each plate was returned to a magnetic plate and washed twice with wash buffer. 6.25 µl per well of detection antibody mix was then added to each sample followed by an incubation at room temperature with shaking at 1700 rpm for 30 min. The plates were then centrifuged quickly (short spin, 900 rpm) to settle down the beads and then placed back on the magnetic plate and washed twice with wash buffer. 12.5 µl Streptavidin-Phycoerythrin (PE) solution was then added to each well, followed by another 30 min incubation with 1700 rpm shaking at room temperature. The plates were centrifuged quickly again (900 rpm) and washed twice on the magnetic plate. 40 µl of reading buffer was then added to the wells followed by shaking at 1700 rpm at room temperature for 5 mins. The samples were then transferred to 96 well plate and 60 µl more of the reading buffer was added per well to make final volume of 100 µl. The plates were then shaken gently at 500 rpm until

measurement. The cytokine levels were measured using Biorad Luminex setup ensuring that the bead count in each well was 50 and above. The measurements were performed in triplicates and plotted as a percentage above cytokine level in just cell culture medium i.e., Neurobasal-A medium (NBA).

3. Results

3.1 Primary microglia mediate removal of hNR1-mAb labelled NMDAR puncta along dendrites.

To explore whether the presence of NMDAR bound with hNR1-mAb leads to an engagement of microglia and removal of bound receptors, we established a co-culture model of primary mouse hippocampal neurons and microglia (Figure 1A). hNR1-mAb was pre-labelled using a Zenon Kit (hNR1-mAb*, Alexa 647) to monitor changes in number of hNR1-mAb* puncta / unit length of dendrite upon microglia addition. As the pre-labelling involves the addition of a fluorophore tag that binds to the Fc region of the hNR1-mAb, a situation which could suppress Fc region dependent effects, unlabelled hNR1-mAb was mixed with the hNR1-mAb* in a 1:1 molar ratio (hNR1-mAb/hNR1-mAb*) making a final concentration of 2 µg/ml. Following the addition of hNR1-mAb/hNR1-mAb* to hippocampal neuronal cultures for 30 mins and washing out unbound autoantibodies, microglia were added to the cultures for 1, 3 and 6 hours (hr). Immunostaining fixed cultures with the presynaptic vesicle marker vGLUT1 revealed a close synaptic co-localization with hNR1-mAb* decorated puncta along dendritic segments (Figure 1B). A significant reduction in hNR1-mAb* puncta per unit length of dendrite was observed only 6 hr (Figure 1E and 1F) after microglia addition and not after 1 and 3 hr (22.34 ±0.7610, 22.31 ± 1.006, 9.964 ± 0.8024 (mean ± SEM) of Ab+/MG+ group after 1, 3 and 6 hr) (Figure 1C, 1D and 1F). Numbers of hNR1-mAb* puncta unit length of dendrite didn't change in absence of microglia at either 1, 3 or 6 hr (22.79 ±0.7698, 20.35 ± 0.8721, 21.63 ± 0.9782 of Ab+/MG- group after 1, 3 and 6 hr) (Figure 1C-F). These data suggest that loss of NMDARs/antibody complexes after 6 hr is due primarily to their removal by microglia and not via other reported mechanisms such as autoantibody-driven internalization which was shown to cause a significant decrease in NMDAR clusters only after 12-24 hr (Hughes et al., 2010; Moscato et al., 2014).

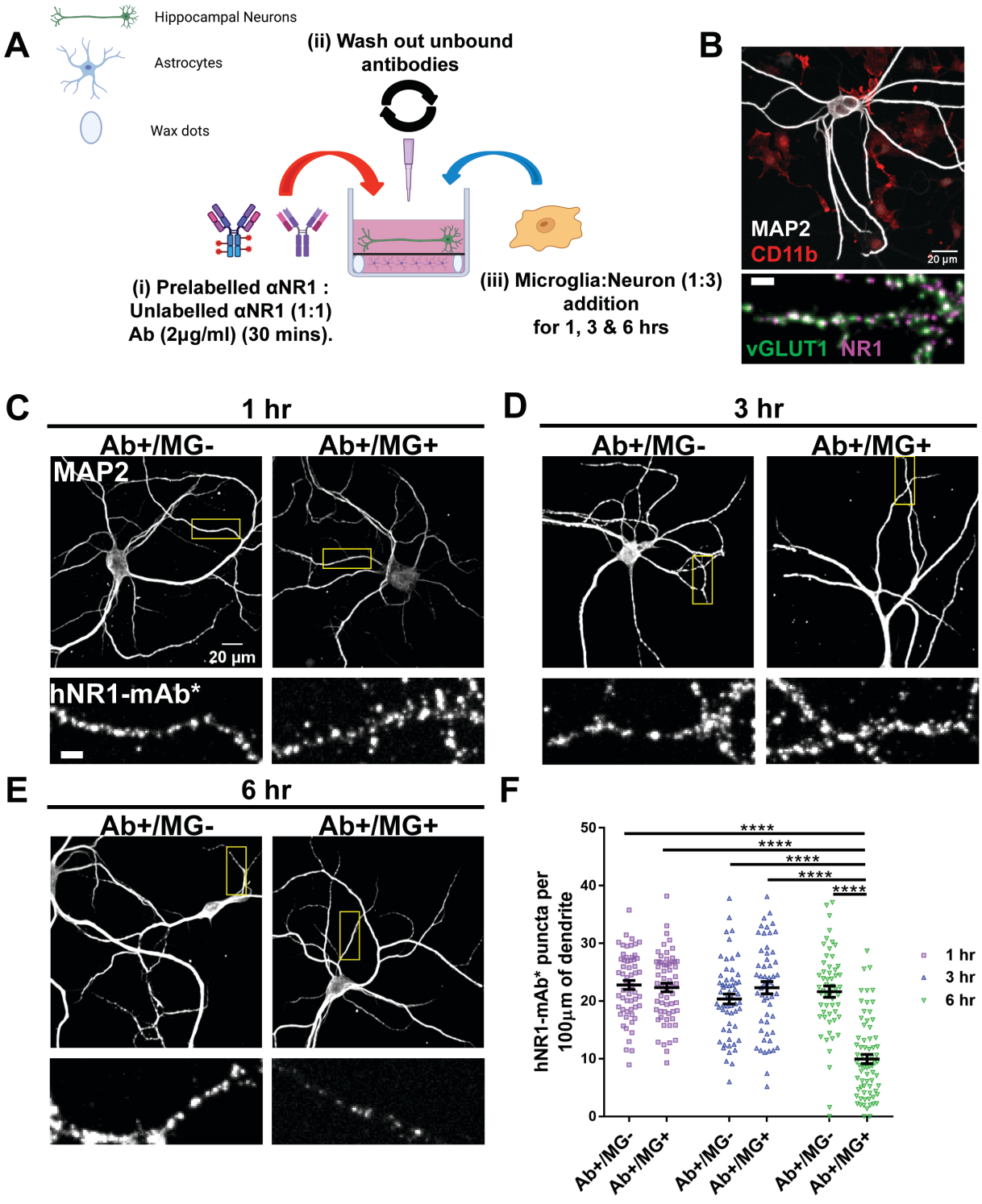

Figure 1| Reduction in hNR1-mAb-bound NMDAR puncta from hippocampal neurons 6hr after co-culture with microglia. (A) Schematic diagram illustrating the experimental setup wherein WT mouse primary hippocampal neurons were grown on glass coverslips on a bed of astrocytes separated by spacer wax dots on to which pre-labeled and unlabeled hNR1-mAb (1:1 molar ratio) was added followed by washing of unbound antibody and microglia addition for 1, 3 and 6 hr. (B) Representative image of neuronal cell stained for dendritic marker MAP2 (grey) co-cultured with CD11b positive microglia (red). Inset depicting a

synaptic staining pattern of hNR1-mAb* (magenta) binding on hippocampal neuron overlapping (white) with pre-synaptic marker vGLUT1 (green). (C) (D) and (E) Representative confocal images of neuronal cells with MAP2 staining (grey) showing punctate pattern of hNR1-mAb* along dendritic segments within selected regions of interest (ROI) with and without co-culture with microglia (Ab+/MG+ and Ab+/MG- respectively) after 1, 3 and 6 hr, respectively. ROI Scale bar = 5 µm. (F) Quantification of hNR1-mAb* puncta per unit length of dendrites in Ab+/MG+ and Ab+/MG- experimental groups after 1, 3 and 6 hr showing significant reduction only in the presence of microglia after 6 hr of co-culture. Each data point represents an ROI from three independent experiments (n = 55-71 ROIs per group). Data points represented as mean ± standard error of mean (SEM). Two-way ANOVA along with Tukey's test for multiple comparison was performed to determine statistical significance (****$p < .0001$). Figure taken from figure 1 (Rahman et al., 2023).

3.2 Microglia accumulates hNR1-mAb* puncta within endo-lysosomal structures.

Accompanying the loss of hNR1-mAb* puncta from dendritic branches, an accumulation of hNR1-mAb* puncta was readily observed within CD11b positive microglial cells. Here, a significant increase in hNR1-mAb* intensity was seen within microglia at 3 and 6 hr after co-culture (Figure 2A, 2B). No changes were seen in the expression levels of CD11b, as measured by staining intensity and microglia area after co-culture 1, 3 and 6 hr (Figure 2C, 2D). Cellular components taken up by microglia have previously been shown to be degraded within the endo-lysosomal compartments (Hong et al, 2016). To test whether hNR1-mAb* taken up microglia also accumulate within endo-lysosomal structures, microglial cells were stained for CD68 (Figure 2F) or Lamp2a (Figure 2E), a monocyte specific and universal lysosomal marker, respectively, 6 hr after co-culture. hNR1-mAb* puncta were found to overlap with CD68 and Lamp2a labelled puncta in microglia indicating that the endo-lysosomal system was involved in degradation of the accumulated hNR1-mAb* (Figure 2E, 2F).

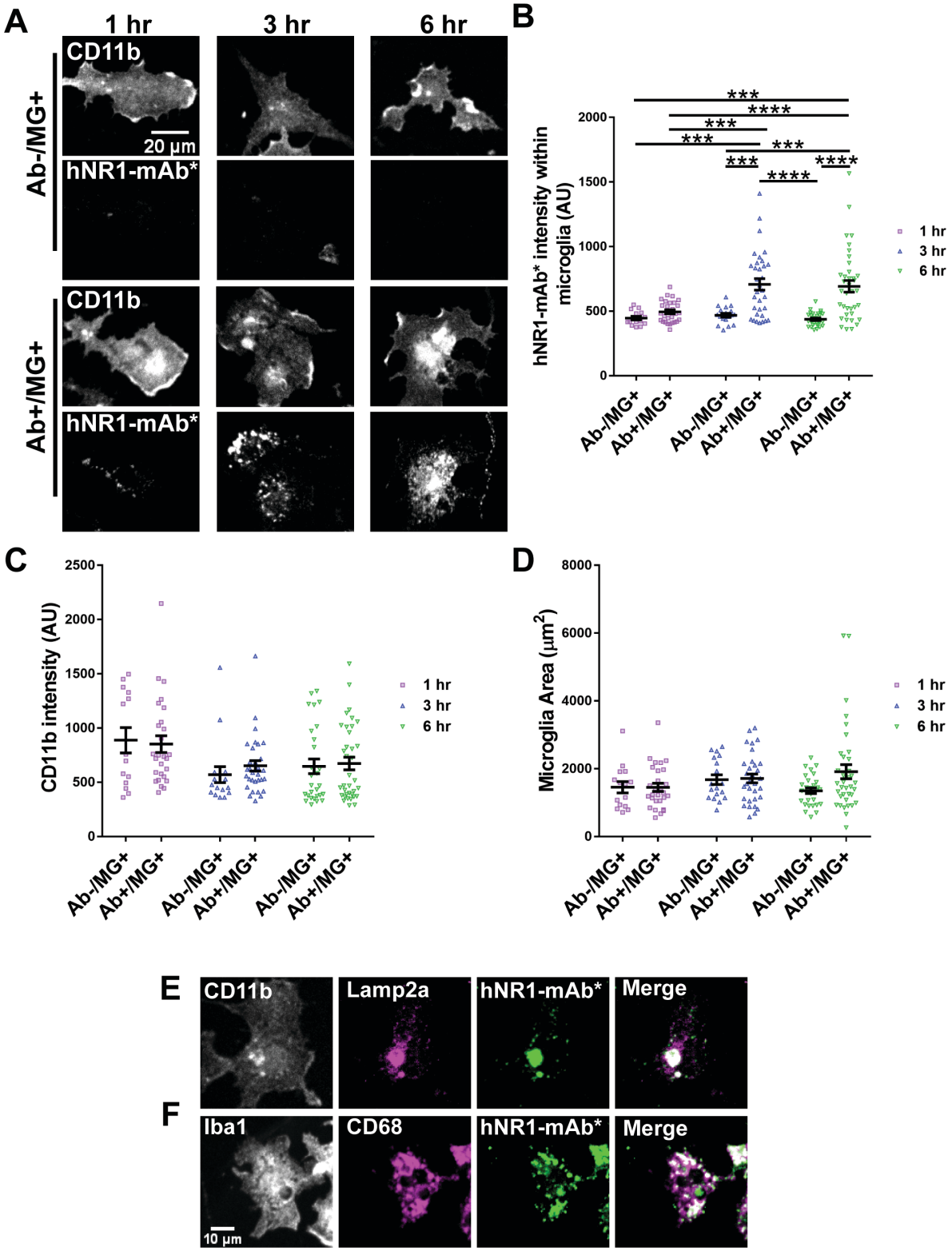

Figure 2| Microglial endo-lysosomes accumulate hNR1-mAb*. (A) Representative images of microglial cells stained for CD11b with hNR1-mAb* signal accumulated within their cell bodies after 1, 3 and 6 hr of co-culture with hippocampal neurons. Images are shown in grey scale. (B) hNR1-mAb* intensity quantifi-

cation inside CD11b positive microglia shows significantly higher accumulation of hNR1-mAb* within microglial cell body after 3 and 6 hr of co-culture. (C) and (D) No appreciable changes were detected in the expression levels of CD11b and microglia area respectively, after co-culture with hNR1-mAb*-bound hippocampal neurons after 1, 3 or 6 hr. Each data point represents a microglia cell from three independent experiments (n = 20-37 cell per group). Data points represented as mean ± SEM. Two-way ANOVA along with Tukey's test for multiple comparison was performed to determine statistical significance (****$p < .0001$). (E) and (F) NMDAR immunoreactivity (green) inside microglial cell stained with CD11b or Iba1 (grey) was seen to co-localize with staining pattern of general lysosomal marker, Lamp2a and a monocyte specific lysosomal marker, CD68 (magenta) respectively. Figure taken from figure 2 (Rahman et al., 2023).

To validate this concept further, electron microscopy (EM) was performed following photo-conversion of Alexa 488 labelled hNR1-mAb (hNR1-mAb≈) in presence of 3,3´-diaminobenzidine tetrahydrochloride (DAB) after co-culturing microglia with hNR1-mAb≈-bound neurons for 90 mins. DAB incubation converts singlet oxygen produced due to photo-bleaching of Alexa 488 into electron dense precipitates. Electron micrographs revealed the presence of photo-converted material within vesicles and lysosomal compartments inside microglia (Figure 3B). This was not observed when hNR1-mAb was not present in the co-culture setup (Figure 3A). Interestingly, in absence of hNR1-mAb only electron dense mitochondrial signal was detected inside microglia, presumably due to the production of reactive oxygen species (ROS) as a part of its role in ATP production (Figure 3A).

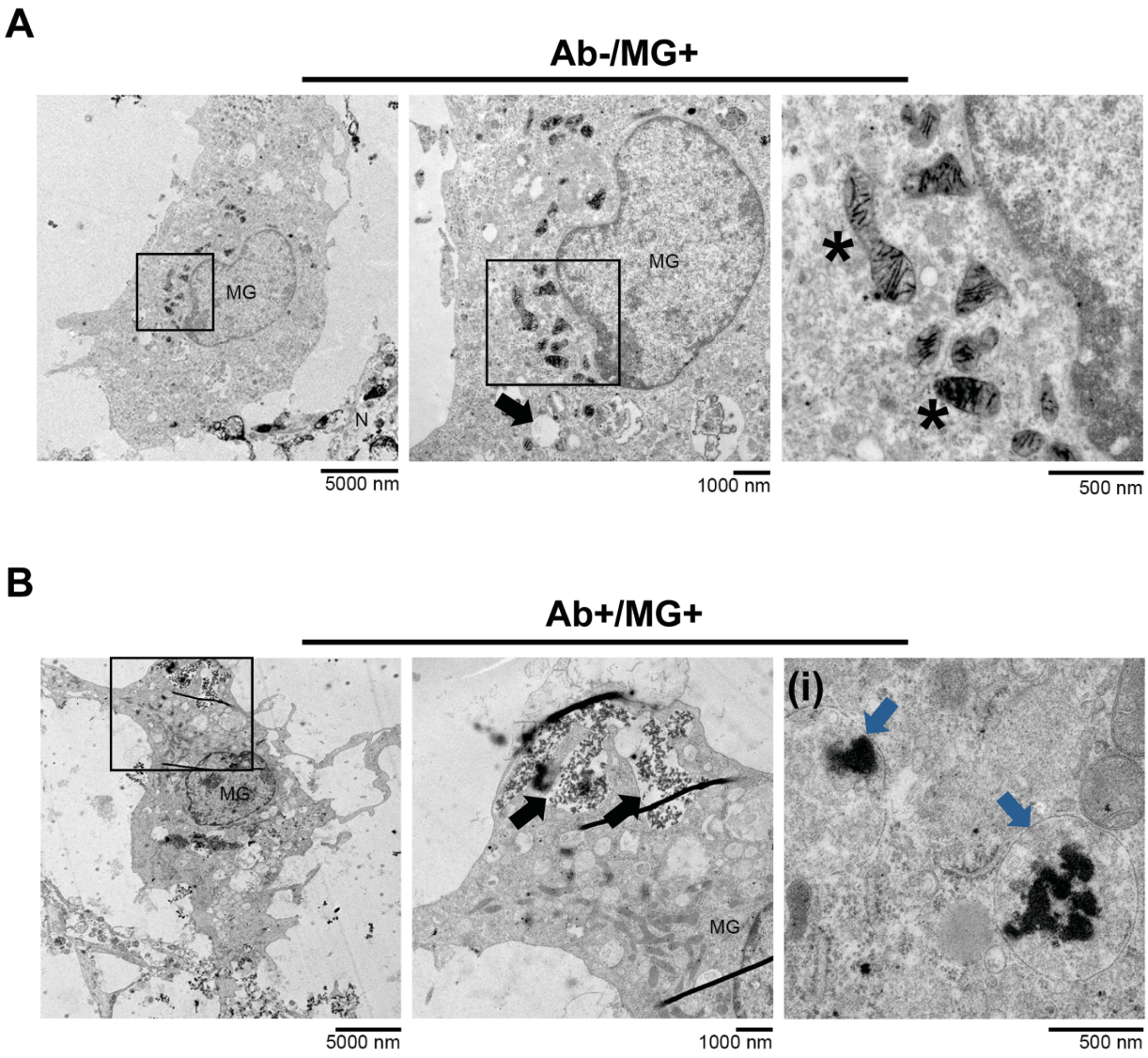

Figure 3| Photo-converted pre-labeled hNR1-mAb≈ present within microglial lysosomal compartments. (A) Electron micrograph of microglia after co-culture in absence of hNR1-mAb≈ (Ab-/MG+) and DAB photo-conversion did not show photo-converted material inside vesicular structures (black arrow). Electron dense signal in absence of hNR1-mAb≈ was seen majorly in microglial mitochondria (asterisks) due the production of singlet oxygen during cellular respiration process that gets photo-converted by DAB. (B) Electron dense photo-converted hNR1-mAb≈ (Alexa 488) was observed inside membrane-bound vesicular structures within microglia (black arrow) after co-culture and DAB photoconversion. Region (i) shows photo-converted material inside bonafide lysosomes (blue arrow). Figure taken from supplementary figure S3 (Rahman et al., 2023).

3.3 hNR1-mAb*-bound NMDARs lead to secretion of inflammatory cytokines.

A fundamental question is whether recognition of antibody/receptor complexes on neurons by microglia, beyond complex phagocytosis, leads to their activation and downstream signalling of other immune cells via the secretion of cytokines. To test this hypothesis, different pro-inflammatory and anti-inflammatory cytokine levels were measured in response to hNR1-mAb-NMDARs engagement 1, 3 and 6 hr after the addition of microglia. The levels of pro-inflammatory cytokines TNFα and IL6 were found to be elevated after 6 hr of co-culture (Figure 4A, 4B). TNFα levels were high even in absence of hNR1-mAb after 6 hr suggesting that it could be due to cellular stress and not specific to the autoantibody (Figure 4A). IL6 levels were significantly higher only in presence of microglia and hNR1-mAb (Figure 4B). The level of IL-1β, another pro-inflammatory cytokine, did not however change appreciably 1, 3 or 6 hr after co-culture (Figure 4C). Anti-inflammatory cytokines, IL10 and IL4, also did not change significantly at different time points of co-culture (Figure 4D, 4E). These data indicate that hNR1-mAb-NMDAR engagement of microglia leads to the activation of microglia and secretion of pro-inflammatory cytokine, e.g., IL6 most profoundly. This increase in IL6 has also been observed in presence of patient derived AQP4 autoantibody (Hinson et al., 2017).

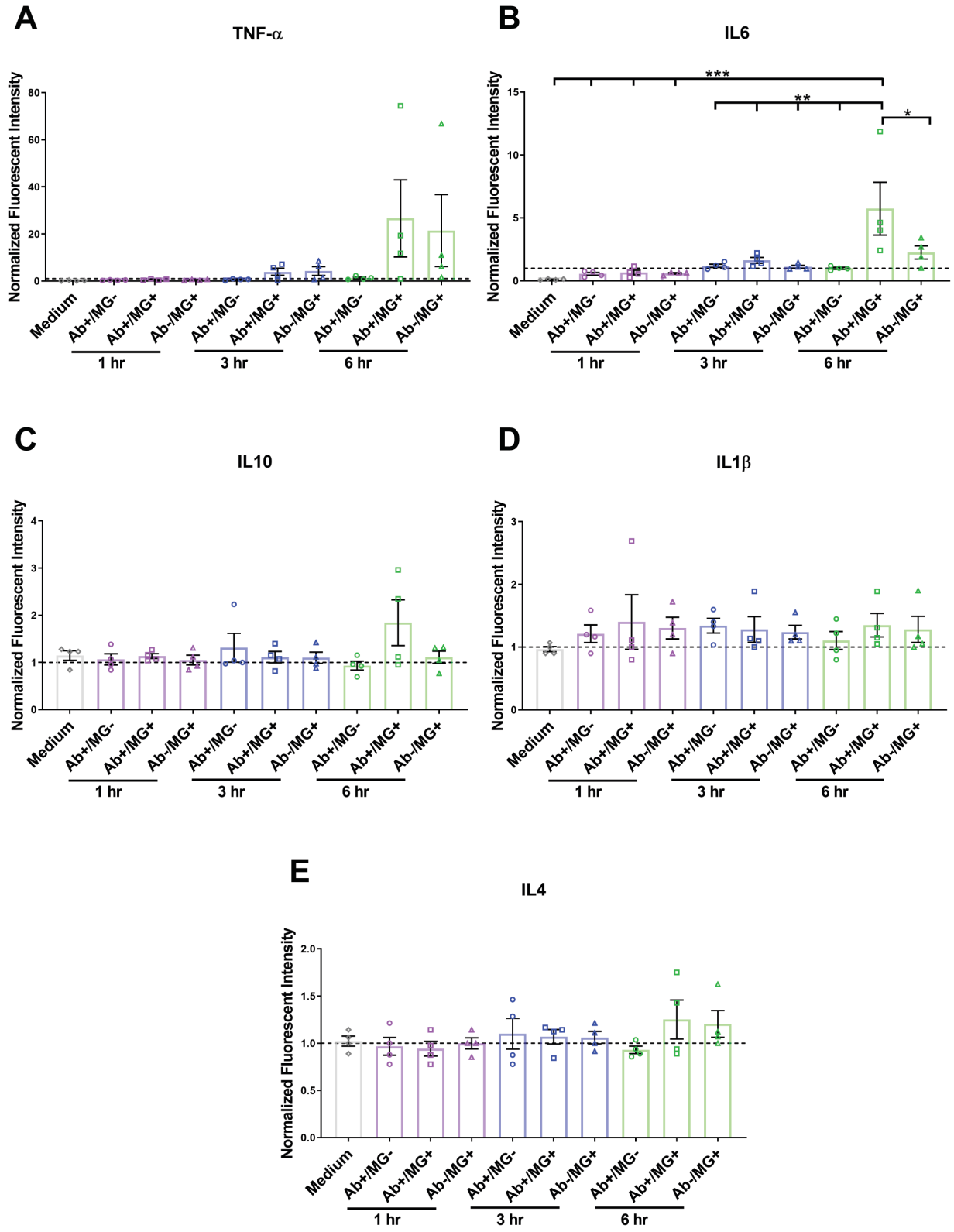
A
TNF-α
Normalized Fluorescent Intensity
Medium
Ab+/MG-
Ab+/MG+
Ab-/MG+
1 hr
3 hr
6 hr
B
IL6
***
**
*
C
IL10
D
IL1β
E
IL4

Figure 4| NMDAR-bound hNR1-mAb leads to production of pro-inflammatory cytokines. (A) TNF-α levels were elevated in supernatants 6 hr after co-culture with microglia. (B) IL6 was significantly higher only in supernatants 6 hr after co-culture in presence of hNR1-mAb (Ab+/MG+). Such an increase was not seen in Ab+/MG-, Ab+/MG+ and Ab-/MG+ experimental groups after 1 and 3 hr of co-culture. (C), (D) and (E) Levels of pro-inflammatory cytokine IL1β and anti-inflammatory cytokines, IL10 and IL4, respectively remained unaltered across all experimental groups after co-culture. Each data point is an average of three technical replicates from each experiment (n=4). Data is represented as mean ± SEM. One-way ANOVA along with Tukey's test for multiple comparison was performed to determine statistical significance (****$p < .0001$).

3.4 Microglia remove hNR1-mAb/NMDAR complexes from dendritic segments.

Conceptually, the presence of hNR1-mAb inside microglia could be due either to the selective removal of bound autoantibodies and/or the co-removal of hNR1-mAb/NMDAR complexes. To test whether microglia physically remove autoantibody-bound receptor complexes, we expressed recombinant NR1-EGFP in hippocampal neurons via a lentivirus under the control of neuron specific Synapsin promoter. NR1-EGFP expressing neurons (DIV 15-17) were then treated with hNR1-mAb/hNR1-mAb* (2 μg/ml) followed by microglia addition for 6 hr (Figure 5A). A significant reduction in the number of NR1-GFP (23.96 ± 1.148 for Ab+/MG-, 15.01 ± 1.164 for Ab+/MG+) and hNR1-mAb*/NR1-EGFP double positive puncta (12.28 ± 0.8791 for Ab+/MG-, 7.424 ± 0.7787 for Ab+/MG+) per unit length of dendrite was observed 6 hr after microglia addition (Figure 5A-C). CD11b positive microglial cells were also found to accumulate hNR1-mAb*/NR1-EGFP double positive puncta in their cytoplasm suggesting that microglia remove hNR1-mAb-bound NMDARs complexes (Figure 5D-E).

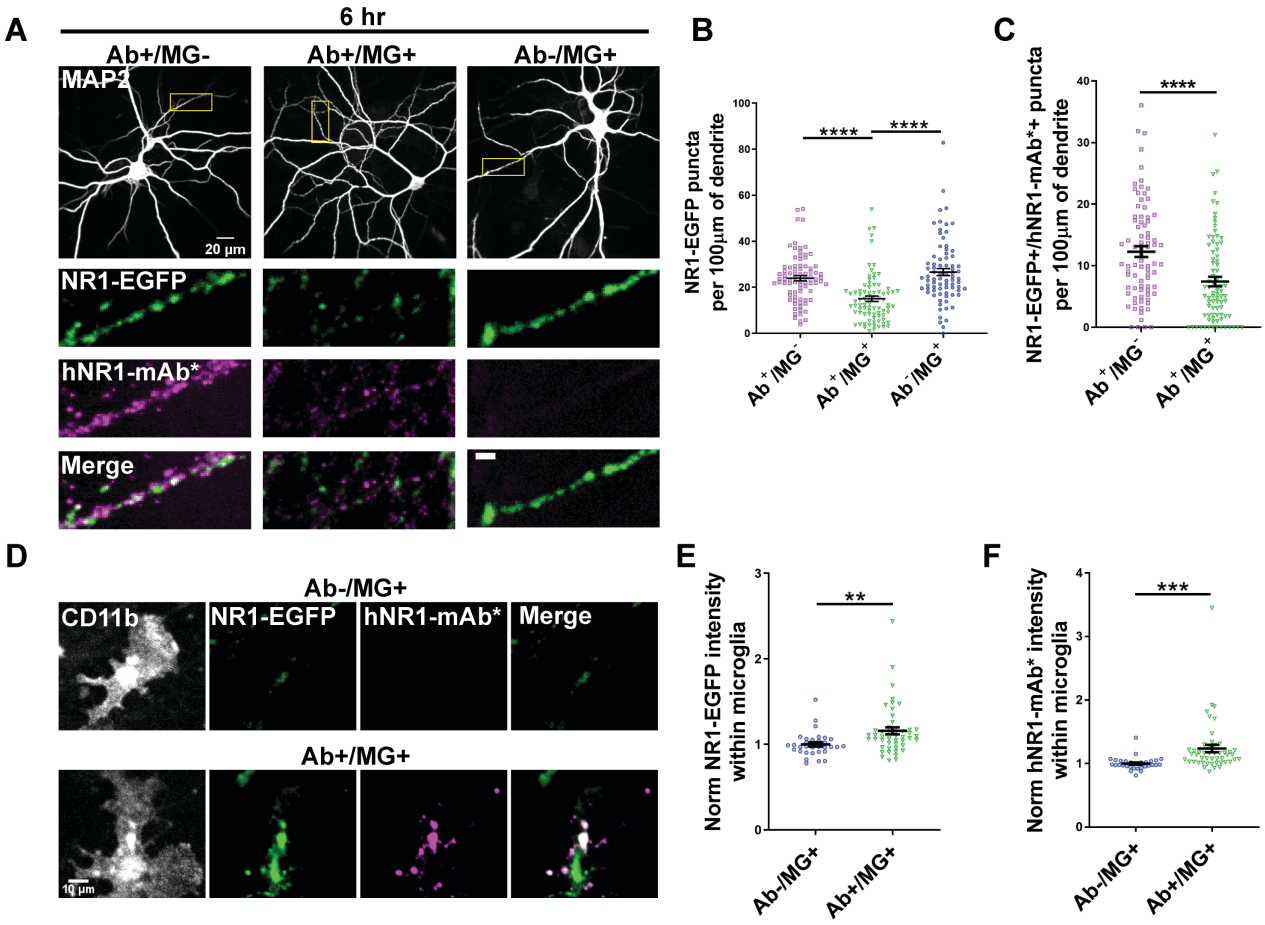

Figure 5| Microglia removes hNR1-mAb bound NMDAR complexes from neuronal surface. (A) Representative images of MAP2 positive (grey) hippocampal neurons expressing NR1-EGFP (green) bound with hNR1-mAb* (magenta) 6 hr after co-culture with microglia (Ab+/MG+) along with Ab+/MG- and Ab-/MG+ control groups. ROI Scale bar = 5 µm. (B) and (C) Quantification of NR1-EGFP and NR1-EGFP+/hNR1-mAb* double positive puncta along dendrite respectively showed a significant reduction in the presence of both hNR1-mAb* and microglia (Ab+/MG+) and not in the absence of either microglia (Ab+/MG-) or antibody (Ab-/MG+). Each data point is an ROI from three independent experiments. (D) Images of microglial cells stained for CD11b (grey) with NR1-EGFP (green) and hNR1-mAb* (magenta) puncta accumulated within its cell body after co-culture in presence of hNR1-mAb* (Ab+/MG+). (E) and (F) Normalized intensity of NR1-EGFP and hNR1-mAb* respectively within microglial cell was significantly higher in Ab+/MG+ group compared to Ab-/MG+ group. Each data point is a microglial cell from three independent experiments. Data points represented as mean ± standard error of mean (SEM). One-way ANOVA with Tukey's test for multiple comparison test was performed to determine statistical significance for NR1-EGFP per unit length quantification (****$p < .0001$) (n = 78-82 ROIs per group). Unpaired t-test with Welch correction for unequal variances was used to determine statistical significance for (C) (n = 78-82 ROIs per group), (E) and (F) (n = 32-48 cells per group). Figure taken from figure 3 (Rahman et al., 2023).

To further explore this finding, live imaging of removal of hNR1-mAb/NMDARs complexes by microglia was performed. Microglia were added to hNR1-mAb* labelled NR1-EGFP expressing neurons for 1 hr, after which the neurons growing on coverslips were imaged live (1 hr) using a confocal microscope. In accordance with immunocytochemical findings, microglial cells were observed to remove and accumulate hNR1-mAb*/NR1-EGFP double positive puncta from dendritic arbours over time (Figure 6). Of note, since lentivirus infection leads to a low/moderate expression of NR1-EGFP, a greater proportion of hNR1-mAb*-bound unlabelled NMDARs was seen on neurons than NR1-EGFP positive NMDARs. This led to a disproportionate higher accumulation of hNR1-mAb* inside microglia as compared to NR1-EGFP (Figure 6B). Nonetheless, the results do support the core finding that microglia remove hNR1-mAb/NMDARs complexes from neurons.

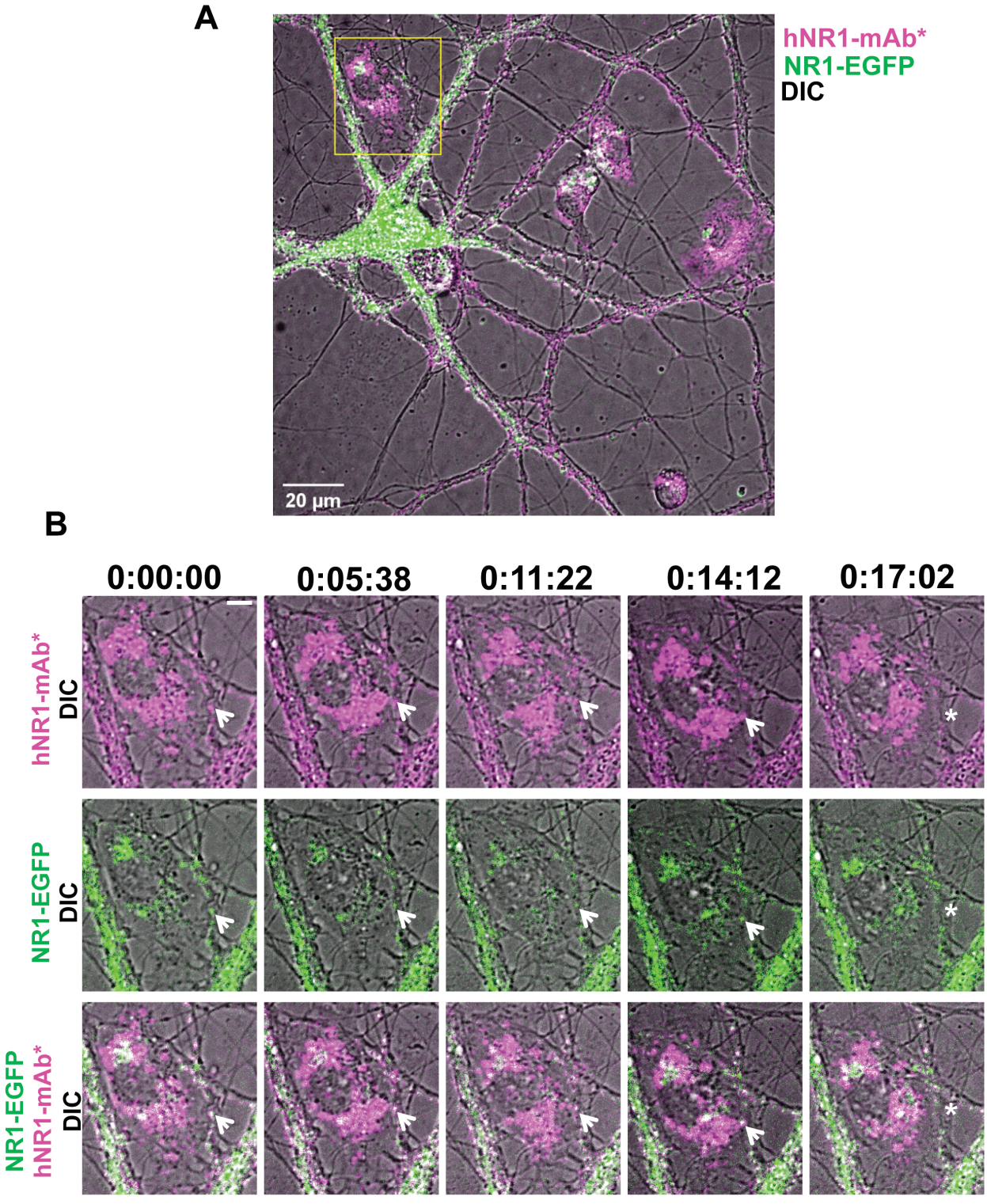

Figure 6| Live imaging of microglia-mediated of hNR1-mAb-bound NMDAR complexes. (A) Representative image of a hippocampal neuron expressing NR1-EGFP (green) bound with hNR1-mAb* (magenta) co-cultured with microglia. Neuronal branches and microglia processes were visualized using the Differential contrast image (DIC) channel simultaneously with fluorescent imaging. Yellow box represents an ROI (B) Time sequence of live images of the ROI showing hNR1-mAb* (magenta), NR1-EGFP (green)

and their overlap (white) being taken up microglia cell (DIC). Arrow represents hNR1-mAb*/NR1-EGFP double positive puncta that gets removed from a dendritic branch (DIC) and accumulated inside neighboring microglial cell (DIC) (~ 17 mins). Asterisks represent loss of the double positive puncta (white) from its dendritic position. ROI Scale bar = 5 µm. Figure taken from figure 4 (Rahman et al., 2023).

3.5 Point mutations in the Fc region of hNR1-mAb prevent microglia-mediated removal of NMDARs.

Fc region of bound antibodies, of IgG subtypes among others, have been shown to drive downstream inflammatory response via activating the complement system and/or by interacting with Fc gamma receptors (FcγR) present on immune cells including macrophages and microglia. To test the hypothesis that the Fc region of NMDAR-bound hNR1-mAb directs microglia-mediated receptor removal, mutations were introduced in the Fc region that blocks two of its downstream interactions. Point mutations replacing leucine residues at 234 and 235th position of the Fc region to alanine (Leu234Ala/Leu235Ala) (LALA) has been reported to block the binding of Fc region of IgGs to FcγRs (Saunders, 2019; Schlothauer et al., 2016). While a mutation at the 329th position, swapping Proline with Alanine (Pro329Ala) (PA), was found to specifically prevent complement binding (Saunders, 2019). A double mutant combining the LALA mutation and a Proline to Glycine mutation at the 329th position (Pro329Gly) (PG) (LALA-PG) of the Fc region of IgG antibodies was shown to prevent both complement and FcγR binding (Saunders, 2019). We thus created recombinant version of these mutations (LALA-PG, LALA, and PA) in hNR1-mAb*, which were subsequently expressed and purified (Figure 7A). As anticipated, hNR1-mAb* containing the LALA-PG triple mutant was observed in *in-vitro* binding assays to have reduced FcγR1 and C1q protein binding (Figure 7C, 7D), consistent with previous studies (Lo et al., 2017; Schlothauer et al., 2016). Interesting, both LALA and PA mutants of hNR1-mAb were found to exhibit reduce binding to both C1q and FcγR1 (Figure 7C, 7D), indicating that with these mutations it was not possible to distinguish between the role of FcγR versus complement interactions with hNR1-mAb* contributing to the removal of hNR1-mAb-NMDAR complexes. Of note, none of these mutations (LALA, PA, and LALA-PG) affected antigen/NR1 binding of the hNR1-mAb, as illustrated by the robust a synaptic co-localization of each with pre-synaptic marker, vGLUT1, similar to WT hNR1-mAb* (Figure 7B).

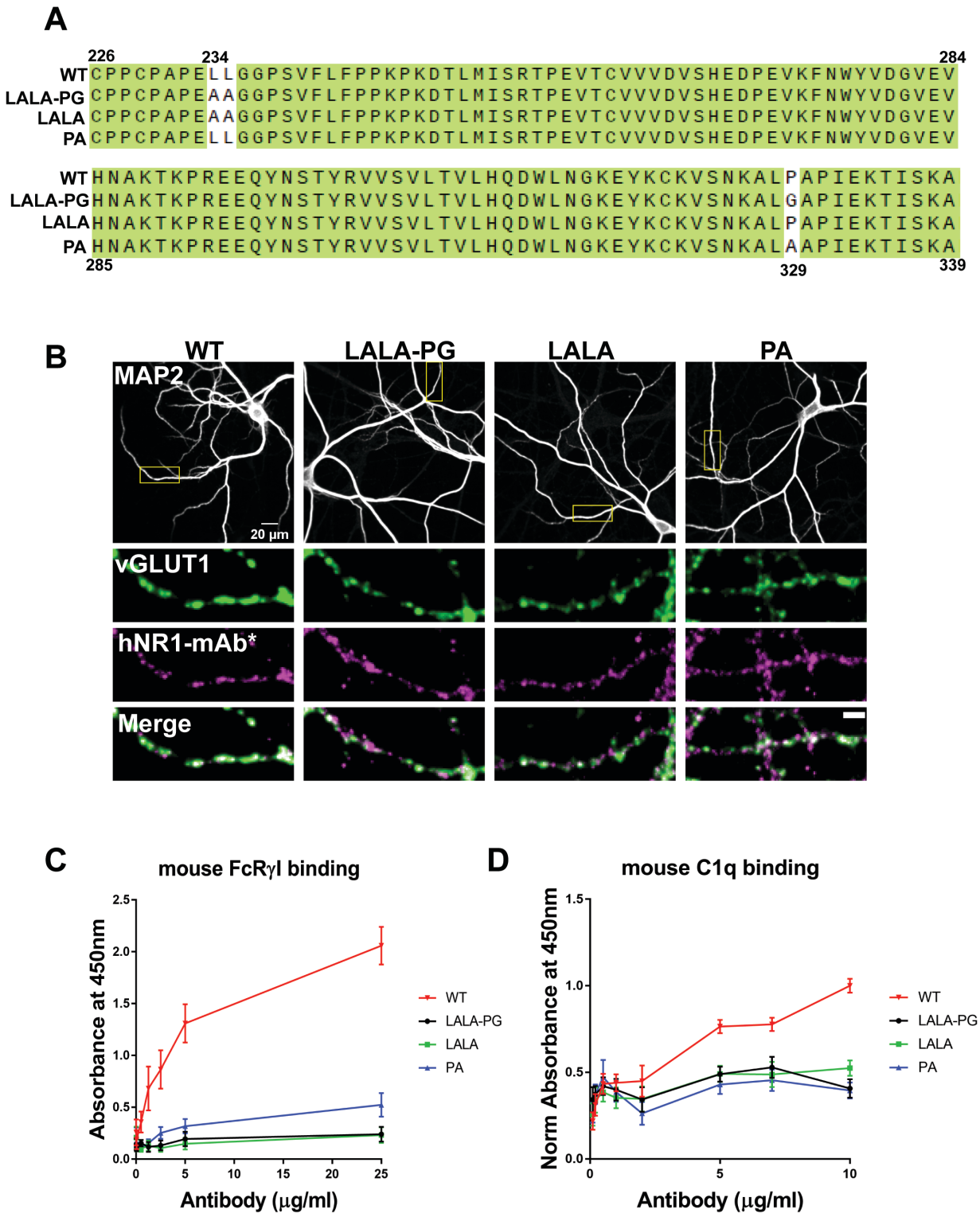

Figure 7| Fc region mutants of hNR1-mAb prevent C1q and FcγRI binding. (A) Amino acid sequence alignment of the Fc region of hNR1-mAb pointing out the introduced mutations. (B) Representative images of hippocampal neurons with bound WT hNR1-mAb* along with the LALA-PG, LALA and PA mutant of hNR1-mAb (magenta) stained for MAP2 (grey) and pre-synaptic marker, vGLUT1 (green). WT and the mutant hNR1-mAb* showed similar punctate synaptic binding pattern reflected by an overlap (white) with

vGLUT1 staining. ROI Scale bar = 5 µm. (C) LALA-PG, LALA and PA mutant of hNR1-mAb had reduced binding to purified FcγRI compared to WT hNR1-mAb in *in-vitro* colorimetric protein binding assays. Each data point represents an average of three independent experiments performed with three technical replicates for each concentration of hNR1-mAb. Error bars represent SEM. (D) Reduced C1q binding was observed in protein binding colorimetric assays for all mutant hNR1-mAb, i.e., LALA-PG, LALA and PA in comparison to WT hNR1-mAb. Each data point represents an average of five independent experiments performed with three technical replicates for each concentration of hNR1-mAb. Error bars represent SEM. Figure taken from supplementary figure S6 (Rahman et al., 2023).

To explore the functional effects of these mutations, WT along with LALA-PG, LALA and PA mutant of hNR1-mAb were used in the co-culture experiment with microglia. A significant reduction in the number of hNR1-mAb* positive puncta per unit length of dendritic segments was only observed when WT hNR1-mAb* (23.04 ± 1.245 for Ab+/MG-, 16.3 ± 0.9746 for Ab+/MG+) was bound to hippocampal neurons in the presence of microglia (Figure 8A, 8E). Such a reduction was not observed when either LALA-PG (24.03 ± 0.9874 for Ab+/MG-, 22.51 ± 1.189 for Ab+/MG+), LALA (27.17 ± 0.7405 for Ab+/MG-, 26.69 ± 0.9778 for Ab+/MG+) or PA (25.56 ± 0.9195 for Ab+/MG-, 25.84 ± 0.9657 for Ab+/MG+) hNR1-mAb* mutants were bound to NMDARs (Figure 8B-D, 8F-H). Concurrently, a higher intensity of WT hNR1-mAb* was measured inside CD11b positive microglia, while the intensity of LALA-PG hNR1-mAb* inside microglia was similar to control levels (i.e., in absence of hNR1-mAb) (1 ± 0.0028 for Ab-/MG+, 1.081 ± 0.0137 for Ab+/MG+ (WT), 1.029 ± 0.0059 for Ab+/MG+ (LALA-PG)) (Figure 8I, 8J). Intriguingly, even though less than WT (1.081 ± 0.0137 for Ab+/MG+), both LALA (1.042 ± 0.0064 for Ab+/MG+) and PA (1.038 ± 0.01028 for Ab+/MG+) mutant hNR1-mAb led to an increase in hNR1-mAb* signal inside microglia (Figure 8I, 8J), without a significant reduction in hNR1-mAb* along dendrites (Figure 8G, 8H). These latter data suggest that the LALA and PA mutants retain some ability to interact with microglia. Together, these results demonstrate that the Fc region of hNR1-mAb is necessary for driving microglia-mediated removal of NMDARs.

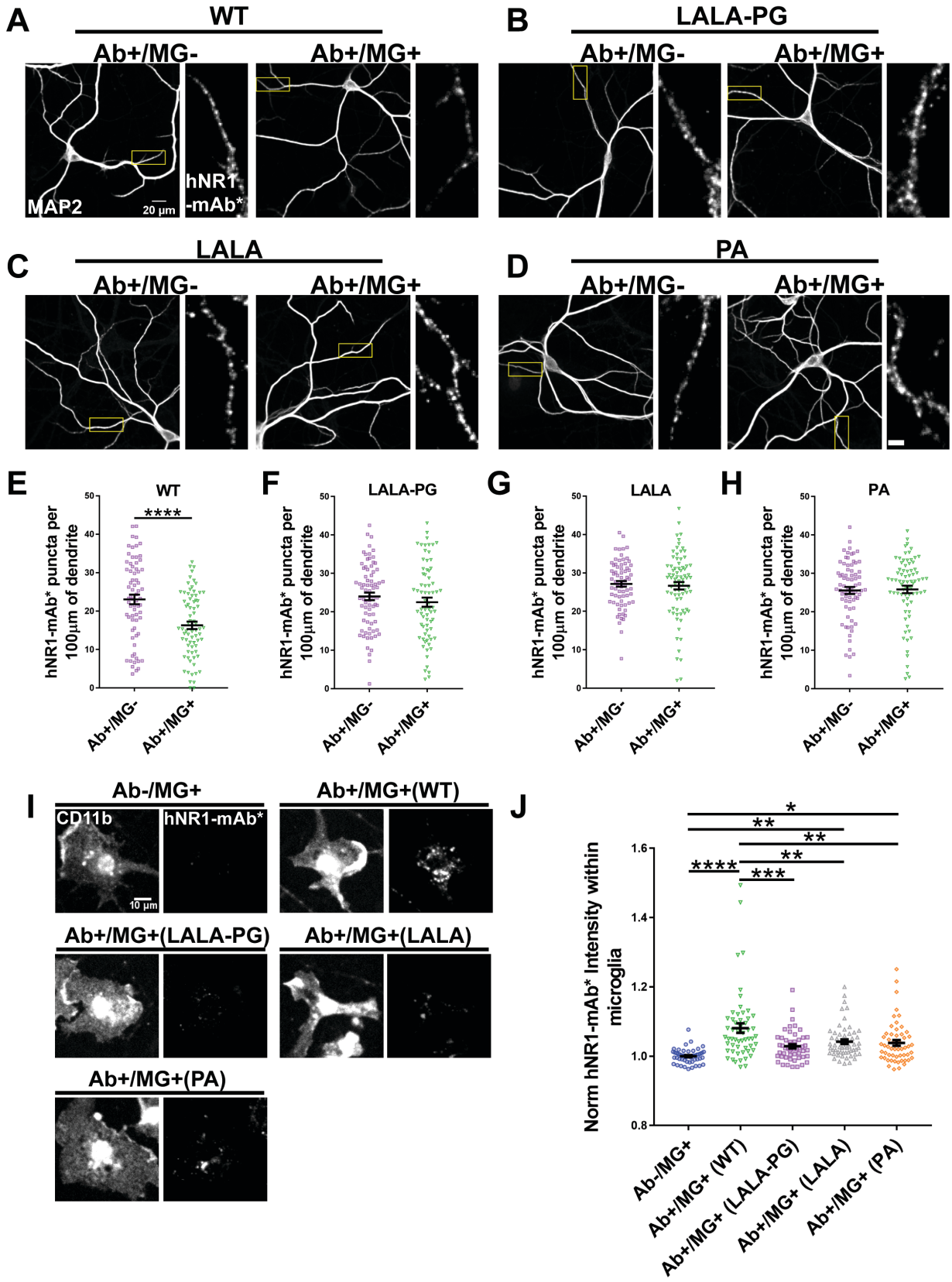
A
WT
Ab+/MG-
Ab+/MG+
MAP2
20 µm
hNR1
-mAb*
B
LALA-PG
Ab+/MG-
Ab+/MG+
C
LALA
Ab+/MG-
Ab+/MG+
D
PA
Ab+/MG-
Ab+/MG+
E
WT
****
hNR1-mAb* puncta per 100µm of dendrite
Ab+/MG-
Ab+/MG+
F
LALA-PG
hNR1-mAb* puncta per 100µm of dendrite
Ab+/MG-
Ab+/MG+
G
LALA
hNR1-mAb* puncta per 100µm of dendrite
Ab+/MG-
Ab+/MG+
H
PA
hNR1-mAb* puncta per 100µm of dendrite
Ab+/MG-
Ab+/MG+
I
Ab-/MG+
CD11b
hNR1-mAb*
10 µm
Ab+/MG+(WT)
Ab+/MG+(LALA-PG)
Ab+/MG+(LALA)
Ab+/MG+(PA)
J
*
**
**
**
****
***
Norm hNR1-mAb* Intensity within microglia
Ab-/MG+
Ab+/MG+ (WT)
Ab+/MG+ (LALA-PG)
Ab+/MG+ (LALA)
Ab+/MG+ (PA)

Figure 8| Blocking complement and FcγR interaction prevents removal of hNR1-mAb-bound NMDARs by microglia. (A) (B) (C) and (D) Representative images of MAP2 positive neurons with bound WT, LALA-PG, LALA and PA hNR1-mAb* respectively with or without co-culture with microglia for 6 hr. Images shown in grey scale. ROI Scale bar = 5 μm. (E) Quantification of puncta per unit length of WT hNR1-mAb* showed a significant decrease in presence of microglia (Ab+/MG+). (F) (G) and (H) No such change was observed in the number of puncta along dendrites for LALA-PG, LALA and PA hNR1-mAb* respectively with or without microglia addition (Ab+/MG+ or Ab+/MG-). Each data point is an ROI from three independent experiments (n = 72-78 ROIs per group). Data points represented as mean ± standard error of mean (SEM). Unpaired t-test with Welch correction for unequal variances was employed to determine statistical significance (****$p < .0001$). (I) Grey scale images of CD11b positive microglial cells showing NMDAR immunoreactivity inside the cell body of microglia in presence of WT and different mutants of hNR1-mAb*. (J) Significantly higher hNR1-mAb* fluorescent intensity was observed inside microglial cells after co-culture with WT hNR1-mAb*-bound hippocampal neurons while no such increase was seen for LALA-PG hNR1-mAb* as compared to negative control (Ab-/MG+). Increased hNR1-mAb* signal inside microglia was also seen for LALA and PA hNR1-mAb* however lower than WT hNR1-mAb*. Each data point represents measurement from one microglial cell from three independent experiments (n = 52-56 cells per group). Data points represented as mean ± SEM. One-way ANOVA with Tukey's test for multiple comparison was performed to determine statistical significance (****$p < .0001$). Figure taken from figure 7 (Rahman et al., 2023).

3.6 WT hNR1-mAb promotes microglia driven reduction in synapse number.

Gestational transfer of NR1 reactive autoantibody to the brains of foetuses is associated with the postnatal decrease in synapse number and microglial activation (García-Serra et al., 2021). The observed removal of synaptic receptors like NMDARs by microglia in presence of hNR1-mAb raised the question whether there is a similar microglia-mediated removal of synapses. To examine this, neurons with either WT or LALA-PG hNR1-mAb bound autoantibodies were co-cultured with microglia for 6 hr. LALA-PG mutant of hNR1-mAb was used here as it was found to be most efficient in blocking interaction with microglia. Cells were stained post-fixation for vGLUT1 and PSD95 as pre- and post-synaptic markers, respectively. Quantifying the number of synapses, defined as vGLUT1+/PSD95+ double positive puncta, we observed a significant reduction (≈ 20 %) in their number/unit length of dendrite when WT hNR1-mAb was bound to NMDARs in presence of microglia for 6 hr (18.4 ± 0.9871 for Ab+/MG-, 13.32 ± 0.8324 for Ab+/MG+) (Figure 9A, 9B). This was not seen when LALA-PG hNR1-mAb was bound to NMDARs (19.65 ± 0.9473 for Ab+/MG-, 20.53 ± 0.9895 for Ab+/MG+) (Figure 9A, 9B). Interestingly for WT hNR1-mAb bound NMDARs, there was as selective decrease in PSD95 positive

post-synapse in presence of microglia (21.94 ± 0.9684 for Ab+/MG-, 15.09 ± 0.8191 for Ab+/MG+) (Figure 9A, 9C), without any notable change in the number of vGLUT1 positive pre-synaptic boutons (24.45 ± 0.9735 for Ab+/MG-, 24.83 ± 0.8595 for Ab+/MG+) (Figure 9A, 9D). No change was detected in the number of PSD95 (22.21 ± 0.9734 for Ab+/MG-, 23.62 ± 0.9876 for Ab+/MG+) or vGLUT1 (27.76 ± 0.8199 for Ab+/MG-, 26.76 ± 0.8691 for Ab+/MG+) puncta along dendrites, when microglia were co-cultured with LALA-PG hNR1-mAb bound NMDARs. In accordance with the loss of PSD95 puncta for WT hNR1-mAb, a higher intensity of PSD95 staining with no change in vGLUT1 staining intensity was detected inside microglia (Figure 9 E-G). Such changes in staining intensities inside microglia were not seen for PSD95 or vGLUT1 in the presence of LALA-PG hNR1-mAb mutant (Figure 9 E-G).

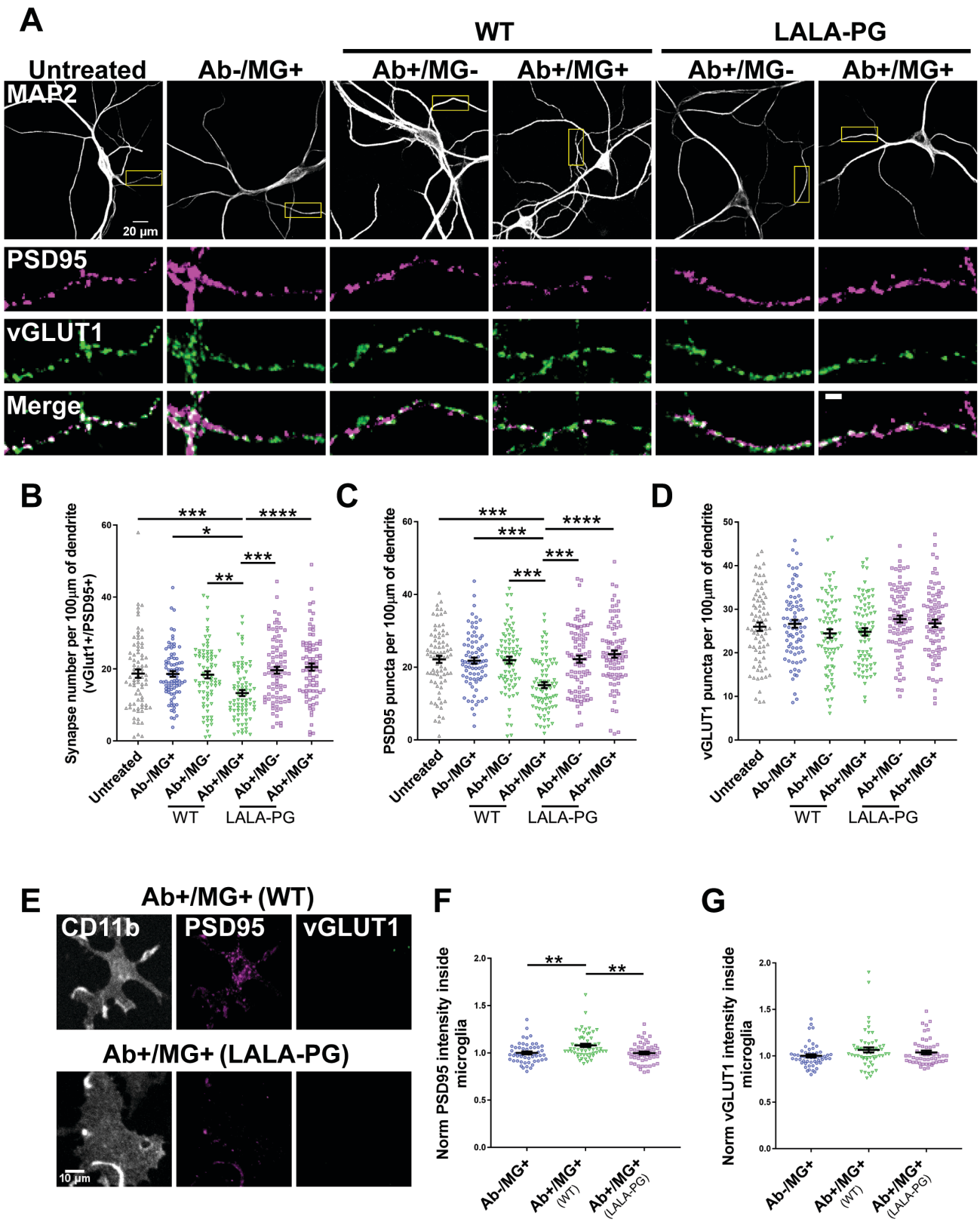

Figure9| Microglia mediates loss of synapses from hippocampal neurons with NMDARs bound by WT hNR1-mAb. (A) Representative neuronal images stained for MAP2 (grey), PSD95 (magenta) and vGLUT1 (green) with or without microglia addition (Ab+/MG+ or Ab+/MG-) in presence of either WT or

LALA-PG hNR1-mAb. Experimental groups with no treatment (Ab-/MG-) or no antibody (Ab-/MG+) were used as controls. Synapses were defined by vGLUT1 and PSD95 double positive (vGLUT1+/PSD95+) puncta (white). ROI Scale bar = 5 µm. (B) Significant decrease in the number of synapses (vGLUT1+/PSD95+) was observed only in the presence of microglia and WT hNR1-mAb. No such reduction was seen for LALA-PG hNR1-mAb in the presence or absence of microglia. (C) PSD95 positive post-synapse number was reduced after co-culture of WT hNR1-mAb-bound hippocampal neuron with microglia and not LALA-PG hNR1-mAb. (D) vGLUT1 positive pre-synaptic bouton number per unit length of dendrite remained unchanged for all experimental group with or without microglia for both WT and LALA-PG hNR1-mAb. Each data point represents an ROI from three independent experiments (n = 78-85 ROIs per group). Data points represented as mean ± SEM. One-way ANOVA with Tukey's test for multiple comparison was performed to determine statistical significance (****$p < .0001$). (E) Microglia images stained for CD11b (grey), PSD95 (magenta) and vGLUT1 (green) after co-culture with either WT or LALA-PG hNR1-mAb-bound hippocampal neurons. (F) Normalized intensity of PSD95 staining was significantly higher within microglia cell body after co-culture with WT hNR1-mAb but not with LALA-PG hNR1-mAb. (G) No change was seen in quantification of vGLUT1 fluorescence imaging inside microglia after co-culture with either WT or LALA-PG hNR1-mAb. Each data point is a measurement from one microglial cell from three independent experiments (n = 51-57 cells per group). Data points represented as mean ± SEM. One-way ANOVA with Tukey's test for multiple comparison was performed to determine statistical significance (****$p < .0001$). Figure taken from figure 8 (Rahman et al., 2023).

3.7 hNR1-mAb causes microglia-mediated loss of post-synaptic proteins in co-culture.

The observation that hNR1-mAb drives microglia-mediated removal of PSD95, but not vGLUT1, indicate that microglia can remove post-synaptic components selectively leaving the pre-synapse intact. This concept was further explored by co-culturing microglia with neurons expressing different combinations of recombinant pre- / post-synaptic markers, including mCherry (mCh)-Synapsin/Homer1 (Homer)-EGFP or Synaptophysin (Syphysin)-EGFP/PSD95-mKate2 bound with WT hNR1-mAb. As observed for endogenous synaptic proteins (Figure 9), a significant reduction was only observed in the numbers of post-synaptic protein puncta i.e., Homer-EGFP (29.76 ± 1.757 for Ab+/MG-, 22.33 ± 1.381 for Ab+/MG+) (Figure 10A, 10B) and PSD95-mKate2 (26 ± 0.8864 for Ab+/MG-, 17.67 ± 1.179 for Ab+/MG+) (Figure 10D, 10E) along dendrites in the presence of microglia with hNR1-mAb-bound NMDARs. No changes were observed in the number of puncta per unit dendrite length for the pre-synaptic proteins mCh-Synapsin (26.17 ± 1.253 for Ab+/MG-, 26.18 ± 1.282 for Ab+/MG+) (Figure 10A, 10C) or Syphysin-EGFP (26.25 ± 0.8186 for Ab+/MG-, 24.86 ± 1.128 for Ab+/MG+) (Figure 10D, 10F). Of note, there was

no detectable change in puncta number for the different pre- and post-synaptic markers under control conditions e.g., transfected neuron grown in the absence of either microglia or hNR1-mAb.

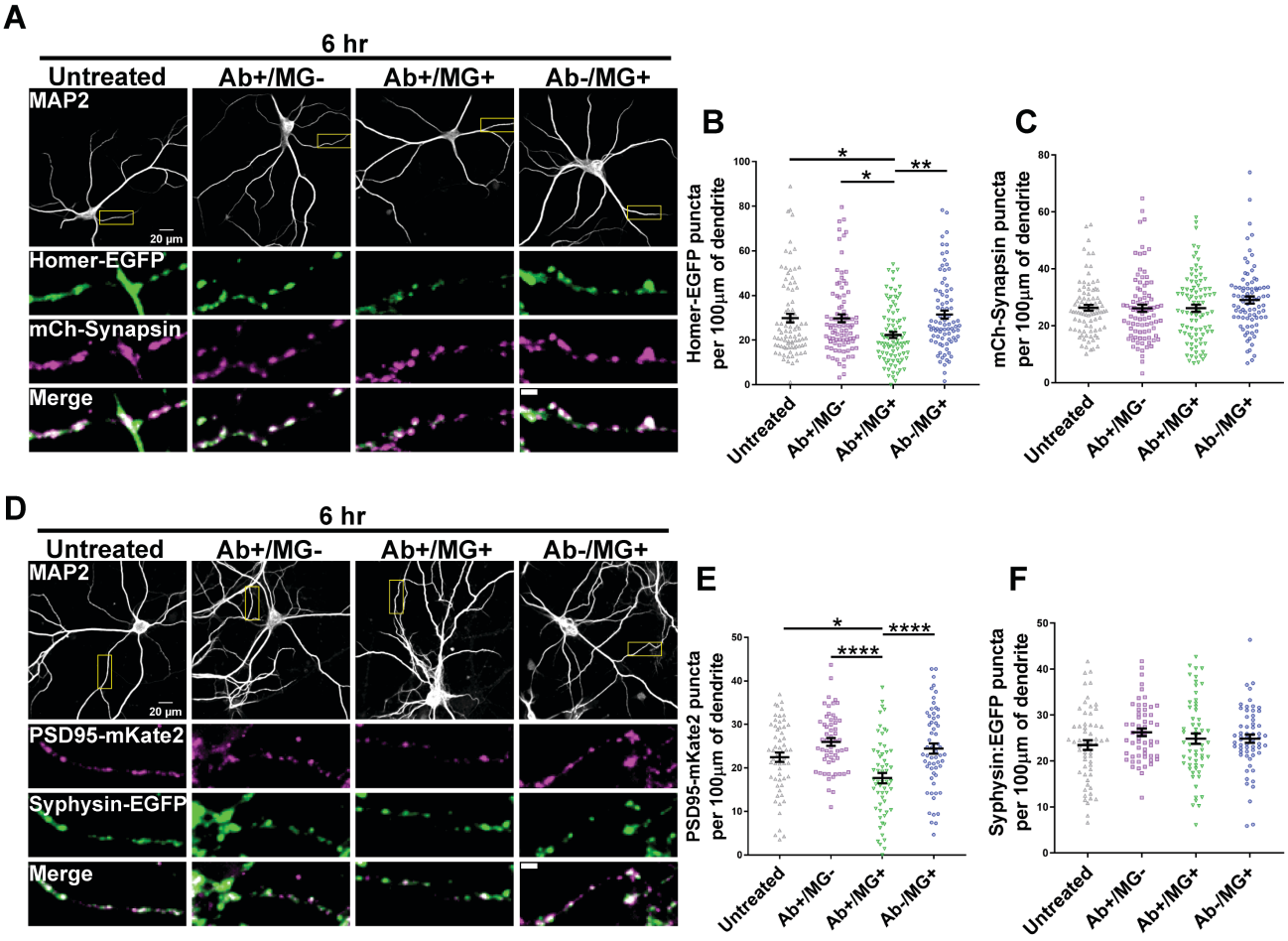

Figure 10| Microglia specifically removes post-synaptic proteins from hNR1-mAb-bound neurons. (A) Representative images hNR1-mAb-bound hippocampal neurons stained for MAP2 (grey) overexpressing Homer-EGFP (green) and mCh-Synapsin (magenta) after 6 hr with or without microglia addition. Experimental groups with no treatment (Ab-/MG-) or no antibody (Ab-/MG+) was used as controls. ROI Scale bar = 5 µm. (B) and (C) Number of Homer-EGFP and mCh-Synapsin puncta along dendritic segments respectively in different experimental groups. Significant reduction was observed only in the number of Homer-EGFP positive post-synapses per unit length of dendrite in presence of microglia and hNR1-mAb. No changes were seen in the number of mCh-Synapsin expressing pre-synaptic boutons in any of the experimental groups. Each data point represents measurement from one microglial cell from three independent experiments (n = 83-89 ROIs per group). Data points represented as mean ± standard error of mean (SEM). One-way ANOVA with Tukey's multiple comparison test was performed to evaluate statistical significance for NR1-EGFP per unit length quantification (****$p < .0001$). (D) Images of MAP2 positive neurons (grey) overexpressing PSD95-mKate (magenta) and Synaptophysin (Syphysin)-EGFP (green) as post and pre-synaptic markers from Untreated (Ab-/MG-), Ab+/MG-, Ab+/MG+ and Ab-/MG+ groups. ROI Scale

bar = 5 µm. (E) Number of PSD95-mKate2 puncta per unit length of dendrite was reduced significantly after co-culture with microglia in presence of hNR1-mAb. (F) No appreciable changes were noticed in the number of Syphysin-EGFP positive pre-synapses in any of the experimental groups. Each data point represents measurement from one microglial cell from two independent experiments (n = 57-60 ROIs per group). Data points represented as mean ± SEM. One-way ANOVA with Tukey's test for multiple comparison was performed to determine statistical significance (****$p < .0001$). Figure taken from figure 6 (Rahman et al., 2023).

To further support the conclusion that the hNR1-mAb promotes the removal of the post-synapse via microglia, we analysed neuronal/microglia co-cultures expressing the post-synaptic protein Homer-EGFP by electron microscopy (EM) 90 mins after antibody/microglia addition. Similar to EM data with the hNR1-mAb≈ (Figure 3), Homer-EGFP/light mediate photo-conversion of DAB, revealed the presence of photo-converted electron dense material within double membraned endo-lysosomal structures inside microglia in presence of hNR1-mAb (Figure 11B, 11C). This was not observed in micrographs from co-cultures lacking hNR1-mAb (Figure 11A), wherein the electron dense signal was restricted primarily to mitochondria within microglial as seen before (Figure 3A), due to ROS generation during ATP production. Together, these demonstrate that microglial mediate removal of hNR1-mAb-NMDARs complexes also leads to a selective loss of post-synaptic proteins, contributing to the loss of functional synapses.

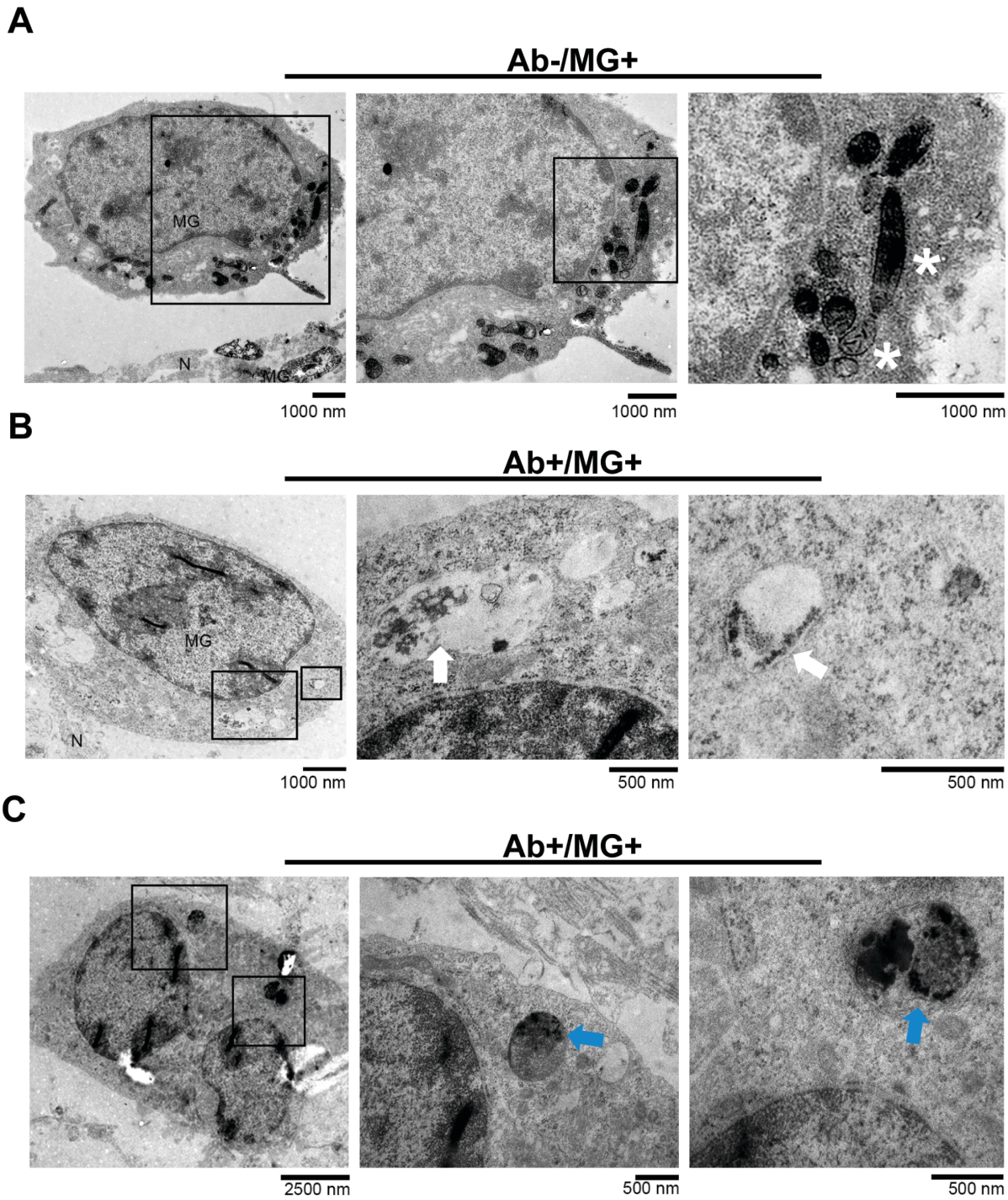

Figure 11| Microglia accumulates photo-converted Homer-EGFP from hNR1-mAb-bound hippocampal neurons inside endo-lysosomal structures. (A) and (B) Electron micrograph showing microglia (M) and neurons (N) after photo-conversion with DAB incubation in presence and absence of hNR1-mAb respectively. Photo-converted Homer-EGFP signal not observed inside membranous compartments inside microglia in absence of hNR1-mAb (A). In absence of hNR1-mAb, mitochondrial signal (asterisk) was mainly observed due to photo-conversion of singlet oxygen species generated during the respiratory cycle. Electron dense photo-converted signal from Homer-EGFP was seen inside double membraned structures

(B) within microglia cell body (white arrow) and bonafied lysosomes (C) (blue arrow) in presence of hNR1-mAb. Figure taken from supplementary figure S5 (Rahman et al., 2023).

3.8 Removal of autoantibody-bound receptors by microglia is selective.

An important unresolved question relates to the specificity of the antibody/microglia-mediated removal and/or whether microglia once activated indiscriminately remove cellular material. To address this question, we compared the specificity of hNR1-mAb to a second patient derived monoclonal autoantibody, of the IgG1 subtype, generated against α1 subunit of $GABA_A$ receptors (α1-$GABA_A$R-mAb). Similar to hNR1-mAb, we observed a significant loss of $GABA_A$R puncta along dendrites 6 hr after microglia addition to α1-$GABA_A$R-mAb*-bound hippocampal neurons (21.88 ± 0.9537 for Ab+/MG-, 11.34 ± 1.001 for Ab+/MG+) (Figure 12A, 12B). Microglia were similarly found to accumulate α1-$GABA_A$R-mAb* puncta within its cell body (Figure 12C, 12D). These data suggest that microglia mediate removal of autoantibody-bound receptors could be a general mechanism for antibodies with functional downstream interactions, i.e., with FcγR and/or complement.

As an initial test of specificity, we performed a time shift experiment, wherein hNR1-mAb and α1-$GABA_A$R-mAb were sequentially added. Here, the first antibody was added, together with microglia for 6 hr, followed by the brief addition/labelling of a different receptor with the second antibody, to assess whether its levels were also affected following microglia activation by the first antibody. For example, in one version of this experiment microglia were added to α1-$GABA_A$R-mAb* (Alexa 647)-bound hippocampal neurons for 6 hr, allowing sufficient time for its removal and microglia activation. These cultures were then incubated/labelled with the hNR1-mAb$^{\#}$ (Alexa 594) for 30 mins before fixation, a time deemed insufficient for microglia selective removal (Figure 12E). An inverse experiment was performed by first labelling cultures with hNR1-mAb* before adding microglia for 6 hr, followed by staining $GABA_A$Rs with α1-$GABA_A$R-mAb$^{\#}$ for 30 mins (Figure 12H). In the former experiment, a significant decrease in the number of for α1-$GABA_A$R-mAb* puncta/unit length of dendrite was observed, in the presence of microglia (25.63 ± 1.019 for Ab+/MG-, 18.22 ± 0.8333 for Ab+/MG+) (Figure 12E, 12F), without any change in the number of hNR1-mAb$^{\#}$-bound NMDARs puncta/unit length of dendrite (24.60 ± 0.8008 for Ab+/MG-, 24.70 ± 0.8437 for Ab+/MG+) (Figure 12E, 12G). Conversely in the latter experiment, we observed a selective decrease in the number of hNR1-mAb* puncta per

unit length of dendrite, when this antibody was added first (26.83 ± 1.006 for Ab+/MG-, 17.38 ± 0.8523 for Ab+/MG+) (Figure 12H, 12I), without affecting the number of α1-$GABA_AR$-mAb$^{\#}$-bound $GABA_ARs$ puncta/unit length of dendrite (24.37 ± 1.032 for Ab+/MG-, 25.74 ± 0.9905 for Ab+/MG+) (Figure 12H, 12J).

The afore mentioned experiments suggest that microglia are capable of selectively removing only antibody labelled receptor complexes. To further explore this conclusion, we initially examined whether microglia can efficiently remove both $GABA_AR$ and NMDARs, simultaneously labelled with the α1-$GABA_AR$-mAb and hNR1-mAb, respectively. This was accomplished by initially pre-labelling α1-$GABA_AR$-mAb$^{\#}$ and hNR1-mAb* with different fluorophores, Alexa 594 and 647, respectively. These were then added at the same time to neurons followed by a 6 hr incubation with microglia (Figure 13A). As expected, we observed a decrease in the number of both α1-$GABA_AR$-mAb$^{\#}$ (22.06 ± 0.8494 for Ab+/MG-, 14.09 ± 0.9742 for Ab+/MG+) and hNR1-mAb* (23.90 ± 1.131 for Ab+/MG-, 14.42 ± 0.9742 for Ab+/MG+) puncta/unit length of dendrites in the presence of microglia (Figure 13A-C). Next, we repeated these experiments utilizing the LALA-PG hNR1-mAb* mutant, instead of the WT hNR1-mAb*, to block FcγR and complement engagement of microglia for just one of the antibodies (Figure 13B). Here, we observed a significant decrease in $GABA_ARs$ bound with α1-$GABA_AR$-mAb$^{\#}$ (22.18 ± 1.248 for Ab+/MG-, 13.19 ± 1.013 for Ab+/MG+) with no change in the number of LALA-PG hNR1-mAb* (25.68 ± 1.143 for Ab+/MG-, 27.37 ± 1.507 for Ab+/MG+)-bound NMDAR puncta per unit length after microglia addition (Figure 13D-F). Taken together, these experiments suggest that microglia both specifically and selectively remove autoantibody receptor complexes via their direct interaction with the Fc region of these IgG1 antibodies.

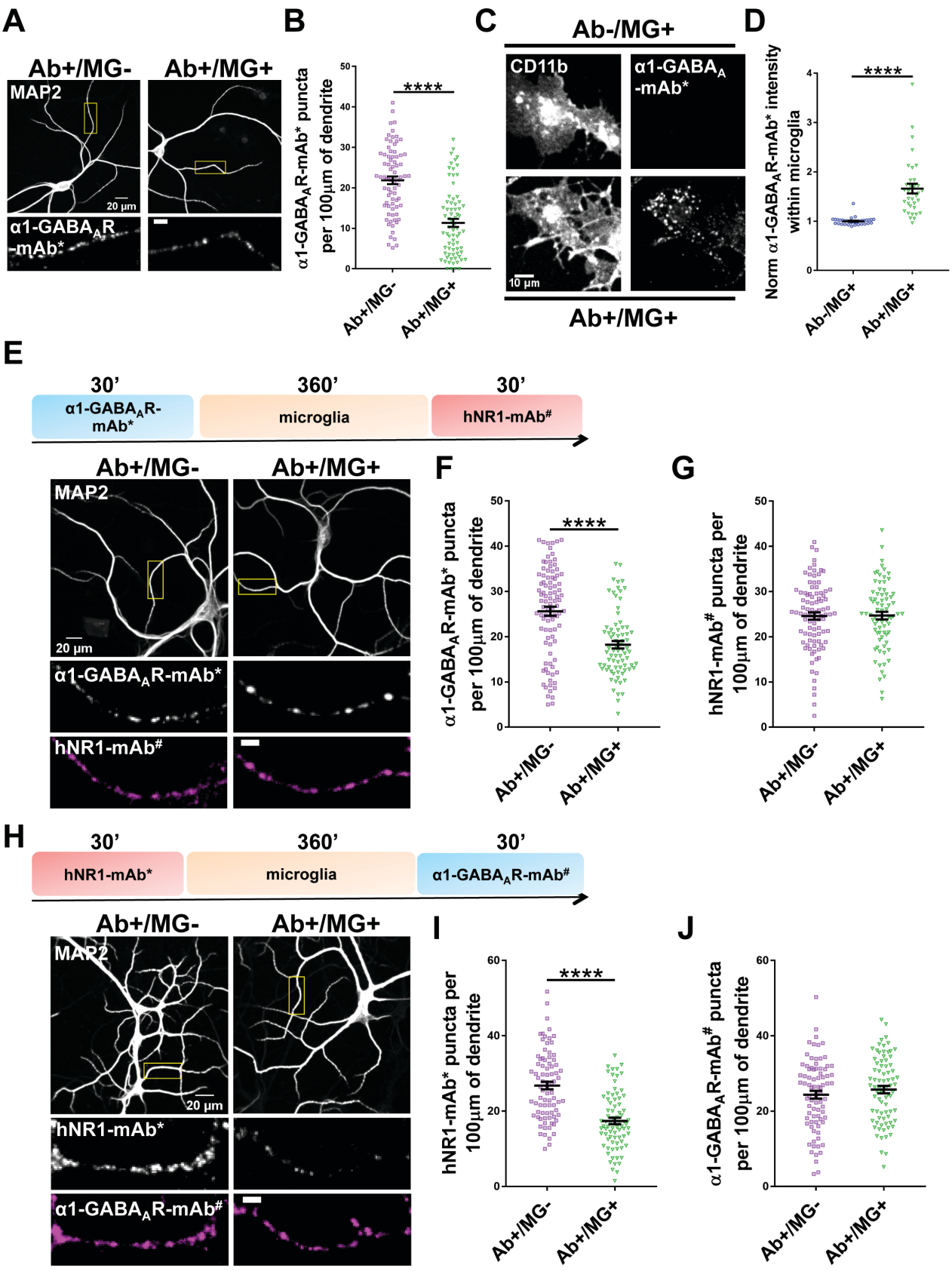
A
Ab+/MG-
Ab+/MG+
MAP2
20 µm
α1-GABA$_A$R -mAb*
B
α1-GABA$_A$R-mAb* puncta per 100µm of dendrite
****
Ab+/MG-
Ab+/MG+
C
Ab-/MG+
CD11b
α1-GABA$_A$ -mAb*
10 µm
Ab+/MG+
D
Norm α1-GABA$_A$R-mAb* intensity within microglia
****
Ab-/MG+
Ab+/MG+
E
30'
α1-GABA$_A$R-mAb*
360'
microglia
30'
hNR1-mAb#
Ab+/MG-
Ab+/MG+
MAP2
20 µm
α1-GABA$_A$R-mAb*
hNR1-mAb#
F
α1-GABA$_A$R-mAb* puncta per 100µm of dendrite
****
Ab+/MG-
Ab+/MG+
G
hNR1-mAb# puncta per 100µm of dendrite
Ab+/MG-
Ab+/MG+
H
30'
hNR1-mAb*
360'
microglia
30'
α1-GABA$_A$R-mAb#
Ab+/MG-
Ab+/MG+
MAP2
20 µm
hNR1-mAb*
α1-GABA$_A$R-mAb#
I
hNR1-mAb* puncta per 100µm of dendrite
****
Ab+/MG-
Ab+/MG+
J
α1-GABA$_A$R-mAb# puncta per 100µm of dendrite
Ab+/MG-
Ab+/MG+

Figure 12| Microglia specifically remove autoantibody-bound neuronal receptors. (A) Images of neurons stained for MAP2 with bound α1-GABA$_A$R-mAb* along dendrites in presence and absence of microglia after 6 hr. Images represented in greyscale. ROI Scale bar = 5 μm. (B) Number of α1-GABA$_A$R-mAb* puncta per unit length of dendrite was significantly reduced in presence of microglia. (C) CD11b positive microglial cells after co-culture with neurons in presence or absence of α1-GABA$_A$R-mAb*. Images represented in greyscale. (D) α1-GABA$_A$R-mAb* fluorescence was significantly higher inside microglial cell body. Each data point represents an ROI (C) (n = 73-77 ROIs per group) and a microglia cell (D) (n = 35 cells per group) from three independent experiments. Data points represented as mean ± SEM. Unpaired t-test with Welch correction for unequal variances was used to determine statistical significance (****$p < .0001$). (E) Hippocampal neurons stained for MAP2 (grey) with bound pre-labeled α1-GABA$_A$R-mAb* (Alexa 647) (grey) with or without microglia addition for 6 hr followed by pre-labeled hNR1-mAb$^{\#}$ (Alexa 594) (magenta) for 30 mins to acutely NMDARs. ROI Scale bar = 5 μm. (F) and (G) Quantification of number of α1-GABA$_A$R-mAb* and hNR1-mAb$^{\#}$ puncta along dendrites, respectively. The number was significantly reduced only for α1-GABA$_A$R-mAb* in presence of microglia while no such changes was seen for hNR1-mAb$^{\#}$ number along dendrites. (H) MAP2 positive (grey) hippocampal neurons with bound pre-labeled hNR1-mAb* (Alexa 647) (grey) with or without microglia addition for 6 hr followed by pre-labeled α1-GABA$_A$R-mAb$^{\#}$ (Alexa 594) (magenta) for 30 mins to acutely label α1-GABA$_A$Rs. ROI Scale bar = 5 μm. (I) and (J) Quantification of number of hNR1-mAb* and α1-GABA$_A$R-mAb$^{\#}$ puncta along dendrites, respectively. The number was significantly reduced only for hNR1-mAb* in presence of microglia, while no such changes was seen for α1-GABA$_A$R-mAb$^{\#}$ number along dendrites. Each data point represents an ROI from three independent experiments (n = 78-94 ROIs per group). Data points represented as mean ± SEM. Unpaired t-test with Welch correction for unequal variances was used to determine statistical significance (****$p < .0001$). Figure taken from figure 9 (Rahman et al., 2023).

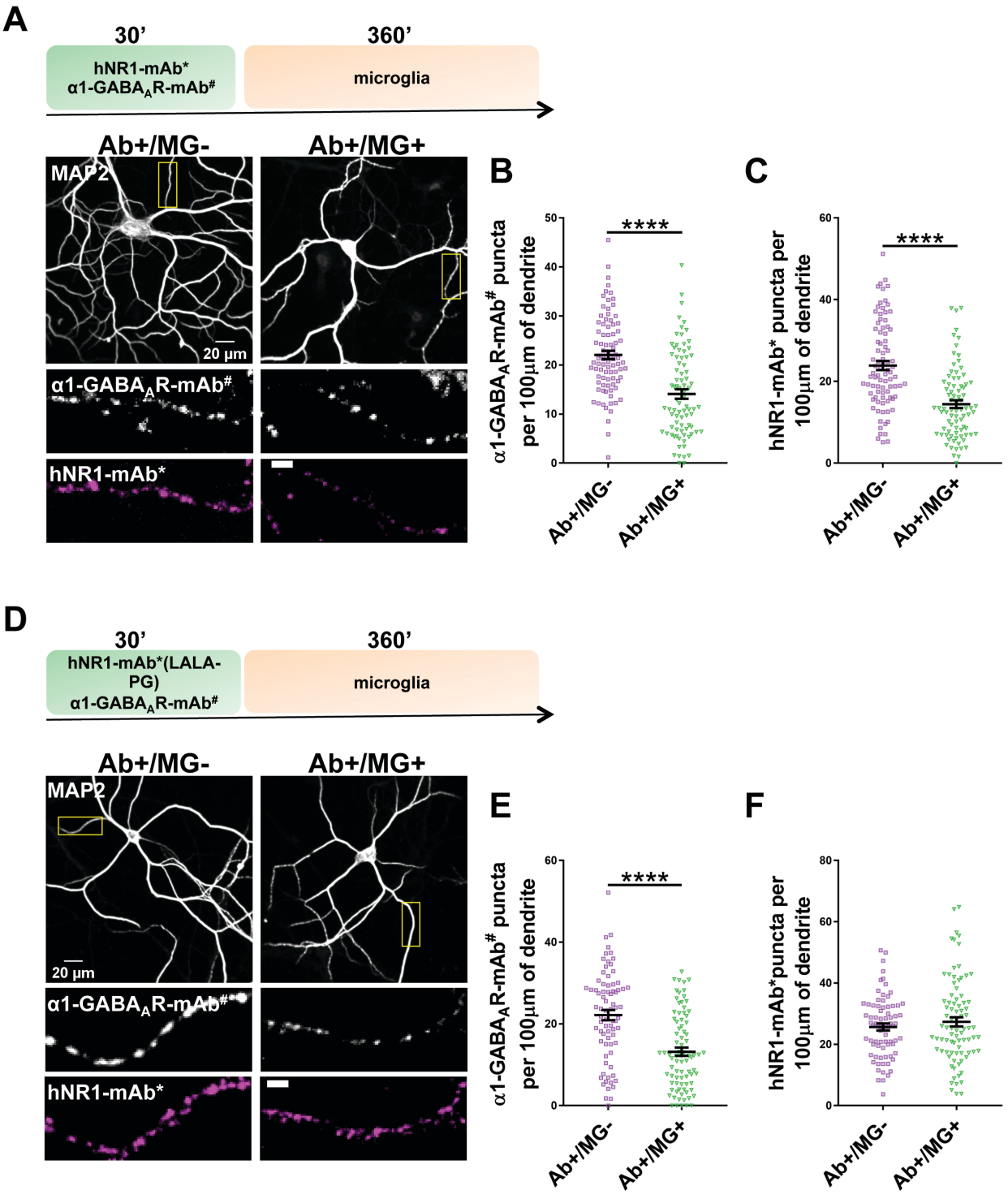

Figure 13| Microglia can selectively remove autoantibody-bound receptors with intact complement and FcγR interactions and not LALA-PG mutant. (A) Representative images of neuronal cells stained for MAP2 (grey) with α1-GABA$_A$R-mAb# (Alexa 594) (grey) and hNR1-mAb* (Alexa 647) (magenta) both bound to α1-GABA$_A$Rs and NMDARs respectively with or without microglia addition for 6 hr. ROI Scale bar = 5 µm. (B) and (C) Number of both α1-GABA$_A$R-mAb# and hNR1-mAb* puncta per unit length of dendrite

respectively, was reduced significantly in presence of microglia. (D) Representative images of MAP2 positive (grey) neuronal cells with α1-GABA$_A$R-mAb$^{\#}$ (Alexa 594) (grey) and LALA-PG hNR1-mAb* mutant (Alexa 647) (magenta) both bound to α1-GABA$_A$Rs and NMDARs respectively with or without microglia addition for 6 hr. ROI Scale bar = 5 µm. (E) Quantification of α1-GABA$_A$R-mAb$^{\#}$ along dendritic segments revealed a significant reduction in the α1-GABA$_A$R-mAb$^{\#}$-bound α1-GABA$_A$Rs after 6 hr in presence of microglia. (F) Number of LALA-PG hNR1-mAb* puncta per unit length of dendrite remained similar in presence or absence of microglia for 6 hr. Each data point represents an ROI from three independent experiments (n = 77-87 ROIs per group). Data points represented as mean ± SEM. Unpaired t-test with Welch correction for unequal variances was used to determine statistical significance (****$p < .0001$). Figure taken from figure 10 (Rahman et al., 2023).

4. Discussion

4.1 Central hypothesis

The role of different immune cells including microglia, peripheral and resident macrophages, T cells and B cells within the CNS are being increasing appreciated. Microglia, resident immune cells of CNS, have been suggested to play vital roles in the healthy brain and various neurodegenerative diseases. For example, microglia via the complement system have been shown to mediate the pruning of synapses during development (Paolicelli et al., 2011; Schafer et al., 2012; Stevens et al., 2007), as well as for aberrant synapse loss in mouse models of Alzheimer's disease (AD) (Hong et al., 2016). This microglia-mediated removal of cellular components has also been studied in a variety of neurodegenerative diseases like AD, Parkinson's Disease (PD), Huntington's as well as different Experimental Animal Encephalitis (EAE) models.

Mechanistically, autoantibodies involved in different forms of autoimmune encephalitis employ different strategies to remove/affect receptors function, including receptor internalization by anti-NMDAR antibodies (Moscato et al., 2014), blocking receptor function with GAB_AAR antibodies (van Casteren et al., 2022) as well as the downstream activation of complement by AQP4 antibodies (Soltys et al., 2019). Recent studies have also reported microglia activation, synapse loss and behavioural deficits in maternal transfer models of both anti-NMDAR (García-Serra et al., 2021) and CASPR2 (Coutinho et al., 2017) encephalitis. These studies however did not explore a direct relationship between these antibodies and microglia and more specifically the contribution of Fc region dependent mechanisms in autoantibody-mediated autoimmune encephalitis, a central hypothesis of this thesis.

4.2 Results and Interpretation

To directly test the central hypothesis that microglia play an active role in the clearance of autoantibody receptor complexes, we established an *in-vitro* co-culture model, wherein primary mouse hippocampal neurons and microglia were cultured in the presence or absence of patient derived auto-antibodies in a temporally controlled manner. In the presence of microglia, we observed a significant reduction in the number of both hNR1-mAb

and NMDAR/hNR1-mAb complexes after 6 hr of co-culture with microglia (Figure 5, 6). These complexes were subsequently shown to appear within endo-lysosomal compartments inside microglia (Figure 2, 3). Such a reduction in hNR1-mAb-bound NMDARs was not observed in the absence of microglia 1, 3, and 6 hr after autoantibody addition (Figure 1). However, previous experiments on time course of internalization had revealed a decrease (~25%) in NMDAR clusters 4 hr after autoantibody addition to hippocampal neurons (Moscato et al., 2014). This decrease, though statistically non-significant, could be due to differences in experimental strategies between the two studies namely use of whole patient CSF with other autoantibodies and factors and absence of a washout step after CSF addition. Nevertheless, it seems reasonable to conclude that both mechanisms contribute to NMDA removal from the cell surface. Importantly, this microglia-mediated removal of autoantibody-bound receptors was found to be specific for hNR1-mAb-NMDARs complexes, as no changes were observed in the number of $GABA_AR$ puncta/unit length of dendrite (Figure 12 H-J). Similarly, using a second patient derived antibody against $GABA_ARs$ (α1-$GABA_AR$-mAb), we observed a microglia dependent loss of $GABA_AR$ puncta without affecting the number of hNR1-mAb puncta/unit length of dendrite (Figure 12 E-G). These results point towards a direct role of microglia engagement in patients with autoimmune encephalitis and a specific removal of autoantibody-bound neuronal receptors by microglia.

Pathogenic autoantibodies in different autoimmune disorders have been shown to be associated with inflammation, e.g., the recruitment of other immune cells and the upregulation of pro-inflammatory cytokines. For example, autoantibodies in Rheumatoid Arthritis (RA) were reported to increase production of TNFα that mediates inflammation of joint and tissues (Burbelo, Iadarola, Keller, & Warner, 2021). Within CNS, AQP4 autoantibodies have been shown to cause the production of IL6 upon binding to astrocytic FcRs (Hinson et al., 2017). Exploring this issue in our co-culture model, we observed an increase in the levels of the pro-inflammatory cytokines, TNFα and IL6, in the presence of autoantibodies and microglia for 6 hr (Figure 4 A, B). Interestingly, unlike TNFα, the levels of IL6 were found to be specific to microglial responses to the presence of hNR1-mAb, as the increase was significantly higher only in Ab+/MG+ experimental group after 6 hr. No changes were seen in the levels of IL1β and anti-inflammatory cytokines like IL10 and IL4 (Figure 4 C-E). Intriguingly, previous studies have highlighted an important role of IL6

in the differentiation and maturation of plasma B cells (Eto et al., 2011; Maeda, Mehta, Drevets, & Coggeshall, 2010). Together, these studies and related observations point towards a potential role of IL6 in autoantibody-mediated autoimmune encephalitis perhaps in promoting the maintenance and differentiation B cell into antibody producing plasma B cells as well as their infiltration into the CNS, allowing a sustained autoantibody production that exacerbates a patient's disease pathology.

Antibodies-bound antigens have been shown to trigger inflammation via their Fc region by directly binding to Fc receptors on myeloid and antigen presenting cells (APCs). For instance, Myelin Oligodendrocyte Glycoprotein (MOG) autoantibodies promote the uptake and presentation of MOG via FcγR binding on APCs (Flach et al., 2016; Kinzel et al., 2016). Another possible mechanism, is the activation of complement system and the deposition of C1q, C3 and others at binding sites of antibodies via their Fc region like in presence of AQP4 autoantibodies (Lucchinetti et al., 2014). Such a complement activation, can lead to cell death as seen with AQP4 autoantibodies (Papadopoulos & Verkman, 2012; Soltys et al., 2019) or engage myeloid cells mediating pro-inflammatory cytokine response following the activation of complement receptors (Lucchinetti et al., 2014). Microglia along with resident and infiltrating macrophagic cells express both FcγRs and complement receptors. Autoantibodies isolated from the serum of patients with NMDARE belong to the IgM, IgA and different subtypes of IgG, with IgG1 being the most prominent (Tüzün et al., 2009). Interestingly, certain subtypes of IgGs bind complement and FcγRs more effectively, like IgG1 and IgG3, among others (Dekkers et al., 2017; Wang, Mathieu, & Brezski, 2018). Both hNR1-mAb and α1-$GABA_A$R-mAb used in this study belongs to the IgG1 subtype. hNR1-mAb was seen to bind strongly to purified FcγR1 and C1q proteins in binding assays *in-vitro* (Figure 7 C, D). Previously studies have identified mutations in the Fc region of IgG1 antibodies to either selectively prevent FcγR (LALA mutant) or complement binding (PA mutant) or both (LALA-PG mutant). Interestingly, all three sets of mutants introduced into the hNR1-mAb were found to dampen both C1q and FcγR1 binding, with minimal specificity, though the LALA-PG was more robust (Figure 7 C, D). This is possibly due to an overlap in the FcγRs and complement receptor binding sites on the Fc region of IgG1 (Vidarsson, Dekkers, & Rispens, 2014). Nonetheless, it was possible for us to use the LALA-PG mutations to block downstream interactions and signalling by these antibodies, preventing the microglia-mediated removal of hNR1-mAb

puncta along dendrites. These data support our conclusion that microglia engagement of antibody/receptor complexes plays a critical role in removal of these receptors (Figure 8).

Microglia mediate the removal of synaptic components during development and in different disorders (Hong et al., 2016; Lawrence & Rosa, 2018; Schafer et al., 2012). Synapse stripping by microglia has been shown to be context dependent, as pre-synapse stripping by microglia was observed during development (Schafer et al., 2012) while mostly post-synapse engulfment was observed in animal models of AD (Hong et al., 2016) and PD (Pérez-Acuña, Shin, Rhee, Kim, & Lee, 2023). In contrast, microglia-mediated removal of both pre-and post-synaptic components was reported upon motor learning in the cerebellum of mice (Morizawa et al., 2022). Maternal transfer studies with anti-NR1 autoantibody also reported a decrease in overall synapse number and microglial activation (García-Serra et al., 2021). Quantifying synapse number in our co-culture setup with hNR1-mAb, using vGLUT1 and PSD95 as pre- and post-synapse marker, revealed a significant decrease in synapse number (vGLUT1+/PSD95+) (Figure 9). Surprisingly, this decrease most directly affected the post-synaptic proteins PSD95 and Homer1, without appreciably changing pre-synaptic proteins including vGLUT1, Synapsin and Synaptophysin (Figure 9, 10). Studies done on oligomeric Abeta (o-Aβ) have shown that o-Aβ specifically binds to post-synapses via NMDARs (Koffie et al., 2009; Lacor et al., 2004). Such a post-synaptic o-Aβ localization was shown to trigger microglia-mediated loss of post-synapses specifically (Hong et al., 2016). These data support our observations that WT hNR1-mAb-bound to NMDARs, that are primarily post-synaptic (Ehlers, Tingley, & Huganir, 1995; Zhang, Peterson, & Liu, 2013), also tags the post-synaptic compartment and/or NMDAR macromolecular complexes for microglia-mediated removal. Interestingly, such a reduction in synapse and post-synaptic markers was not observed when LALA-PG hNR1-mAb mutant was used in our co-culture experiments (Figure 9). This further supports the idea that FcγRs and complement binding mediate autoantibody driven losses of neuronal receptors and synapses by microglia (Figure 14) and ultimately in patients with autoimmune encephalitis. An unresolved issue is how mechanistically microglia work to remove synapses/receptors. A general tagging of the pre/post compartments by complement could promote engulfment of entire synapses. Presumably antibody tagging could be yet more selective e.g. only removing receptors signalling complexes. If this was to occur in the context of receptors embedded in the PSD, e.g. like NMDARs, then non-selective removal

of both pre-/post-synaptic compartments needs to be considered. Alternatively, autoantibody mediated displacement of such receptor complex into the peri-/extra-synaptic space would allow their removal from synapses without initially affecting synapse integrity. Given that trans-synaptic signalling is key to synapse stability and integrity, the stripping of subsets of component could also lead to the selective loss of synaptic sub-compartments, e.g. the PSD as seen with the NMDAR autoantibodies.

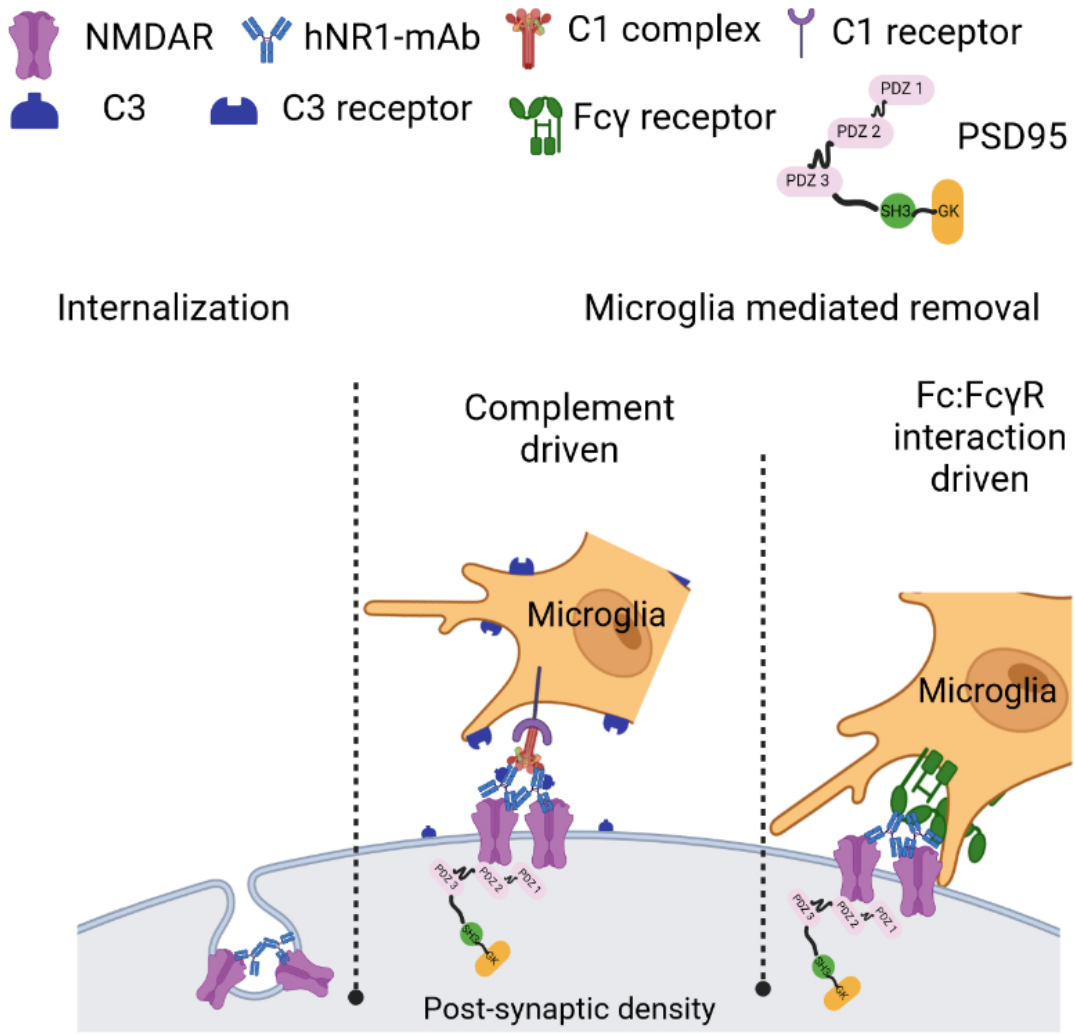

Figure 14| Proposed mechanism of action of microglia-mediated removal of hNR1-mAb-bound NMDARs with intact downstream complement and FcγR binding. hNR1-mAb bound to NMDARs, in addition to driving internalization of the bound surface NMDARs via clustering mediated by their Fc regions, can engage microglia triggering them to remove antibody bound NMDARs. Such an engagement involves deposition of complement proteins that have corresponding complement receptors on microglial surface and/or a direct interaction of hNR1-mAb Fc region and microglial FcγRs. Figure taken from Table of Content Image (TOCI) (Rahman et al., 2023).

4.3 Strengths and weaknesses of the study(s)

This work highlights new roles of microglia in autoimmune encephalitis of CNS. In addition to previously studied pathogenic antibody driven mechanism, this thesis sheds light on the role of immune cells specifically microglia not only in the removal of receptors and synapses, but also the induction in downstream inflammatory response that could facilitate disease progression. One obvious limitation of this study is that it utilises *in-vitro* co-culture system, which cannot completely recapitulate *in-vivo* physiological conditions. Thus, it would be prudent to replicate these observations in *in-vivo* models of autoimmune disorders. In addition, the lack of specificity of the LALA and PA hNR1-mAb mutants to selectively block FcγR or complement binding, respectively, precluded our ability to distinguish between the relative contribution of FcγR or complement receptors in the microglia-mediated removal of NMDARs. More specific mutations and/or the use of receptor loss of function strategies will be needed to clarify this important issue. Additionally, it remains unclear whether microglia selectively remove extra-synaptic antibody-tagged receptor/post-synaptic protein complexes or whether they can also access proteins within the synaptic cleft, thus directly removing whole post-synaptic density (PSD). Further work needs to be done to answer these questions in better *in-vivo* models of autoimmune encephalitis.

4.4 Implications for practice and/or future research

This study is the first to report a direct involvement of microglia in the removal of autoantibody-bound neuronal receptors. Since such a removal was found to depend on Fc region driven interactions with FcγR or complement receptors, implying all pathogenic autoantibodies that engage these downstream effectors (e.g., IgG1 and IgG3 subtypes) could trigger a similar microglia response. Hence, the engagement of microglia could be a potential common mechanism across different autoantibody mediated autoimmune encephalitis of CNS, making it an attractive therapeutic target.

Exciting unanswered questions in this field include how different immune cells communicate with each other in orchestrating the immune response within the CNS? How this triggers the infiltration of peripheral cells? Whether microglia are key mediators in this process and what signals to they respond to and send? Equally important is what role

microglia play during later stages of disease pathology when peripheral cells reach CNS? One answer could be linked to the role of pro-inflammatory cytokines in such disorders. Further work is required to understand the role of secreted pro-inflammatory cytokines like IL6, TNFα and IL17 in mediating infiltration of peripheral and brain border associated T cells and B cells causing a clinically relevant inflammatory response. This study along with others point towards IL6 being an important mediator of inflammation in such disorders. The role of IL6 in the differentiation of B cells into autoantibody producing plasma cells locally within the CNS also needs to be explored in the context of autoimmune encephalitis. Interestingly, tocilizumab, a humanized monoclonal antibody against soluble and membrane-bound IL6 receptor, was shown to improve clinical response in NMDARE patients initially refractive to the conventional anti-CD20 (rituximab) treatment (W. J. Lee et al., 2016). However, tocilizumab treatment was also associated with tumor development as a potential side-effect in 10% of patient's post-treatment (W. J. Lee et al., 2016). Thus, improved anti-IL6 therapies could be a viable complement or alternative to the existing immune dampening treatment options like B cell elimination by rituximab or plasmapheresis, immunosuppressants etc.

5. Conclusions

The data presented here argues for a potential active involvement of microglia in the pathology of NMDARE. The reported mechanism of removal of autoantibody-tagged NMDARs by microglia adds to the previously reported and well-studied concept of internalization driven loss of NMDARs in such disorders contributing to disease outcome (Hughes et al., 2010; Moscato et al., 2014). This microglia-mediated removal of bound neuronal receptors and synaptic components could be a common mechanism in many autoimmune encephalitis, wherein the pathogenic autoantibodies are of subtypes capable of binding to FcRs and complement proteins like IgG1 and IgG3. This study paves the way for future work in trying to understand the role of microglia and other cells of the innate and adaptive immune system like macrophages, T cells and B cells within CNS in these disorders. Understanding the biology of immune involvement in these disorders has great potential in developing innovative therapies that alleviates disease outcomes, without leading to massive suppression of the immune system reducing the chances of comorbidities and relapses.

Taken together, this thesis is an important first step in understanding the role of microglia in autoimmune encephalitis of CNS. Studies in different *in-vivo* models and autopsied tissues could further unravel the involved mechanisms and strengthen the concept of innate immune system involvement in such disorders. This in turn can provide new therapeutic targets to augment and/or improve currently used treatment options for patients with autoimmune encephalitis.

Reference list

Andrzejak, E., Rabinovitch, E., Kreye, J., Prüss, H., Rosenmund, C., Ziv, N. E., Garner, C. C., & Ackermann, F. (2022). Patient-derived anti-NMDAR antibody disinhibits cortical neuronal networks through dysfunction of inhibitory neuron output. *J Neurosci*. doi:10.1523/JNEUROSCI.1689-21.2022

Ben Achour, S., & Pascual, O. (2010). Glia: The many ways to modulate synaptic plasticity. *Neurochemistry International, 57*(4), 440-445. doi:https://doi.org/10.1016/j.neuint.2010.02.013

Bien, C. G., Vincent, A., Barnett, M. H., Becker, A. J., Blümcke, I., Graus, F., Jellinger, K. A., Reuss, D. E., Ribalta, T., Schlegel, J., Sutton, I., Lassmann, H., & Bauer, J. (2012). Immunopathology of autoantibody-associated encephalitides: clues for pathogenesis. *Brain, 135*(5), 1622-1638. doi:10.1093/brain/aws082

Burbelo, P. D., Iadarola, M. J., Keller, J. M., & Warner, B. M. (2021). Autoantibodies Targeting Intracellular and Extracellular Proteins in Autoimmunity. *Front Immunol, 12*, 548469. doi:10.3389/fimmu.2021.548469

Coutinho, E., Menassa, D. A., Jacobson, L., West, S. J., Domingos, J., Moloney, T. C., Lang, B., Harrison, P. J., Bennett, D. L. H., Bannerman, D., & Vincent, A. (2017). Persistent microglial activation and synaptic loss with behavioral abnormalities in mouse offspring exposed to CASPR2-antibodies in utero. *Acta Neuropathol, 134*(4), 567-583. doi:10.1007/s00401-017-1751-5

Dalmau, J., Gleichman, A. J., Hughes, E. G., Rossi, J. E., Peng, X., Lai, M., Dessain, S. K., Rosenfeld, M. R., Balice-Gordon, R., & Lynch, D. R. (2008). Anti-NMDA-receptor encephalitis: case series and analysis of the effects of antibodies. *The Lancet Neurology, 7*(12), 1091-1098. doi:https://doi.org/10.1016/S1474-4422(08)70224-2

Dalmau, J., Tüzün, E., Wu, H.-y., Masjuan, J., Rossi, J. E., Voloschin, A., Baehring, J. M., Shimazaki, H., Koide, R., King, D., Mason, W., Sansing, L. H., Dichter, M. A., Rosenfeld, M. R., & Lynch, D. R. (2007). Paraneoplastic anti–N-methyl-D-aspartate receptor encephalitis associated with ovarian teratoma. *Annals of Neurology, 61*(1), 25-36. doi:https://doi.org/10.1002/ana.21050

Dekkers, G., Bentlage, A. E. H., Stegmann, T. C., Howie, H. L., Lissenberg-Thunnissen, S., Zimring, J., Rispens, T., & Vidarsson, G. (2017). Affinity of human IgG subclasses to mouse Fc gamma receptors. *MAbs, 9*(5), 767-773. doi:10.1080/19420862.2017.1323159

Ehlers, M. D., Tingley, W. G., & Huganir, R. L. (1995). Regulated Subcellular Distribution of the NR1 Subunit of the NMDA Receptor. *Science, 269*(5231), 1734-1737. doi:doi:10.1126/science.7569904

Eto, D., Lao, C., DiToro, D., Barnett, B., Escobar, T. C., Kageyama, R., Yusuf, I., & Crotty, S. (2011). IL-21 and IL-6 Are Critical for Different Aspects of B Cell Immunity and Redundantly Induce Optimal Follicular Helper CD4 T Cell (Tfh) Differentiation. *PLOS ONE, 6*(3), e17739. doi:10.1371/journal.pone.0017739

Flach, A.-C., Litke, T., Strauss, J., Haberl, M., Gómez, C. C., Reindl, M., Saiz, A., Fehling, H.-J., Wienands, J., Odoardi, F., Lühder, F., & Flügel, A. (2016). Autoantibody-boosted T-cell reactivation in the target organ triggers manifestation of autoimmune CNS disease. *Proceedings of the National Academy of Sciences, 113*(12), 3323-3328. doi:doi:10.1073/pnas.1519608113

García-Serra, A., Radosevic, M., Pupak, A., Brito, V., Ríos, J., Aguilar, E., Maudes, E., Ariño, H., Spatola, M., Mannara, F., Pedreño, M., Joubert, B., Ginés, S.,

Planagumà, J., & Dalmau, J. (2021). Placental transfer of NMDAR antibodies causes reversible alterations in mice. *Neurology - Neuroimmunology Neuroinflammation, 8*(1), e915. doi:10.1212/nxi.0000000000000915

Heneka, M. T., Kummer, M. P., Stutz, A., Delekate, A., Schwartz, S., Vieira-Saecker, A., Griep, A., Axt, D., Remus, A., Tzeng, T.-C., Gelpi, E., Halle, A., Korte, M., Latz, E., & Golenbock, D. T. (2013). NLRP3 is activated in Alzheimer's disease and contributes to pathology in APP/PS1 mice. *Nature, 493*(7434), 674-678. doi:10.1038/nature11729

Hinson, S. R., Clift, I. C., Luo, N., Kryzer, T. J., & Lennon, V. A. (2017). Autoantibody-induced internalization of CNS AQP4 water channel and EAAT2 glutamate transporter requires astrocytic Fc receptor. *Proc Natl Acad Sci U S A, 114*(21), 5491-5496. doi:10.1073/pnas.1701960114

10.1073/pnas.1701960114. Epub 2017 May 1.

Hong, S., Beja-Glasser, V. F., Nfonoyim, B. M., Frouin, A., Li, S., Ramakrishnan, S., Merry, K. M., Shi, Q., Rosenthal, A., Barres, B. A., Lemere, C. A., Selkoe, D. J., & Stevens, B. (2016). Complement and microglia mediate early synapse loss in Alzheimer mouse models. *Science, 352*(6286), 712-716. doi:doi:10.1126/science.aad8373

Hughes, E. G., Peng, X., Gleichman, A. J., Lai, M., Zhou, L., Tsou, R., Parsons, T. D., Lynch, D. R., Dalmau, J., & Balice-Gordon, R. J. (2010). Cellular and synaptic mechanisms of anti-NMDA receptor encephalitis. *J Neurosci, 30*(17), 5866-5875. doi:10.1523/JNEUROSCI.0167-10.2010

Jézéquel, J., Johansson, E. M., Dupuis, J. P., Rogemond, V., Gréa, H., Kellermayer, B., Hamdani, N., Le Guen, E., Rabu, C., Lepleux, M., Spatola, M., Mathias, E., Bouchet, D., Ramsey, A. J., Yolken, R. H., Tamouza, R., Dalmau, J., Honnorat, J., Leboyer, M., & Groc, L. (2017). Dynamic disorganization of synaptic NMDA receptors triggered by autoantibodies from psychotic patients. *Nature Communications, 8*(1), 1791. doi:10.1038/s41467-017-01700-3

Kamma, E., Lasisi, W., Libner, C., Ng, H. S., & Plemel, J. R. (2022). Central nervous system macrophages in progressive multiple sclerosis: relationship to neurodegeneration and therapeutics. *J Neuroinflammation, 19*(1), 45. doi:10.1186/s12974-022-02408-y

Kinzel, S., Lehmann-Horn, K., Torke, S., Häusler, D., Winkler, A., Stadelmann, C., Payne, N., Feldmann, L., Saiz, A., Reindl, M., Lalive, P. H., Bernard, C. C., Brück, W., & Weber, M. S. (2016). Myelin-reactive antibodies initiate T cell-mediated CNS autoimmune disease by opsonization of endogenous antigen. *Acta Neuropathologica, 132*(1), 43-58. doi:10.1007/s00401-016-1559-8

Koffie, R. M., Meyer-Luehmann, M., Hashimoto, T., Adams, K. W., Mielke, M. L., Garcia-Alloza, M., Micheva, K. D., Smith, S. J., Kim, M. L., Lee, V. M., Hyman, B. T., & Spires-Jones, T. L. (2009). Oligomeric amyloid β associates with postsynaptic densities and correlates with excitatory synapse loss near senile plaques. *Proceedings of the National Academy of Sciences, 106*(10), 4012-4017. doi:doi:10.1073/pnas.0811698106

Kreye, J., Wenke, N. K., Chayka, M., Leubner, J., Murugan, R., Maier, N., Jurek, B., Ly, L. T., Brandl, D., Rost, B. R., Stumpf, A., Schulz, P., Radbruch, H., Hauser, A. E., Pache, F., Meisel, A., Harms, L., Paul, F., Dirnagl, U., Garner, C., Schmitz, D., Wardemann, H., & Prüss, H. (2016). Human cerebrospinal fluid monoclonal N-methyl-D-aspartate receptor autoantibodies are sufficient for encephalitis pathogenesis. *Brain, 139*(Pt 10), 2641-2652. doi:10.1093/brain/aww208

Lacor, P. N., Buniel, M. C., Chang, L., Fernandez, S. J., Gong, Y., Viola, K. L., Lambert, M. P., Velasco, P. T., Bigio, E. H., Finch, C. E., Krafft, G. A., & Klein, W. L. (2004). Synaptic Targeting by Alzheimer's-Related Amyloid β Oligomers. *The Journal of Neuroscience, 24*(45), 10191-10200. doi:10.1523/jneurosci.3432-04.2004

Lawrence, R., & Rosa, C. P. (2018). Microglia-Mediated Synapse Loss in Alzheimer's Disease. *The Journal of Neuroscience, 38*(12), 2911. doi:10.1523/JNEUROSCI.1136-17.2017

Lee, S. H., Le Pichon, C. E., Adolfsson, O., Gafner, V., Pihlgren, M., Lin, H., Solanoy, H., Brendza, R., Ngu, H., Foreman, O., Chan, R., Ernst, J. A., DiCara, D., Hotzel, I., Srinivasan, K., Hansen, D. V., Atwal, J., Lu, Y., Bumbaca, D., Pfeifer, A., Watts, R. J., Muhs, A., Scearce-Levie, K., & Ayalon, G. (2016). Antibody-Mediated Targeting of Tau In Vivo Does Not Require Effector Function and Microglial Engagement. *Cell Rep, 16*(6), 1690-1700. doi:10.1016/j.celrep.2016.06.099

Lee, W. J., Lee, S. T., Moon, J., Sunwoo, J. S., Byun, J. I., Lim, J. A., Kim, T. J., Shin, Y. W., Lee, K. J., Jun, J. S., Lee, H. S., Kim, S., Park, K. I., Jung, K. H., Jung, K. Y., Kim, M., Lee, S. K., & Chu, K. (2016). Tocilizumab in Autoimmune Encephalitis Refractory to Rituximab: An Institutional Cohort Study. *Neurotherapeutics, 13*(4), 824-832. doi:10.1007/s13311-016-0442-6

Lo, M., Kim, H. S., Tong, R. K., Bainbridge, T. W., Vernes, J. M., Zhang, Y., Lin, Y. L., Chung, S., Dennis, M. S., Zuchero, Y. J., Watts, R. J., Couch, J. A., Meng, Y. G., Atwal, J. K., Brezski, R. J., Spiess, C., & Ernst, J. A. (2017). Effector-attenuating Substitutions That Maintain Antibody Stability and Reduce Toxicity in Mice. *J Biol Chem, 292*(9), 3900-3908. doi:10.1074/jbc.M116.767749

Locatelli, G., Theodorou, D., Kendirli, A., Jordão, M. J. C., Staszewski, O., Phulphagar, K., Cantuti-Castelvetri, L., Dagkalis, A., Bessis, A., Simons, M., Meissner, F., Prinz, M., & Kerschensteiner, M. (2018). Mononuclear phagocytes locally specify and adapt their phenotype in a multiple sclerosis model. *Nat Neurosci, 21*(9), 1196-1208. doi:10.1038/s41593-018-0212-3

Lucchinetti, C. F., Guo, Y., Popescu, B. F. G., Fujihara, K., Itoyama, Y., & Misu, T. (2014). The Pathology of an Autoimmune Astrocytopathy: Lessons Learned from Neuromyelitis Optica. *Brain Pathology, 24*(1), 83-97. doi:https://doi.org/10.1111/bpa.12099

Maeda, K., Mehta, H., Drevets, D. A., & Coggeshall, K. M. (2010). IL-6 increases B-cell IgG production in a feed-forward proinflammatory mechanism to skew hematopoiesis and elevate myeloid production. *Blood, 115*(23), 4699-4706. doi:10.1182/blood-2009-07-230631

Malhotra, S., Costa, C., Eixarch, H., Keller, C. W., Amman, L., Martínez-Banaclocha, H., Midaglia, L., Sarró, E., Machín-Díaz, I., Villar, L. M., Triviño, J. C., Oliver-Martos, B., Parladé, L. N., Calvo-Barreiro, L., Matesanz, F., Vandenbroeck, K., Urcelay, E., Martínez-Ginés, M.-L., Tejeda-Velarde, A., Fissolo, N., Castilló, J., Sanchez, A., Robertson, A. A. B., Clemente, D., Prinz, M., Pelegrin, P., Lünemann, J. D., Espejo, C., Montalban, X., & Comabella, M. (2020). NLRP3 inflammasome as prognostic factor and therapeutic target in primary progressive multiple sclerosis patients. *Brain, 143*(5), 1414-1430. doi:10.1093/brain/awaa084

Monje, M. L., Toda, H., & Palmer, T. D. (2003). Inflammatory Blockade Restores Adult Hippocampal Neurogenesis. *Science, 302*(5651), 1760-1765. doi:doi:10.1126/science.1088417

Morizawa, Y. M., Matsumoto, M., Nakashima, Y., Endo, N., Aida, T., Ishikane, H., Beppu, K., Moritoh, S., Inada, H., Osumi, N., Shigetomi, E., Koizumi, S., Yang, G., Hirai, H., Tanaka, K., Tanaka, K. F., Ohno, N., Fukazawa, Y., & Matsui, K. (2022).

Synaptic pruning through glial synapse engulfment upon motor learning. *Nat Neurosci, 25*(11), 1458-1469. doi:10.1038/s41593-022-01184-5

Moscato, E. H., Peng, X., Jain, A., Parsons, T. D., Dalmau, J., & Balice-Gordon, R. J. (2014). Acute mechanisms underlying antibody effects in anti-N-methyl-D-aspartate receptor encephalitis. *Ann Neurol, 76*(1), 108-119. doi:10.1002/ana.24195

Paolicelli, R. C., Bolasco, G., Pagani, F., Maggi, L., Scianni, M., Panzanelli, P., Giustetto, M., Ferreira, T. A., Guiducci, E., Dumas, L., Ragozzino, D., & Gross, C. T. (2011). Synaptic Pruning by Microglia Is Necessary for Normal Brain Development. *Science, 333*(6048), 1456-1458. doi:doi:10.1126/science.1202529

Papadopoulos, M. C., & Verkman, A. S. (2012). Aquaporin 4 and neuromyelitis optica. *The Lancet Neurology, 11*(6), 535-544. doi:https://doi.org/10.1016/S1474-4422(12)70133-3

Pérez-Acuña, D., Shin, S. J., Rhee, K. H., Kim, S. J., & Lee, S.-J. (2023). α-Synuclein propagation leads to synaptic abnormalities in the cortex through microglial synapse phagocytosis. *Molecular Brain, 16*(1), 72. doi:10.1186/s13041-023-01059-1

Pike, A. F., Longhena, F., Faustini, G., van Eik, J.-M., Gombert, I., Herrebout, M. A. C., Fayed, M. M. H. E., Sandre, M., Varanita, T., Teunissen, C. E., Hoozemans, J. J. M., Bellucci, A., Veerhuis, R., & Bubacco, L. (2022). Dopamine signaling modulates microglial NLRP3 inflammasome activation: implications for Parkinson's disease. *Journal of Neuroinflammation, 19*(1), 50. doi:10.1186/s12974-022-02410-4

Pozzo, E. D., Tremolanti, C., Costa, B., Giacomelli, C., Milenkovic, V. M., Bader, S., Wetzel, C. H., Rupprecht, R., Taliani, S., Settimo, F. D., & Martini, C. (2019). Microglial Pro-Inflammatory and Anti-Inflammatory Phenotypes Are Modulated by Translocator Protein Activation. *Int J Mol Sci, 20*(18). doi:10.3390/ijms20184467

Rahman, K. A., Orlando, M., Boulos, A., Andrzejak, E., Schmitz, D., Ziv, N. E., Prüss, H., Garner, C. C., & Ichkova, A. (2023). Microglia actively remove NR1 autoantibody-bound NMDA receptors and associated post-synaptic proteins in neuron microglia co-cultures. *Glia*. doi:10.1002/glia.24369

Saijo, K., & Glass, C. K. (2011). Microglial cell origin and phenotypes in health and disease. *Nat Rev Immunol, 11*(11), 775-787. doi:10.1038/nri3086

Saunders, K. O. (2019). Conceptual Approaches to Modulating Antibody Effector Functions and Circulation Half-Life. *Front Immunol, 10*, 1296. doi:10.3389/fimmu.2019.01296

Schafer, Dorothy P., Lehrman, Emily K., Kautzman, Amanda G., Koyama, R., Mardinly, Alan R., Yamasaki, R., Ransohoff, Richard M., Greenberg, Michael E., Barres, Ben A., & Stevens, B. (2012). Microglia Sculpt Postnatal Neural Circuits in an Activity and Complement-Dependent Manner. *Neuron, 74*(4), 691-705. doi:https://doi.org/10.1016/j.neuron.2012.03.026

Schlothauer, T., Herter, S., Koller, C. F., Grau-Richards, S., Steinhart, V., Spick, C., Kubbies, M., Klein, C., Umaña, P., & Mössner, E. (2016). Novel human IgG1 and IgG4 Fc-engineered antibodies with completely abolished immune effector functions. *Protein Eng Des Sel, 29*(10), 457-466. doi:10.1093/protein/gzw040

Sierra, A., Encinas, J. M., Deudero, J. J., Chancey, J. H., Enikolopov, G., Overstreet-Wadiche, L. S., Tsirka, S. E., & Maletic-Savatic, M. (2010). Microglia shape adult hippocampal neurogenesis through apoptosis-coupled phagocytosis. *Cell Stem Cell, 7*(4), 483-495. doi:10.1016/j.stem.2010.08.014

Smith, J. A., Das, A., Ray, S. K., & Banik, N. L. (2012). Role of pro-inflammatory cytokines released from microglia in neurodegenerative diseases. *Brain Res Bull, 87*(1), 10-20. doi:10.1016/j.brainresbull.2011.10.004

Soltys, J., Liu, Y., Ritchie, A., Wemlinger, S., Schaller, K., Schumann, H., Owens, G. P., & Bennett, J. L. (2019). Membrane assembly of aquaporin-4 autoantibodies regulates classical complement activation in neuromyelitis optica. *J Clin Invest, 129*(5), 2000-2013. doi:10.1172/jci122942

Stevens, B., Allen, N. J., Vazquez, L. E., Howell, G. R., Christopherson, K. S., Nouri, N., Micheva, K. D., Mehalow, A. K., Huberman, A. D., Stafford, B., Sher, A., Litke, Alan M., Lambris, J. D., Smith, S. J., John, S. W. M., & Barres, B. A. (2007). The Classical Complement Cascade Mediates CNS Synapse Elimination. *Cell, 131*(6), 1164-1178. doi:10.1016/j.cell.2007.10.036

Tremblay, M.-È., Stevens, B., Sierra, A., Wake, H., Bessis, A., & Nimmerjahn, A. (2011). The Role of Microglia in the Healthy Brain. *The Journal of Neuroscience, 31*(45), 16064-16069. doi:10.1523/jneurosci.4158-11.2011

Tüzün, E., Zhou, L., Baehring, J. M., Bannykh, S., Rosenfeld, M. R., & Dalmau, J. (2009). Evidence for antibody-mediated pathogenesis in anti-NMDAR encephalitis associated with ovarian teratoma. *Acta Neuropathologica, 118*(6), 737. doi:10.1007/s00401-009-0582-4

van Casteren, A. C. M., Ackermann, F., Rahman, K. A., Andrzejak, E., Rosenmund, C., Kreye, J., Prüss, H., Garner, C. C., & Ichkova, A. (2022). Differential Modes of Action of α1- and α1γ2-Autoantibodies Derived from Patients with GABA_AR Encephalitis. *eneuro, 9*(6), ENEURO.0369-0322.2022. doi:10.1523/eneuro.0369-22.2022

Vidarsson, G., Dekkers, G., & Rispens, T. (2014). IgG subclasses and allotypes: from structure to effector functions. *Front Immunol, 5*, 520. doi:10.3389/fimmu.2014.00520

Wang, X., Mathieu, M., & Brezski, R. J. (2018). IgG Fc engineering to modulate antibody effector functions. *Protein & Cell, 9*(1), 63-73. doi:10.1007/s13238-017-0473-8

Zhang, Z.-w., Peterson, M., & Liu, H. (2013). Essential role of postsynaptic NMDA receptors in developmental refinement of excitatory synapses. *Proceedings of the National Academy of Sciences, 110*(3), 1095-1100. doi:doi:10.1073/pnas.1212971110

Statutory Declaration

“I, Kazi Atikur Rahman, by personally signing this document in lieu of an oath, hereby affirm that I prepared the submitted dissertation on the topic **Role of microglia in removal of autoantibody-bound NMDA receptors and post-synaptic proteins, Rolle der Mikroglia bei der Entfernung von an Autoantikörper gebundenen NMDA-Rezeptoren und postsynaptischen Proteinen**, independently and without the support of third parties, and that I used no other sources and aids than those stated.

All parts which are based on the publications or presentations of other authors, either in letter or in spirit, are specified as such in accordance with the citing guidelines. The sections on methodology (in particular regarding practical work, laboratory regulations, statistical processing) and results (in particular regarding figures, charts and tables) are exclusively my responsibility.

Furthermore, I declare that I have correctly marked all of the data, the analyses, and the conclusions generated from data obtained in collaboration with other persons, and that I have correctly marked my own contribution and the contributions of other persons (cf. declaration of contribution). I have correctly marked all texts or parts of texts that were generated in collaboration with other persons.

My contributions to any publications to this dissertation correspond to those stated in the below joint declaration made together with the supervisor. All publications created within the scope of the dissertation comply with the guidelines of the ICMJE (International Committee of Medical Journal Editors; http://www.icmje.org) on authorship. In addition, I declare that I shall comply with the regulations of Charité – Universitätsmedizin Berlin on ensuring good scientific practice.

I declare that I have not yet submitted this dissertation in identical or similar form to another Faculty.

The significance of this statutory declaration and the consequences of a false statutory declaration under criminal law (Sections 156, 161 of the German Criminal Code) are known to me.”

Date Signature

Declaration of your own contribution to the publications

Kazi Atikur Rahman contributed the following to the below listed publications:

Publication 1: Rahman, K. A., Orlando, M., Boulos, A., Andrzejak, E., Schmitz, D., Ziv, N. E., Prüss, H., Garner, C. C., & Ichkova, A. (2023). Microglia actively remove NR1 autoantibody-bound NMDA receptors and associated post-synaptic proteins in neuron microglia co-cultures. *Glia*.

Contribution:

Planning of the experiments:
Kazi Atikur Rahman, Ewa Andrzejak, Dietmar Schmitz, Harald Prüss, Craig C. Garner, Aleksandra Ichkova

Execution of experiments:
Immunocytochemistry (Fig 1, 2, 5, 7, 8, 9, 10, 12, 13) – Kazi Atikur Rahman
Electron Imaging (Figure 3, 11) – Kazi Atikur Rahman, Marta Orlando
ELISA (Figure 4) – Kazi Atikur Rahman
Live Imaging (Figure 6) – Kazi Atikur Rahman, Ayub Boulos, Noam E Ziv
Cloning and Testing of mutant Antibodies (Figure 7) – Kazi Atikur Rahman, Aleksandra Ichkova

Data analysis:
Analysis of Immunocytochemistry: Kazi Atikur Rahman
Analysis of Electron Imaging: Marta Orlando
Analysis of ELISA: Kazi Atikur Rahman

Data visualization: Kazi Atikur Rahman

Writing and editing of the manuscript:
Initial draft by Kazi Atikur Rahman, editing by Craig C. Garner, Aleksandra Ichkova and Kazi Atikur Rahman with input from all the authors.

_____

Signature, date and stamp of first supervising university professor / lecturer

_____

Signature of doctoral candidate

Printing copy(s) of the publication(s)

Received: 2 November 2022 | Revised: 15 March 2023 | Accepted: 20 March 2023
DOI: 10.1002/glia.24369

GLIA
WILEY

RESEARCH ARTICLE

Microglia actively remove NR1 autoantibody-bound NMDA receptors and associated post-synaptic proteins in neuron microglia co-cultures

Kazi Atikur Rahman[1,2,3] | Marta Orlando[1,2] | Ayub Boulos[4] | Ewa Andrzejak[5] | Dietmar Schmitz[1,2,3,5,6,7] | Noam E. Ziv[4] | Harald Prüss[1,5,8] | Craig C. Garner[1,2,5] | Aleksandra Ichkova[5]

[1]Corporate Member of Freie Universität Berlin, Humboldt-Universität Berlin and Berlin Institute of Health, Neuroscience Research Center, Charité-Universitätsmedizin Berlin, Berlin, Germany

[2]Corporate Member of Freie Universität Berlin, Humboldt-Universität Berlin and Berlin Institute of Health, NeuroCure Cluster of Excellence, Charité-Universitätsmedizin Berlin, Berlin, Germany

[3]Corporate Member of Freie Universität Berlin, Humboldt-Universität Berlin and Berlin Institute of Health, Einstein Center for Neuroscience, Charité-Universitätsmedizin Berlin, Berlin, Germany

[4]Technion Faculty of Medicine, Rappaport Institute and Network Biology Research Laboratories, Haifa, Israel

[5]German Center for Neurodegenerative Diseases (DZNE) Berlin, Berlin, Germany

[6]Bernstein Center for Computational Neuroscience, Humboldt-Universität zu Berlin, Berlin, Germany

[7]Max Delbrück Center for Molecular Medicine in the Helmholtz Association, Berlin, Germany

[8]Corporate Member of Freie Universität Berlin, Humboldt-Universität Berlin and Berlin Institute of Health, Department of Neurology and Experimental Neurology, Charité-Universitätsmedizin Berlin, Berlin, Germany

Correspondence
Aleksandra Ichkova, German Center for Neurodegenerative Diseases (DZNE) Berlin, 10117 Berlin, Germany.
Email: aleksandra.ichkova@dzne.de

Craig C. Garner, Charité-Universitätsmedizin Berlin, corporate member of Freie Universität Berlin, Humboldt-Universität Berlin and Berlin Institute of Health, Neuroscience Research Center, 10117 Berlin, Germany.
Email: craig.garner@charite.de

Funding information
Bundesministerium für Bildung und Forschung, Grant/Award Numbers: 01GM1908D, 01GQ1420B; Deutsche Forschungsgemeinschaft, Grant/Award Numbers: 184695641, 327654276, 415914819, 431572356; Deutsches Zentrum für Neurodegenerative Erkrankungen; Einstein Stiftung Berlin; Germany's Excellence Strategy, Grant/Award Numbers: Exc-2049-390688087, PR1274/3-1, PR1274/4-1, PR1274/5-1; H2020 European Research Council, Grant/Award Number: 810580; Helmholtz-Gemeinschaft, Grant/Award Number: HIL-A03

Abstract

Autoantibodies against the NR1 subunit of NMDA receptors (NMDARs) have been shown to promote crosslinking and internalization of bound receptors in NMDAR encephalitis (NMDARE). This internalization-mediated loss of NMDARs is thought to be the major mechanism leading to pathogenic outcomes in patients. However, the role of bound autoantibody in engaging the resident immune cells, microglia, remains poorly understood. Here, using a patient-derived monoclonal NR1 autoantibody (hNR1-mAb) and a co-culture system of microglia and neurons, we could show that hNR1-mAb bound to hippocampal neurons led to microglia-mediated removal of hNR1-mAb bound NMDARs. These complexes were found to accumulate inside endo-lysosomal compartments of microglia. Utilizing another patient isolated monoclonal autoantibody, against the α1-subunit of $GABA_A$ receptors (α1-$GABA_A$-mAb), such removal of receptors was found to be specific to the antibody-bound receptor targets. Interestingly, along with receptor removal, we also observed a reduction in synapse number, more specifically in the numbers of post-synaptic proteins like PSD95 and Homer 1, when microglia were present in the culture. Importantly, mutations in the Fc region of hNR1-mAb,

blocking its Fcγ receptor (FcγR) and complement binding, attenuated hNR1-mAb driven loss of NMDARs and synapses, indicating that microglia engagement by bound hNR1-mAb is critical for receptor and synapse loss. Our data argues for an active involvement of microglia in removal of NMDARs and other receptors in individuals with autoimmune encephalitis, thereby contributing to the etiology of these diseases.

KEYWORDS
antibody mediated autoimmune encephalitis; autoantibodies; microglia, hippocampal neurons, co-culture, pre-labeling; NMDAR

1 | INTRODUCTION

NMDA receptor encephalitis (NMDARE), initially described as a paraneoplastic syndrome, is a neuro autoimmune disorder where autoantibodies are formed, most commonly, against NR1 subunit of NMDA receptor (NMDAR) (Josep Dalmau et al., 2007). NMDARE patients show myriad of symptoms including psychosis, impaired consciousness, behavioral changes (Day et al., 2011) autonomic dysfunction and catatonia (Barry et al., 2011; Josep Dalmau et al., 2019; Prüss, 2021). The mechanism of action of NR1 autoantibodies was reported to be receptor crosslinking by bound autoantibody, leading to internalization of receptor antibody complexes thereby reducing the number of NR1 positive NMDAR from the surface of neurons (Hughes et al., 2010). The crosslinking of receptors by bound antibody was shown to be mediated by Fc region of the autoantibody (Hughes et al., 2010). This crosslinking dependent receptor internalization was not observed when F(ab) fragments of NR1 reactive autoantibody, which lacks the Fc region, was bound to NMDARs on cultured hippocampal neurons (Hughes et al., 2010).

Apart from receptor crosslinking by bound antibody, Fc regions of sub-types of antibodies (IgG1, IgG3, among others) are also known to mediate downstream immune responses including binding to Fc receptors (FcRs) present on cells of monocytic lineage and antigen presenting cells (APCs) (Wang et al., 2018) as well as activating the complement pathway (Vidarsson et al., 2014). For example, autoantibody against aquaporin-4 (AQP4) in Neuromyelitis optica (NMO) has been reported to bind not only to AQP4 on astrocytes, but also engage astrocytic Fc gamma receptors (FcγRs), via their Fc region, leading to clustering and internalization of AQP4 from the surface of astrocytes (Hinson et al., 2017). Bound AQP4 reactive autoantibody also activates C1q, due to their Fc-Fc region interaction, providing a scaffold for complement deposition, which leads to complement-dependent cytotoxicity (CDC) (Soltys et al., 2019). In another study, therapeutic antibodies targeting tau, thereby blocking its cell to cell spreading, were found to engage FcγRs on microglia promoting inflammation and the secretion of pro-inflammatory cytokines contributing to poor neuronal health (Lee et al., 2016).

Microglia are resident immune cells, of monocytic lineage, of the central nervous system (CNS) (Saijo & Glass, 2011). Within the CNS, microglia perform several important functions including synaptic pruning during development (Schafer et al., 2012) and degenerative disorders like Alzheimer's Disease (Hong et al., 2016). They also produce pro-inflammatory and anti-inflammatory cytokines and chemokines such as IL6, TNF-α (Smith et al., 2012) and IL10, IL4 (Pozzo et al., 2019), respectively. They are also actively engaged in the phagocytosis of cellular debris, arising from damaged neurons, via phagocytic receptors such as Toll-like receptors (TLRs), FcγRs and complement receptors, among others (Fu et al., 2014). Studies on post-mortem tissues from patients with NMDAR encephalitis have shown marked microglia activation and microgliosis in the hippocampus (Camdessanché et al., 2011; Josep Dalmau et al., 2007; Tüzün et al., 2009). Recent studies on maternal transfer of autoantibodies have also hinted at the role of microglia in autoimmune encephalitis. For example, the gestational transfer of Contactin-associated protein-like2 (CASPR2) autoantibodies induced long-term microglial activation related to synaptic loss and behavioral deficits (Coutinho et al., 2017). Similarly, brains from fetuses with placental transfer of NMDAR reactive autoantibodies showed decreased NMDAR clusters, reduced synapse number, poor behavioral performance and microglia activation (García-Serra et al., 2021). However, the casual link between the autoantibody-induced phenotypes and microglial activation remains unexplored.

Here, we investigated the capacity of patient-derived monoclonal NR1 reactive autoantibody (hNR1-mAb) to elicit a downstream immune reaction, by engaging microglia, in a neuron:microglia co-culture system. Our data revealed that microglia not only proactively remove hNR1-mAb bound NMDARs complexes, but also excitatory post-synaptic proteins in a highly specific and selective manner. Furthermore, we could show that by introducing mutations in the Fc region that blocks Fc region-driven microglia engagement prevented the loss of NMDARs and post-synaptic proteins. Similarly, utilizing patient-derived monoclonal autoantibody targeting α1 subunit of the $GABA_A$ receptor (α1-$GABA_A$R-mAb), we could also show that microglia selectively removes autoantibody-bound $GABA_A$Rs, but not antibody-free NMDARs and vice versa. These results provide evidence that microglia could play an active role in removing

antibody/receptor complexes, contributing to disease progression, in patients with autoimmune encephalitis.

2 | MATERIALS AND METHODS

2.1 | Preparation of hippocampal neurons

Wild type (WT) hippocampal neurons from both sexes of C57BL/6J mouse pups were plated on glass coverslips (VWR, 18 mm) supported with wax spacer dots over a bed of astrocytes, using a Banker protocol (Banker & Goslin, 1988; Meberg & Miller, 2003). In brief, astrocytes from WT cortices (P0-P2) were plated on 12 well plates at a density of 10,000 cells per 1 cm^2 6–7 days in Dulbecco's Modified Eagle's Medium (DMEM, Invitrogen, Thermo Fisher Scientific) with 10% FBS, 5% PenStrep (Thermo Fisher Scientific). Astrocytes were treated with 1% floxuridine (FUDR) at 4 days *in-vitro* (DIV) to stop mitogenesis prior to addition of neurons. The medium of the astrocytes is changed to Neurobasal-A (NBA) medium with 2% B27, 1% Glutamax, 0.2% PenStrep (Thermo Fisher Scientific) at 7 DIV prior to addition of neurons. Hippocampal neurons were dissected from WT P0-P2 pups in cold Hanks' Balanced Salt solution (HBSS, Millipore). The dissected hippocampus was incubated for 30 min in enzyme solution DMEM with 3.3 mM Cystein, 2 mM $CaCl_2$, 1 mM EDTA and 20 U/ml Papain (Worthington) at 37°C. Papain activity was inhibited by incubating hippocampus in inhibitory solution, DMEM with 10% FCS (Thermo Fisher Scientific), 38 mM BSA (Sigma-Aldrich) and 95 mM trypsin inhibitor (Sigma-Aldrich) for 5 min. Cells were titrated in NBA medium with 2% B27, 1% Glutamax, and 0.2% PenStrep by gently pipetting. Isolated neurons were then plated at a density of 20,000 cells per 1 cm^2 on nitric acid washed, poly-L-lysine coated glass coverslips with paraffin wax spacer dots at the bottom in NBA medium with 2% B27, 1% Glutamax, 0.2% P/S. Coverslips were transferred, with neurons facing upwards, 1.5 h later on to the wells with astrocytes in NBA medium with 2% B27, 1% Glutamax, 0.2% P/S. The neurons were cultured with astrocytes for 15-17 DIV before each experiment.

2.2 | Mixed glial cultures

WT cortices from P0-P2 pups were used to prepare mixed glial cultures, that is, astrocytes and microglia. The cortices were incubated with 0.05% Trypsin-EDTA (Gibco) at 37°C shaking at 800 rpm for 20 min. The trypsin was subsequently blocked with pre-warmed DMEM with 10% FBS, 5% PenStrep at 37°C. The cells were then titrated by pipetting until the cell suspension was homogenous. The cell suspension was then added to T75 flasks containing pre-warmed DMEM with 10% FBS, 5% PenStrep at 37°C. Medium was replaced at 24 h post culturing and again at DIV 6. The cells were cultured for 15–17 DIV prior to microglia isolation.

2.3 | Lentivirus production

All lentiviral particles were produced at the Viral Core Facility of the Charité-Universitätsmedizin, Berlin (https://vcf.charite.de/ed/) as described previously (Lois et al., 2002). In brief, HEK293T cells were co-transfected with 10 µg of shuttle vector, 5 µg of helper plasmid pCMVsR8.9 and 5 µg pf pVSV.G with X-tremeGENE 9 DNA transfection reagent (Roche Diagnostics). Cell culture supernatant containing the viral particles was collected 72 h post transfection and purified via filtration. Aliquots were flash frozen in liquid nitrogen and stored at −80°C. WT hippocampal neurons were infected with 100 µL per well of lentivirus at 3–4 DIV.

2.4 | Isolation and production of recombinant monoclonal antibody

A human IgG1 autoantibody reactive to the NR1 subunit of NMDAR (#003-102) was isolated and cloned from the CSF of patient-derived B-cells with acute NMDAR encephalitis (Kreye et al., 2016). The NR1 #003-102 was recombinantly expressed using paired expression vectors encoding for heavy and light chain by transient transfection in HEK293 cell. Following expression, the recombinant NR1 reactive autoantibody (hNR1-mAb) was purified from the supernatant as described previously (Kreye et al., 2016). The hNR1-mAb concentration was determined using anti-human IgG ELISA following the manufacturer's instructions (3850-1AD-6, Mabtech). An IgG1 autoantibody against the α1 subunit of the $GABA_AR$ (α1-$GABA_AR$-mAb) (Kreye et al., 2021) was also isolated, cloned, expressed and purified, as mentioned above.

2.5 | Mutant hNR1-mAb cloning and purification

Several mutations within the Fc region of human IgG1 antibodies have been shown to block its interaction with complement proteins and FcγR. Some of these were identified to block either both of these interactions-, (Leu234Ala/Leu235Ala/Pro329Gly (LALA-PG)) or selectively complement (Pro329Ala (PA)) or FcγR binding (Leu234Ala/Leu235Ala (LALA)) (Lo et al., 2017; Saunders, 2019). Recombinant heavy chain constant region DNA segments, containing these mutations were designed and synthesized (EurofinsGenomics). The fragments were then PCR amplified with 5′-CTCAGCGTCGACCAAGGGACCATCGGTCTTC-3′ (Forward Primer) and 5′-CATGAGCGTACGTCATTTGCCGGGGCTCAGG-3′ (Reverse Primer), introducing SalI and BsiWI restriction sites at the front and back of the inserts, respectively, before subcloning into the SalI and BsiWI sites in the pCMV-hNR1-mAb (Kreye et al., 2016) vector using Quick Ligation kit (NEB, M2200). This led to the generation of expression vectors coding WT, LALA-PG, PA and LALA hNR1-mAb, respectively. Antibodies were then produced and purified from these expression vectors by new/Era/mabs GmbH, Potsdam, DE.

2.6 | Mouse FcγR1 and C1q binding ELISAs

WT and mutant hNR1-mAb binding to FcγR1 and C1q were measured as reported previously (Lo et al., 2017). In brief: for FcγR1 binding, purified FcγR1 protein (Sino Biological, 50086-M08H) was coated at a concentration of 1 μg/mL in PBS overnight at 4°C on 96 well plates (Corning, Costar, 3595). These were washed with PBS containing 0.05% Tween 20 (PBS-T) followed by blocking with PBS containing 0.5% BSA, 15 ppm Proclin (Sigma Aldrich, 49376-U), pH 7.4 for 1 h at room temperature (RT). Plates were further washed with PBS-T. WT and mutant (LALA-PG, PA and LALA) hNR1-mAbs (50–0.2 μg/mL in triplicates) in PBS-T containing 0.5% BSA and 15 ppm Proclin, pH 7.4, were added to the plates and incubated at RT for 2 h. Plates were washed with PBS-T and then incubated with goat F(ab′)2 anti-human F(ab′)2 conjugated with Horseradish Peroxidase (HRSP) (1:5000) (Jackson ImmunoResearch, 109-035-006) for 90 min at RT. Plates were washed with PBS-T and bound autoantibody was detected by using 3,3′,5,5′-teramethylbenzidine (TMB) as a substrate (Sera Care, 5120-0047). Plates were developed with TMB in the dark at RT for 1 h. The reaction was stopped by the addition of 1 M H_3PO_4 (Sigma Aldrich, 345245). The absorbance was then measure at 450 nm, using absorbance at 620 nm as background, using an Infinite 200PRO Tecan plate reader. The absorbance curves were subsequently plotted using GraphPad.

For mouse C1q binding, 96 well plates (Corning, Costar, 3595) were coated overnight with WT and mutant (LALA-PG, LALA and PA) hNR1-mAbs (0.1–10 μg/mL) in PBS at 4°C. Plates were then washed with PBS-T and blocked with PBS-T containing 0.5% BSA, 15 ppm Proclin and 10% blocker Caesin (ThermoFisher Scientific, 37582) (pH 7.4) for 1 h at RT. Purified mouse C1q (Complement Technology, M099) was added to the plate at a concentration of 0.5 μg/mL in PBS-T and incubated 1.5 h at RT. Plates were washed with PBS-T and bound C1q was detected by addition of biotinylated anti mouse C1q (Hycult Technologies, HM1096BT-50UG) at a concentration of 20 ng/mL for 1.5 h at RT followed by an incubation with HRSP-conjugated Streptavidin (Cytiva, RPN 1231) at a ratio of 1:5000 for 1 h at RT. Plates were washed with PBS-T and developed using TMB substrate for 1 h in the dark. The reaction was subsequently stopped using 1 M H_3PO_4. The absorbance was then measured at 450 and 620 nm, using Infinite 200PRO Tecan plate reader, which automatically subtracts the background signal at 620 nm. The absorbance curves were subsequently plotted using GraphPad. Note, washing was always done at least three times with PBS-T while maintaining reaction volume at 100 μL per well. Gentle shaking (50 rpm) was performed during each incubation step.

2.7 | Pre-labeling of hNR1-mAb

hNR1-mAb autoantibody, 1 μg per coverslip, was pre-labeled using Zenon Human IgG Labeling Kit (Molecular Probes, Z-25408, Z-25407 or Z-25402), following the manufacturer's protocol. Briefly, 1 μg of hNR1-mAb in PBS was incubated with 5 μL of labeling Reagent A (200 μg Fab fragment/ml, 5 mM azide) followed by 5 min incubation at RT. Five microliters of blocking Reagent B (5 mg IgG/ml, 5 mM azide) was then added to the solution and incubated at RT for 5 min. Note, pre-labeling involves attachment of Fab fragments tagged to fluorophores at the Fc region of the antibody, which could interfere with binding to complement proteins and/or FcγRs. Thus, cells were incubated with a 1:1 mixture of pre-labeled and unlabeled autoantibody. Previous studies have used different concentration of hNR1 autoantibody *in-vitro* like 0.5 μg/mL (Kreye et al., 2016) or 1 μg/mL (Andrzejak et al., 2022) without washing out for 24 h. Here, a final concentration of 2 μg/mL of the autoantibody (pre- and unlabeled at 1 μg/mL each) was added to co-culture set up as this amount was found to optimally label NMDARs within the acute time frame of 30 min. Such an amount was found to be sufficient to saturation binding, while 95% of added hNR1-mAb was washed off after 30 min.

2.8 | Neuron microglia co-culture

2.8.1 | Bound hNR1-mAb removal experiment

Cultured hippocampal neurons were incubated with hNR1-mAb at DIV 15-17. Here, 1 μg of the pre-labeled (hNR1-mAb*) and unlabeled (hNR1-mAb) hNR1-mAb mixture (1:1) was added to the coverslips making the final concentration 2 μg/mL. hNR1-mAb*/hNR1-mAb were allowed to bind to the neurons for 30 min at 37°C. Medium with unbound autoantibodies were then removed and replenished with fresh pre-warmed NBA medium with 2% B27, 1% Glutamax, and 0.2% PenStrep.

Primary mouse microglia, grown for 15-17 DIV, were isolated by tapping mixed glial flasks manually for 6 min. The supernatant containing microglia was centrifuged at 200*g* at 22°C for 5 min. The cell pellet was resuspended in pre-warmed NBA medium at 37°C with 2% B27, 1% Glutamax, 0.2% P/S. Cell number was counted using hemocytometer. Microglia cells were added to the autoantibody-bound neurons at a density, ensuring a 1:3 microglia:neuron ratio. Different ratios of microglia to neuron, 1:2, 1:3 and 1:5, were also tested, yet 1:3 microglia to neuron ratio was found to be optimal in both cellular health and density of both cell types and thus used for all subsequent experiments. Microglial cells were incubated with autoantibody-bound neurons for 1, 3 and 6 h at 37°C following which the cells were fixed with pre-warmed 4% paraformaldehyde (PFA) for 10 min, prior to immunocytochemical staining (see below).

2.8.2 | NMDAR/hNR1-mAb complex removal experiment

For studying microglia-mediated removal of NMDAR/hNR1-mAb complexes, WT hippocampal neurons were initially infected with 200 μL per well of lentiviruses expressing NR1-EGFP under the neuron specific Synapsin promoter at 3–4 DIV, and subsequently incubated with hNR1-mAb*/hNR1-mAb (2 μg/mL) at 37°C for 30 min at

(15–17 DIV). After incubation and removal of unbound autoantibody, microglia were added to the neurons in 1:3 ratio of microglia to neuron for 6 h at 37°C. Cells were then fixed with pre-warmed 4% PFA for 10 min. Cells were stained with anti-GFP (1:1000, mouse, Abcam, #ab1218) antibody to enhance NR1-EGFP signal.

2.8.3 | Synapse quantification experiment

WT hippocampal neurons (DIV 15–17) were treated with unlabeled hNR1-mAb for 30 min at 37°C. Directly after unbound hNR1-mAb removal, microglia were added to autoantibody-bound neurons for 6 h as described above. Cells were fixed with pre-warmed 4% PFA and later stained for the post-synaptic and pre-synaptic marker proteins, PSD95 and vGLUT1, respectively.

To directly monitor the loss of synapses in presence of microglia, in some experiments WT hippocampal neurons were doubly infected with lentiviruses expressing either mCh-Synapsin/Homer-EGFP (Homer-1) or Synaptophysin-EGFP/PSD95-mKate2 on DIV 3–4 under the neuron specific Synapsin promoter. Neurons overexpressing different combinations of pre- and post-synaptic markers were then treated with unlabeled hNR1-mAb (2 μg/mL) for 30 min at 37°C, before washing and adding microglia for 6 h as described above. Finally, the cells were fixed in 4% PFA and subsequently processed for immunocytochemistry.

2.8.4 | Mutant hNR1-mAb experiments

As described above for experiments with WT hNR1-mAb*/hNR1-mAb, we also treated WT hippocampal neurons with LALA-PG or LALA or PA mutants of hNR1-mAb prepared in a 1:1 mixture of pre-labeled:unlabeled autoantibodies. Following the removal of unbound antibodies by washing, microglia were added for 6 h at 37°C. Cells were then fixed with pre-warmed 4% PFA for 10 min.

2.8.5 | Antibody specificity experiments

To study the specificity of microglia-mediated removal of bound autoantibody, we compared the ability of microglia to remove the hNR1-mAb*/hNR1-mAb to that of a second patient-derived autoantibody against the alpha1 subunit of the $GABA_AR$ (α1-$GABA_AR$-mAb). Here, pre-labeling of α1-$GABA_AR$-mAb ($GABA_AR$-mAb*) was performed as mentioned before, however in this case 8.3 μL of Reagent A and Reagent B of Zenon kit (Alexa 647, Molecular Probes, Z-25408) was used as the labeling was not uniform for lower antibody to reagent ratios. Initially, we checked if bound α1-$GABA_AR$-mAb could also trigger microglia-mediated loss of α1-$GABA_AR$-mAb puncta similar to hNR1-mAb. This was accomplished similar to hNR1-mAb experiments in that neurons were first treated with α1-$GABA_AR$-mAb*/α1-$GABA_AR$-mAb (1:1) (2 μg/mL) for 30 min followed by removal of unbound antibody and the addition of microglia for 6 h.

In co-labeling experiments, we initially incubated cultures for 30 min with α1-$GABA_AR$-mAb*/α1-$GABA_AR$-mAb (1:1) (2 μg/mL) before washing and adding microglia for 6 h as described above. After 6 h, pre-labeled hNR1-mAb# (Zenon kit Z25407, Alexa 594) (1 μg/mL) was added for 30 min to label the NMDARs. Cells were then washed with pre-warmed NBA culture medium before fixation with 4% PFA. The converse experiment was performed by first adding hNR1-mAb*/hNR1-mAb (1:1) (2 μg/mL) for 30 min, washing, adding microglia for 6 h followed by incubating cultures with the α1-$GABA_AR$-mAb# to label $GABA_ARs$ for 30 min.

In competitive experiments, we simultaneously added different combinations of antibodies: for example, (a) both WT $GABA_AR$-mAb and hNR1-mAb or (b) $GABA_AR$-mAb and LALA-PG mutant of hNR1-mAb (LALA-PGhNR1-mAb) to our co-culture setup. Here, WT hippocampal neurons were pre-treated with either hNR1-mAb*(Alexa 647)/hNR1-mAb (1:1) and α1-$GABA_AR$-mAb# (Alexa 594)/α1-$GABA_AR$-mAb (1:1) or LALA-PG-hNR1-mAb* (Alexa 647)/LALA-PG-hNR1-mAb (1:1) and α1-$GABA_AR$-mAb# (Alexa 594)/α1-$GABA_AR$-mAb (1:1) at a concentration of 2 μg/mL for each autoantibody at 37°C for 30 min. After washing of unbound antibody, microglia were added for 6 h at 37°C. Cells were then fixed with 4% PFA for 10 min.

2.9 | Immunocytochemistry

Cells fixed in PFA were washed two times with PBS followed by incubation with ice cold 25 mM glycine in PBS for 20 min to quench background fluorescence. Cells were then permeabilized and blocked with a solution containing 5% Normal Goat Serum (NGS), 2% BSA and 0.1% Triton in PBS for 1 h at RT. Cells were then incubated with primary antibodies in PBS containing 5% NGS and 2% BSA for 1 h at RT. The following primary antibodies were used: MAP2 (1:2000, chicken, Millipore, #AB5543), CD11b (1:1000, rat, Abcam, #ab8878), Iba1 (1:500, rabbit, Wako, #019-19741), P2Y12R (1:400, rabbit, AnaSpec, #AS-55043A), PSD95 (1:500, mouse, Abcam, #ab2723), vGLUT1 (1:4000, guinea pig, Synaptic Systems, #135 304), Lamp2a (1:1000, rabbit, Abcam, #ab18528), CD68 (1:1000, rabbit, Abcam, #ab125212) and GFP (1:1000, mouse, Abcam, #ab1218). The cells were then washed three times with PBS containing 5% NGS and 2% BSA for 10 min each. This was followed by incubation with secondary antibody diluted in PBS containing 5% NGS and 2% BSA for 1 h at RT. Differentially labeled (Alexa fluorophore) secondary antibodies (1:1000, Invitrogen, Thermo Fisher Scientific) were used. Cells were then washed three times once with PBS containing 5% NGS and 2% BSA followed by two times with cold PBS for 10 min each. Finally, coverslips were dipped in H_2O and mounted on Mowiol mounting media.

2.10 | Electron microscopy

To study microglia-mediated removal of antibody complexes and post-synaptic proteins in the presence of bound hNR1-mAb by

electron microscopy (EM), we adapted a photo-conversion protocol that was previously described (Meisslitzer-Ruppitsch et al., 2013). This is based on the oxidation of the chromogen 3,3′-diaminobenzidine tetrahydrochloride (DAB), in presence of singlet oxygen generated by photo-bleaching, and the formation of precipitates that are electron-dense and thus can be imaged and analyzed with EM. WT hippocampal neurons were treated with pre-labeled hNR1-mAb≈ (Zenon kit Z25402, Alexa 488) and unlabeled hNR1-mAb in 1:1 ratio (hNR1-mAb≈ /hNR1-mAb) (2 µg/mL) for 30 min following which unbound antibodies were washed off. For studying removal of post-synaptic proteins, lentivirally infected neurons overexpressing Homer-EGFP under the Synapsin promoter were used, followed by addition of hNR1-mAb (2 µg/mL) for 30 min and washing away of unbound hNR1-mAb. Microglia were then added to and incubated for 90 min at 37°C. The cells were fixed in pre-warmed 1.25% glutaraldehyde (ThermoFisher) in 0.066 M sodium cacodylate buffer (Sigma Aldrich). Cells were washed three times with 0.1 M sodium cacodylate buffer for 10 min per wash. To prevent nonspecific background DAB reaction cells were blocked for 30 min at 4°C in blocking buffer (50 mM glycine and 5 mM aminotriazole in 0.1 M sodium cacodylate). This was followed by incubation with 100 mM ammonium chloride at 4°C for 1 h and washing with 0.1 M sodium cacodylate buffer. 1 mg/mL DAB (Sigma, D5905) in Tris Buffer Saline (TBS) pH 7.4 was oxygenated for 5 min at 4°C. The cells with or without bound hNR1-mAb≈ were then bleached using a mercury lamp (491 nm excitation laser) of Zeiss confocal microscope under 20× objective at 100% intensity for 30 min in presence of oxygenated ice cold 1 mg/mL DAB in TBS. The cells were then washed with chilled 0.1 M sodium cacodylate followed by 1 h incubation with 1% osmium tetroxide (Science Services) in 0.1 M sodium cacodylate. After this, cells were en-bloc stained and embedded in Epoxy resin (Epon 812 Kit, Science Services) following steps 3–15 of this protocol https://www.protocols.io/view/chemical-fixation-and-embedding-of-cultured-cells-eq2lyp5yplx9/v1. The photo-converted area from each experimental group was visible due to the formation of a brown precipitate. The photo-converted region was subsequently cut with a Ultracut ultramicrotome (Leica) equipped with a 45° Ultra diamond knife (Diatom). Sixty nanometers thick ultrathin sections were collected on formvar coated copper grids (Science. Services) stained for 5 min with 1% uranyl acetate and for 1 min with 1% lead citrate and imaged at an EM900 Transmission Electron Microscope (Zeiss) operating at 80 kV and equipped with a 2k × 2k digital camera (Olympus). To note, either Alexa 488 pre-labeled hNR1-mAb≈ or Homer-EGFP was used as fluorophores of choice for photo-conversion as they have the highest yield of reactive oxygen species (ROS) upon bleaching which ensures efficient DAB precipitation.

2.11 | Live imaging

For live imaging of microglia-mediated removal of NMDAR/hNR1-mAb complexes, WT hippocampal neurons infected with lentiviruses expressing NR1-EGFP at 3 DIV were treated with pre-labeled/unlabeled hNR1-mAb*/hNR1-mAb (1:1) (2 µg/mL) for 30 min at 37°C at 15–17 DIV. After washing away unbound antibody, microglia were added to the neurons for 1 h. The coverslips with hNR1-mAb bound neurons and microglia were then carefully transferred to a live imaging chamber (Quick Change Chamber for 18 mm, RC-41LP, Warner Instruments) together with 500 µL of NBA culture media. Coverslips were then imaged using a Nikon Spinning Disk Confocal Microscope (AMBIO Facility, Charité-Universitätsmedizin, Berlin) under 40× water objective. Six different regions with neuron and microglia were selected and the focus and Z plane of each of these regions were defined. Images were taken using DualCamera set up of the microscope with one camera for taking differential interference contrast (DIC) images while the other collected fluorescence images. The cells were imaged live at 37°C for 1 h under perfect focus setting of the confocal microscope with no wait time. Note, after the sixth image the microscope immediately returns to the first region of interest (ROI). The images were processed with volume projection in time series using Imaris 9.0.0 software.

2.12 | Image acquisition and quantification

Fluorescent images were acquired on either a spinning disk confocal microscope (Carl Zeiss Axio Observer.Z1 with Andor spinning disk and cobolt, omricon, i-beam laser) (Carl Zeiss, Andor) using a 40× (1.3 NA) Plan-Apochromat oil objective and an iXon ultra (Andor) camera controlled by iQ software (Andor) or a Nikon Spinning Disk Confocal under 40× (1.3 NA) objective. All images were taken with a Z stack of 5 µm with a step size of 0.5 µm. Neuronal cells of visibly similar morphology with extensive dendritic branches were imaged. Microglial cells adjacent to neuronal dendritic branches were imaged.

Images were processed and analyzed using ImageJ/FIJI software. The images were first converted into maximum intensity projections using ImageJ codes. For NMDAR and $GABA_AR$ puncta analysis, secondary dendrites (one from each quadrant per image) of around the same thickness from each experimental group were selected. ROI selection was based solely on MAP2 staining to eliminate bias. The length of the dendrite within each ROI was measured and recorded. Numbers of NMDAR/$GABA_AR$ puncta along each dendritic segment were counted using Time Series Analyzer plugin of ImageJ. Briefly, circles of 6 × 6 pixels were manually placed over NMDAR puncta along each dendrite. Puncta with intensity above a set threshold value (average intensity of least intense puncta) were counted as positive puncta. The number of puncta and intensity of each puncta was recorded using Time Series Analyzer and plotted as the number of puncta per 100 µm length of dendrite (referred henceforth as puncta/unit length).

The number of co-localizing pre- (vGLUT1 or mCh-Synapsin1 or Synaptophysin-EGFP) and post-synaptic markers (PSD95 or Homer-EGFP or PSD95-mKate2) along dendritic segments were determined as described above. In brief, synapse counting (e.g., double positive for vGLUT1+/PSD95+) was performed by placing 6 × 6 pixels circles over PSD95 positive puncta (with intensity above the set threshold

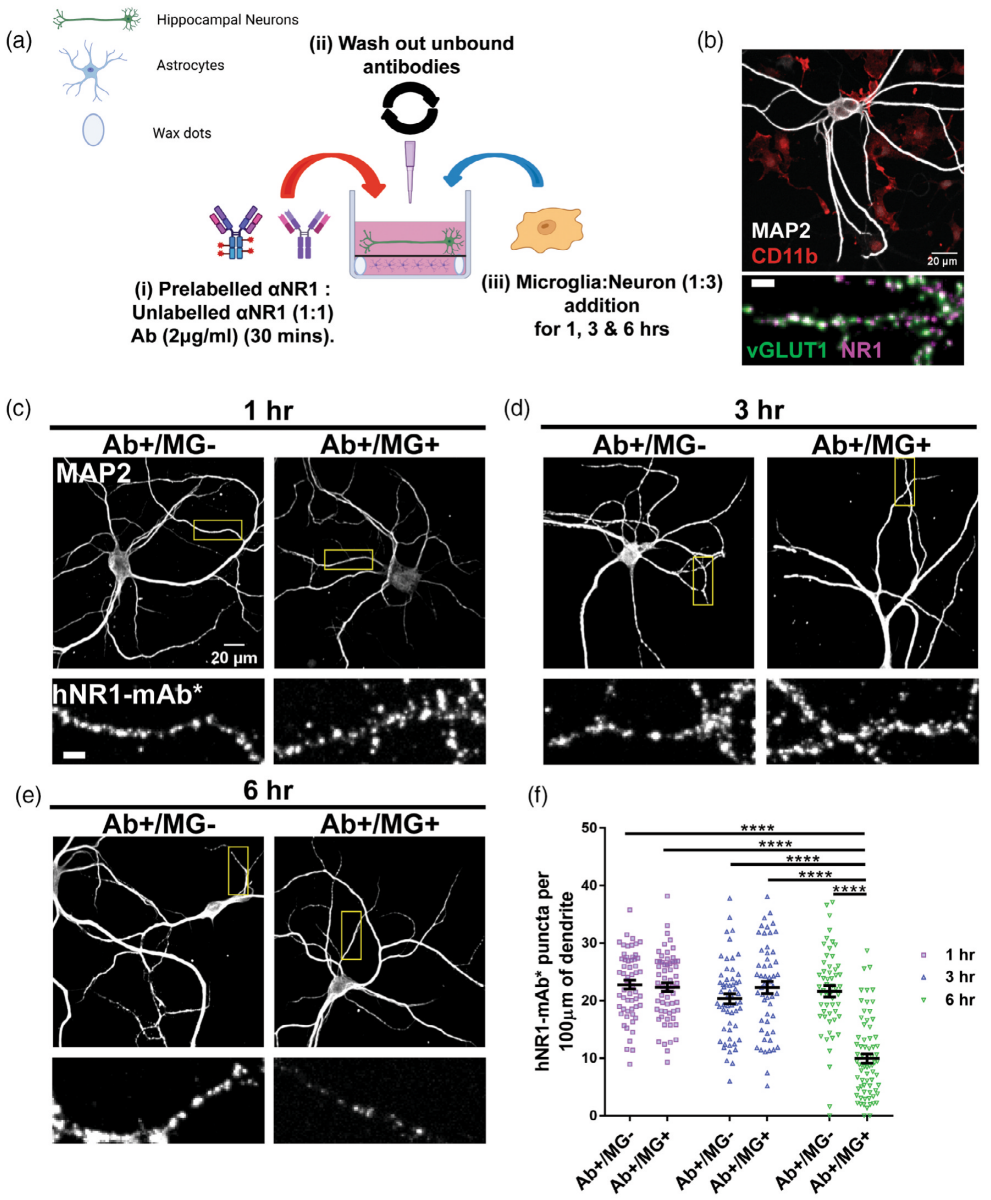

FIGURE 1 Reduction in hNR1-mAb labeled NR1 puncta 6 h after co-culturing hNR1-mAb bound hippocampal neurons with microglia. (a) Schematic of co-culture setup of hNR1-mAb bound neuron and microglia for different time points (1, 3 and 6 h) in "Banker" like culture in which neurons are placed face up on coverslips supported by wax spacer dots over a bed of astrocytes. (b) Image of a hippocampal neuron co-cultured with microglia stained for the dendritic marker MAP2 (gray) and CD11b (red), respectively. Zoom view of dendritic segment showing synaptic co-localization (white) of bound pre-labeled hNR1-mAb* (Alexa 647) (magenta) puncta with the pre-synaptic marker vGLUT1 (green). Scale bar, 5 μm. (c–e) Representative images of hippocampal neurons stained for MAP2 (gray) with selected Region Of Interests (ROIs) showing bound pre-labeled hNR1-mAb* (gray) along dendritic segments with or without microglia addition (Ab+/MG+ and Ab+/MG−, respectively) for 1, 3 and 6 h, respectively. Scale bar, 5 μm. (f) Quantitation of hNR1-mAb* puncta number along 100 μm of dendrite (unit length) with and without microglia. Significant reduction in puncta number was only seen 6 h after the addition of microglia to hNR1-mAb* bound hippocampal neurons. Each data point is an ROI from three independent experiments ($n = 55–71$ ROIs for each group). Error bars represent standard error of mean (SEM). Two-way ANOVA with Tukey's multiple comparison test was used to evaluate statistical significance (****$p < .0001$).

1.5× above background) along dendritic segments followed by measuring intensity of both PSD95 and vGLUT1 at these locations. The number of vGLUT1+/PSD95+ double positive synapses was then plotted per unit length of dendrite.

For analyzing uptake of different receptors and synaptic markers by microglia, microglial cells, labeled with the CD11b antibody, were selected using the Polygon selection tool of ImageJ. Then the average mean intensity of different synaptic markers within each labeled microglia area was measured. These were normalized to intensities within microglia in no autoantibody control (Ab−/MG+).

To eliminate bias, neuronal cells were selected, imaged and analyzed based solely on MAP2 staining. All ROIs after selection were numbered randomly without specifying the experimental conditions to ensure analysis was blinded.

2.13 | Experimental design and statistical analyses

All figures represent data from at least three independent experiments from independent cultures. Statistical design for all experiments can be found in figure legends. GraphPad Prism was used to perform all statistical tests and graphical representations. Unpaired *t*-tests with Welch correction, when the variances were different, was used to determine statistical significance. One way and Two-way ANOVA with Tukey's multiple comparison tests were used to compare means of different experimental groups. All data are represented as mean ± standard error of mean (SEM) with p values <.05 representing statistical significance. Schematics were made using BioRender.com.

3 | RESULTS

3.1 | Primary mouse microglia promote the removal of hNR1-mAb labeled NR1 puncta from hippocampal neurons

To test our hypothesis that NMDAR/NR1-mAb complexes on the surface of neurons could lead to microglia engagement and receptor removal by phagocytosis, we developed an *in-vitro* co-culture system comprised of primary mouse hippocampal neuron and microglia, wherein the addition of antibodies and/or microglia could be temporally controlled (Figure 1a,b). To monitor changes in antibody/receptor distribution, we used the Zenon-system to fluorescently tag hNR1-mAb (hNR1-mAb*, #003-102) (Kreye et al., 2016). hNR1-mAb* along with unlabeled hNR1-mAb (hNR1-mAb*/hNR1-mAb) in a ratio of 1:1 were added to live hippocampal neurons (15–17 DIV) for 30 min, allowing surface synaptic and extra-synaptic receptors to be labeled. Unbound antibodies were removed by medium exchange before addition of isolated cortical microglia at a ratio of 1:3 to neurons for various times (e.g., 1–6 h). In neuronal cultures, lacking microglia, the fluorescently labeled hNR1-mAb* puncta readily decorated the surfaces of MAP2 positive dendrites in pattern that co-localized with the pre-synaptic glutamatergic synaptic vesicle marker vGLUT1 (Figure 1b), consistent with the post-synaptic localization of NMDARs and this antibody, as previously described (Kreye et al., 2016). In cultures that also received microglia for 1, 3 or 6 h, we observed a qualitative decrease in the number of hNR1-mAb* positive puncta along dendrites over time (Figure 1c–e). Quantifying the number of puncta/unit length of dendrite at 1, 3 and 6 h after microglia addition, revealed a significant decrease in the number of hNR1-mAb* positive puncta 6 h after the addition of microglia to the hippocampal neuronal cultures (22.34 ± 0.761, 22.31 ± 1.006 and 9.964 ± 0.8024 of Ab+/MG+ for 1,3 and 6 h, respectively, $p < .0001$) (Figure 1e,f). No significant decrease in the number of hNR1-mAb* positive puncta/unit length of dendrite was detected either at 1 h (Figure 1c,f) or 3 h (Figure 1d,f) post microglia addition. Importantly, no change in the number of NR1-mAb* positive puncta was observed in the absence of microglia for 1, 3 or 6 h (22.79 ± 0.7698, 20.35 ± 0.8721 and 21.63 ± 0.9782 of Ab+/MG− for 1, 3 and 6 h, respectively) (Figure 1f), indicating that antibody-mediated receptor internalization does not play significant role in removal of bound receptors in this time frame, consistent with previous studies (van Casteren et al., 2022). Note, several studies have reported that the internalization driven the loss of NMDARs and NMDA currents in presence of hNR1 autoantibody at longer time points, that is, 12–24 h (Andrzejak et al., 2022; Jézéquel et al., 2017; Moscato et al., 2014). To explore the effect of microglia-mediated removal of bound hNR1-mAb at longer time scales, we performed the co-culture experiment for 6 and 24 h with or without microglia addition. Here, we found a similar significant decrease in the number of hNR1-mAb* puncta along dendrite 6 h after microglia addition (Figure S1a,b). Interestingly, an almost significant decrease ($p = .056$) in hNR1-mAb* puncta number was seen after 24 h even without microglia addition which could be due to previously reported internalization of NMDARs bound with hNR1-mAb. However, microglia addition led to a further decrease in hNR1-mAb* after 24 h (Figure S1a,b). Hence, to reduce the contribution of internalization-driven effects, all subsequent co-culture experiments were performed for 6 h.

3.2 | Bound hNR1-mAb is removed by microglia and accumulates in microglial endo-lysosomes

To investigate whether microglia physically removed the bound hNR1 autoantibody, we analyzed whether the hNR1-mAb* accumulated in the soma of microglia, following the 1, 3 or 6 h incubation with hNR1-mAb*/hNR1-mAb bound hippocampal neurons. In cultures fixed and stained with antibodies against CD11b, a microglia marker, clear hNR1-mAb* positive puncta could be detected within CD11b positive microglia at significantly higher levels 3 and 6 h (Figure 2a,b) after co-culturing with NR1-mAb bound hippocampal neurons. These increases were not associated with appreciable changes in the fluorescent intensity of CD11b in these hNR1-mAb* positive microglial

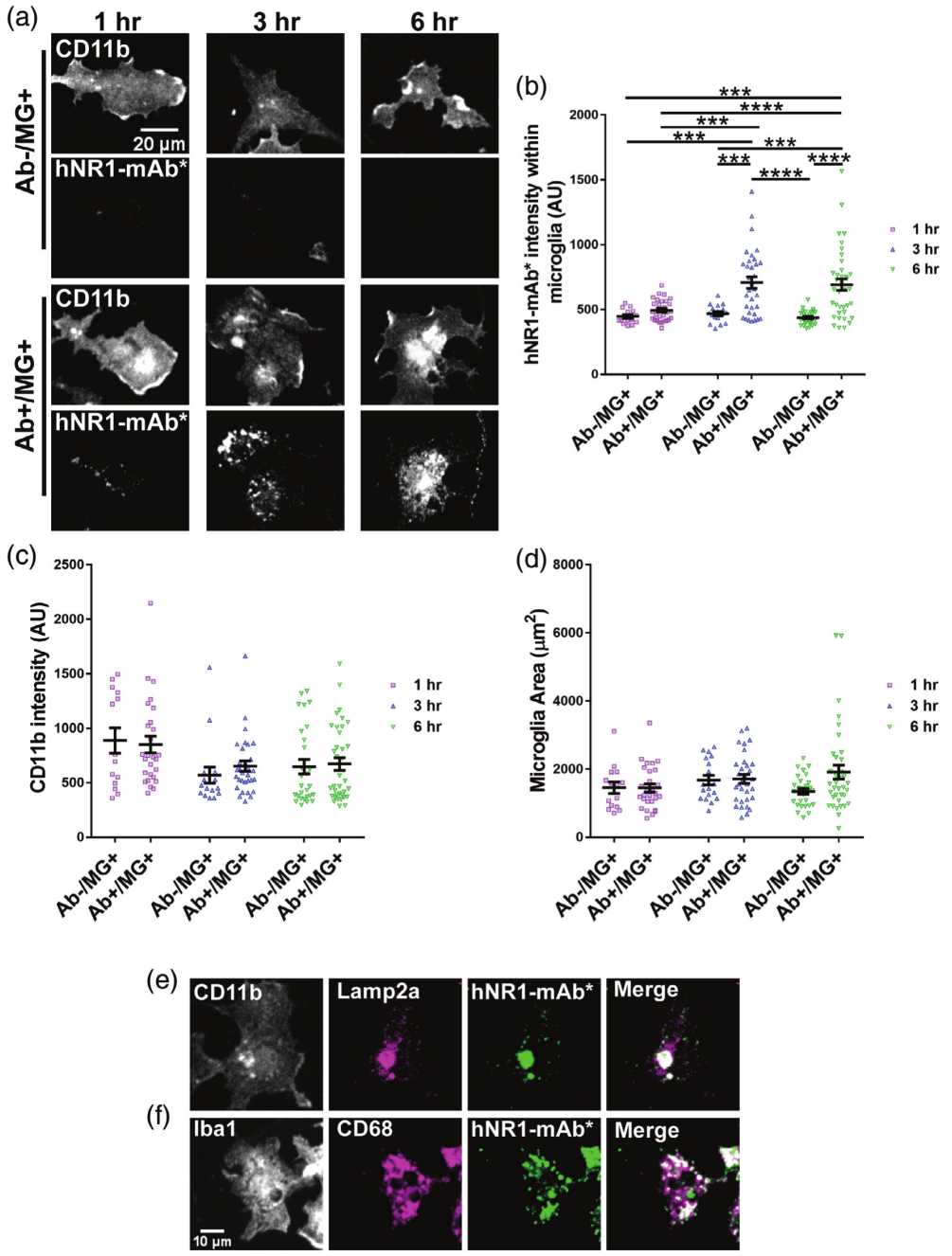

FIGURE 2 NMDAR immuno-reactivity accumulates within microglial endo-lysosomes. (a) Images of microglia, stained for CD11b (gray), 1, 3 and 6 h after co-culture with neurons with or without hNR1-mAb* (Ab+/MG+ and Ab−/MG+, respectively). hNR1-mAb* (gray) puncta accumulate in microglia when co-cultured with hNR1-mAb* bound neurons (Ab+/MG+). (b) Increased hNR1-mAb* immunoreactivity inside CD11b positive microglia after 3 and 6 h of co-culture with neurons in presence of hNR1-mAb*. Each data point represents one microglial cell from three independent experiments ($n = 20–37$ cells for each group). Error bars represent standard error of mean (SEM). Two-way ANOVA with Tukey's multiple comparison test was used to evaluate statistical significance (***$p < .0002$; ****$p < .0001$). (c and d) CD11b intensity and microglia area, respectively, remained unchanged 1, 3 and 6 h after co-culture with or without bound hNR1-mAb*. Each data point represents one microglial cell from three independent experiments ($n = 20–37$ cells for each group). Error bars represent SEM. Two-way ANOVA with Tukey's multiple comparison test was used to evaluate statistical significance. (e and f) hNR1-mAb* puncta (green) inside CD11b or Iba-1 positive microglia cell (gray) co-localized with a pan lysosomal marker, Lamp2a or monocytic lysosomal marker, CD68 (magenta), respectively.

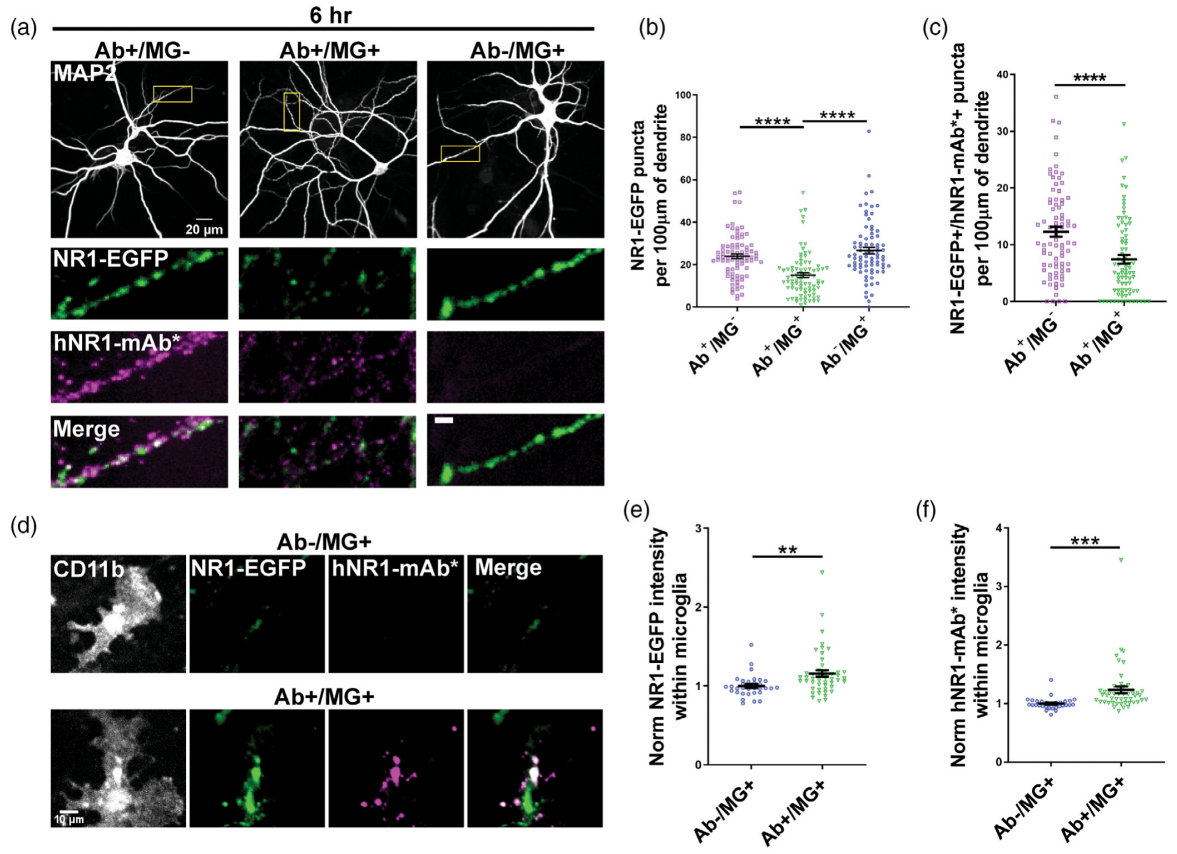

FIGURE 3 hNR1-mAb induces microglial-dependent removal of NR1-EGFP from hippocampal neurons. (a) Representative images of neurons overexpressing NR1-EGFP co-cultured with microglia for 6 h with or without bound pre-labeled hNR1-mAb* (Ab+/MG+ and Ab−/MG+, respectively) and stained for MAP2 (gray). Ab+/MG− experimental group without microglia addition to hNR1-mAb* bound NR1-EGFP overexpressing neurons was also included. Selected ROIs shows NR1-EGFP (green), hNR1-mAb* (magenta) and their merge (white) puncta along dendritic segments (scale bar, 5 µm). (B) Quantitation of NR1-EGFP puncta number per unit length of dendrite. There is a significant reduction of NR1-EGFP puncta number only in presence of microglia and hNR1-mAb (Ab+/MG+) after 6 h of co-culture. Each data point represents an ROI from three independent experiments ($n = 82$ for Ab+/MG−, $n = 82$ for Ab+/MG+ and $n = 78$ for Ab−/MG+). Error bars represent SEM. One-way ANOVA with Tukey's multiple comparison test was used to evaluate statistical significance (****$p < .0001$). (c) Quantification of NR1-EGFP/hNR1-mAb* double positive puncta along dendrites. A significant reduction was seen in Ab+/MG+ compared to Ab−/MG+ group after 6 h. Each data point represents an ROI from three independent experiments ($n = 78$ for Ab−/MG+ and $n = 82$ for Ab+/MG+). Unpaired *t*-test was used to evaluate statistical significance (****$p < .0001$). (d) Images of CD11b positive microglia cells (gray), revealing immunoreactivity for both NR1-EGFP (green) and hNR1-mAb* (magenta) in the Ab+/MG+ group after 6 h of co-culture. Such NR1-EGFP (green) and hNR1-mAb* (magenta) puncta were not seen inside microglia in absence of hNR1-mAb (Ab−/MG+). (e and f) Normalized intensity of NR1-EGFP and hNR1-mAb* inside microglia was significantly higher in Ab+/MG+ compared to the Ab−/MG+ group. Each data point represents a microglia cell over three independent experiments ($n = 32$ for Ab−/MG+ and $n = 48$ for Ab+/MG+). Error bars represent SEM. Unpaired *t*-test with Welch correction was used to evaluate statistical significance (**$p = .0019$ ***$p = .0003$).

(Figure 2a,c). To assess whether the addition of antibodies affects the activation state of added microglia, we monitored the *in-vitro* expression of several other physiologically relevant microglial markers, including Iba1 and P2Y12R, which have previously also been used to determine the activation state of microglia (Hovens et al., 2014; Walker et al., 2020). Microglial cells used in our co-culture experiments were found to express both Iba1 and P2Y12R with no appreciable changes in morphology (Figure S2a). Moreover, we also found that the expression levels of both Iba1 and P2Y12R did not change significantly 1 and 6 h after co-culture (Figure S2b–d). These data could imply that our co-culture conditions do not led to significant microglia activation.

Typically, antibody/receptor complexes phagocytosed by microglia are subsequently degraded via the endo-lysosomal system. To explore this possibility, microglia were immuno-stained 6 h after co-culture with antibodies against Lamp2a, a lysosomal-associated

membrane protein or CD68, an endo-lysosomal associated membrane protein in cells of the monocytic lineage. Here, hNR1-mAb* positive puncta were found to co-localize with Lamp2a or CD68 positive endo-lysosomes within CD11b or Iba1 positive microglia, respectively (Figure 2e,f), consistent with their clearance via this degradative system.

To further validate the observation that microglia remove and internalize bound hNR1-mAb from the surface of neurons, we performed EM following DAB incubation and Alexa 488 photo conversion 90 min after microglia addition to hippocampal neurons bound with pre-labeled hNR1-mAb≈ (Zenon Kit Z25402, Alexa 488) and unlabeled hNR1-mAb, hNR1-mAb/hNR1-mAb≈ (1:1). EM images of microglia revealed the presence of electron-dense material inside membrane bound structures within microglia in the Ab+/MG+ condition (Figure S3b). This was rarely detectable in cultures lacking the hNR1-mAb, that is, Ab−/MG+ condition (Figure S3a). Instead, in the latter, we observed electron-dense signal restricted to mitochondria, due to the photo-conversion of reactive oxygen species that are generated during the mitochondrial ATP generation process (Figure S3a, b). These data support our immunocytochemistry results showing that bound hNR1-mAb can be removed from the surface of neurons by microglia (Figure 2).

3.3 | Microglia removes NMDAR/hNR1-mAb complexes from the surface of neurons

Given our experimental design, namely that unbound antibody is washed away following a 30 min incubation, we anticipated that the appearance of hNR1-mAb* within microglia is associated with and involved in the co-removal of antibody/NMDAR complexes by microglia. To formally test this hypothesis, we infected mouse hippocampal neuron with a lentivirus expressing NR1-EGFP under the neuron specific Synapsin promoter at DIV 3. At 15-16 DIV, these cultures were initially incubated with hNR1-mAb*/hNR1-mAb for 30 min, washed to remove unbound antibody and incubated with microglia for 6 h. This led to a significant decrease in the number of NR1-EGFP puncta per unit length of dendrite in the presence of microglia (23.96 ± 1.148 for Ab+/MG− vs. 15.01 ± 1.164 for Ab+/MG+, $p < .0001$) (Figure 3a,b). Moreover, this decrease was associated with a decline in the number of NR1-mAb* and NR1-EGFP double positive puncta after 6 h of co-culture (12.28 ± 0.8791 for Ab+/MG− vs. 7.424 ± 0.7787 for Ab+/MG+, $p < .0001$) (Figure 3c). No decrease in NR1-EGFP puncta number was detected after 6 h of co-culture with microglia in the absence of bound hNR1-mAb* (23.96 ± 1.148 for Ab+/MG− vs. 26.64 ± 1.573 for Ab−/MG+, $p = .3170$) (Figure 3a,b). Importantly, we also observed a concomitant increase in the fluorescent intensity of NR1-EGFP and hNR1-mAb* double positive puncta inside microglial cells (Figure 3d–f).

To complement these experiments, we also performed live experiments to monitor the real-time removal of NR1-EGFP decorated with hNR1-mAb*/hNR1-mAb by microglia. Using differential interference contrast (DIC) and fluorescence imaging, we could simultaneously visualize neuronal networks and microglia in addition to NR1-EGFP and hNR1-mAb* fluorescence (Figure 4a). Live imaging 1 h after the addition of microglia revealed the active uptake of double positive hNR1-mAb* and NR1-EGFP puncta by microglia from dendritic branches (Figure 4b) (Figure S4a,b). In some cases, we could visualize long microglial processes removing NR1-EGFP/hNR1-mAb* puncta and the pulling of these complexes toward its cell body from dendritic arbors (Figure S4c). Notably, a greater accumulation of hNR1-mAb* was observed inside microglia as compared to NR1-EGFP (Figure 4b). This could be due to the low/moderate expression of NR1-EGFP following transfection, compared to the higher levels of NMDAR-bound hNR1-mAb* to these neurons. Moreover, it is well appreciated that EGFP is more effectively quenched inside acidic lysosomes compared to Alexa 647, used in the pre-labeling of hNR1-mAb* (A. K. Chen et al., 2008). Together these data indicate that microglia can indeed actively remove NMDAR/hNR1-mAb complexes within 1 h of their initial engagement.

3.4 | hNR1-mAb promotes microglia-mediated synapse loss

Intrauterine exposure to IgG1 from anti-NMDAR encephalitis patient was recently shown to cause synapse loss and microglia activation in the brains of postnatal mice (García-Serra et al., 2021). This raises a fundamental question of whether synapse loss is secondary to the removal of antibody/NMDARs complexes and/or whether microglia encounter these complexes and simultaneously remove/strip away excitatory synapses. As an initial test of this concept, we co-cultured hNR1-mAb*/hNR1-mAb bound hippocampal neuron with microglia for 6 h and then analyzed changes in the number of synapses, defined as puncta double positive for the excitatory pre-/post-synaptic markers, vGLUT1 and PSD95, respectively (Figure 5a). Here, we observed a significant decrease (~20%) in the number of vGLUT1+/PSD95+ double positive puncta/unit length of dendrite in the presence of autoantibody and microglia after 6 h (18.87 ± 0.9258 for Ab+/MG− vs. 14.19 ± 0.7152 for Ab+/MG+, $p = .0005$) (Figure 5b). Interestingly, a similar decrease was observed only in the number of PSD95 positive puncta (22.03 ± 0.7569 for Ab+/MG− vs. 15.8 ± 0.7200 for Ab+/MG, $p < .0001$) (Figure 5c), but not in the number of vGLUT1 positive puncta/unit length of dendrite (22.57 ± 0.9887 for Ab+/MG− vs. 21.89 ± 0.0.9218 for Ab+/MG+, $p = .9586$) (Figure 5d), suggesting that microglia preferential remove the post-synaptic components of excitatory synapses. Importantly, no decrease was observed in any of the other experimental conditions, that is, untreated, no microglia (Ab+/MG−) or no NR1 autoantibody (Ab−/MG+). To assess whether these changes were due to their engulfment by microglia, we also analyzed whether either protein accumulated in microglia after 6 h of co-culture. Similar to results

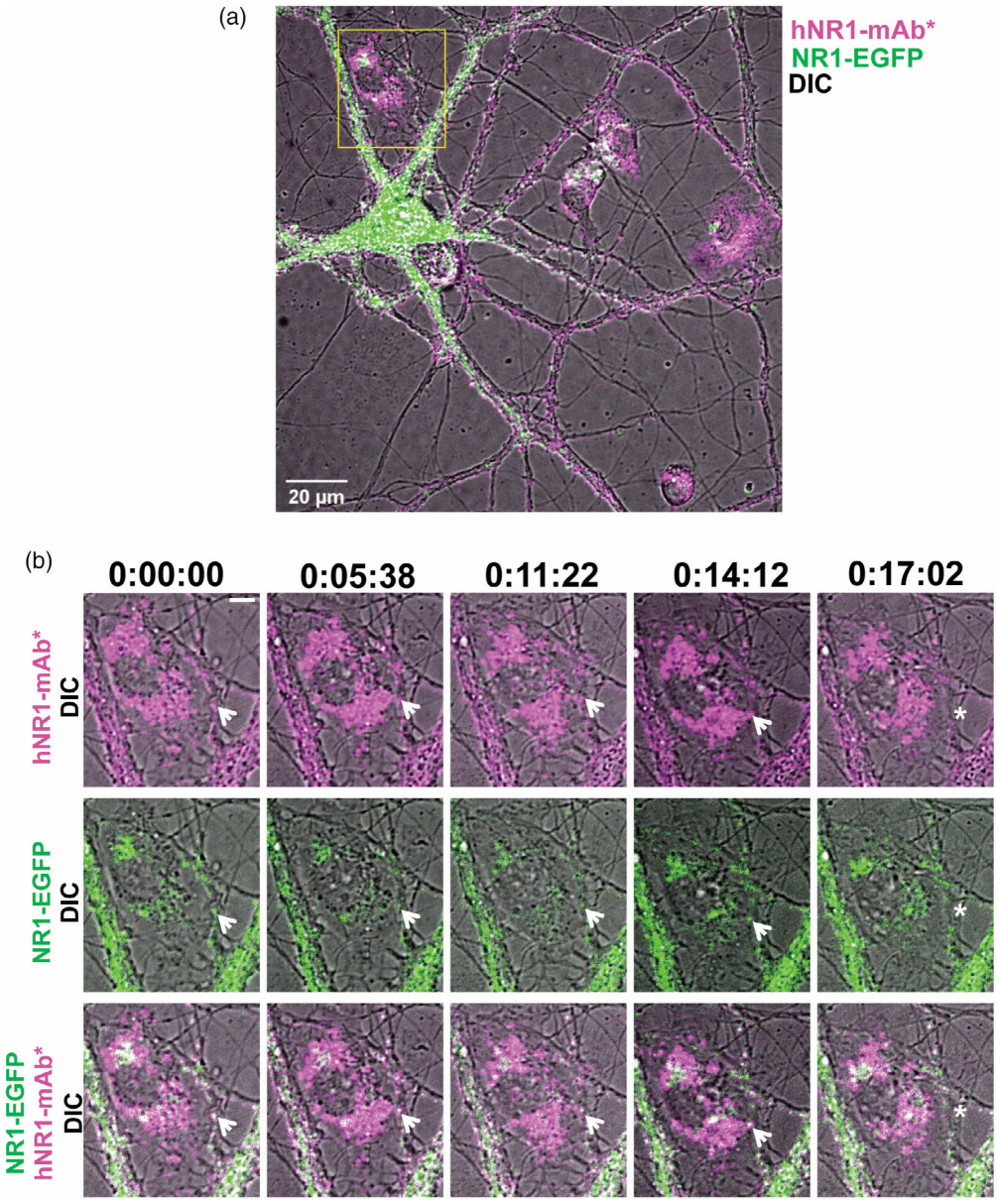

FIGURE 4 Live imaging of microglia-mediated removal of NR1-EGFP/hNR1-mAb* complexes from neurons. (a) Live cell imaging of NR1-EGFP (green) transfected hippocampal neurons with bound hNR1-mAb* (magenta) co-cultured with microglia for 1 h before imaging for 1 h. DIC images were taken simultaneously to visualize axonal and dendritic branches and microglia. Yellow box represents zoomed ROI. (b) Time sequence images of selected ROI showing either hNR1-mAb* (magenta), NR1-EGFP (green) or merge of NR1-EGFP/ hNR1-mAb* (white) together with DIC at different time points. Arrow represents NR1-EGFP/ hNR1-mAb* double positive puncta along a dendritic segment which over time ends up being lost from its location (asterisk) (~17 min) and taken up by an adjacent microglia with accumulated NR1-EGFP/ hNR1-mAb* inside its cell body. Scale bar, 5 µm.

obtained for NR1-EGFP and hNR1-mAb* (Figure 3e,f), we observed higher immunoreactivity for PSD95 (Figure 5e,f), but not vGLUT1 (Figure 5e,g), within microglia in the presence of bound NR1 autoantibody, implying that microglia can distinguish and selectively removed antibody decorated sub-synaptic structures. Note, vGLUT1 only positive puncta could either represent orphan-presynaptic boutons or simply synaptic vesicle (SV) rich axonal varicosities (Krueger et al., 2003).

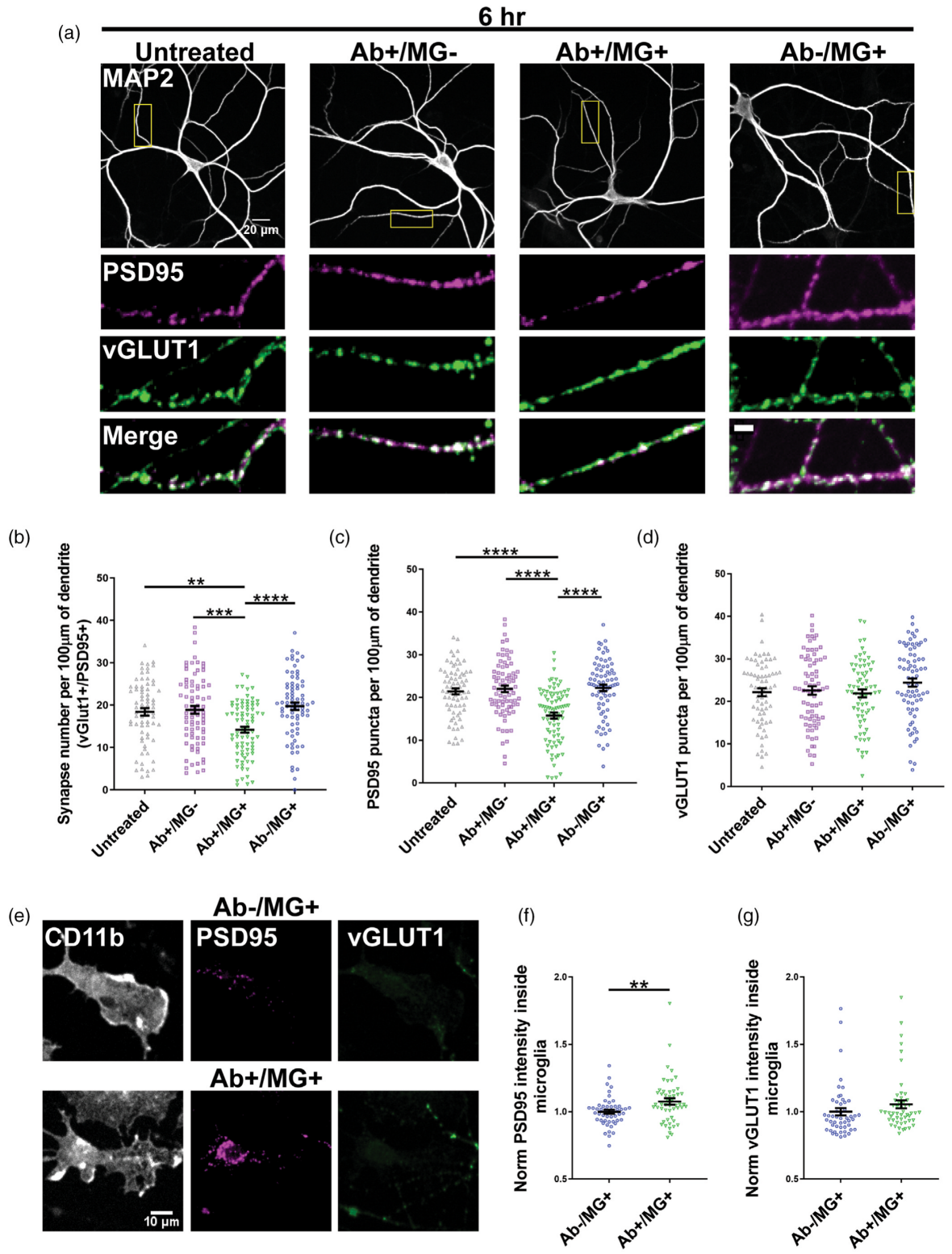

FIGURE 5 Legend on next page.

3.5 | hNR1-mAbs triggers microglia-mediated loss of different post-synaptic but not pre-synaptic reporters

To further explore the idea that microglia can selectively remove decorated post-synaptic components, we co-infected neurons with lentiviruses expressing different combinations of fluorescently tagged pre- and post-synaptic reporters (Homer-EGFP/mCherry-Synapsin or Synaptophysin-EGFP/PSD95-mKate2). Here, we observed a significant decrease in the number of Homer-EGFP (29.76 ± 1.757 for Ab+/MG− vs. 22.33 ± 1.381 for Ab+/MG+, $p = .0123$) (Figure 6a,b) or PSD95-mKate2 (26 ± 0.8864 for Ab+/MG− vs. 17.67 ± 1.179 for Ab+/MG+, $p < .0001$) (Figure 6d,e) positive puncta along dendrites, 6 h after co-culture with microglia in the presence of hNR1-mAb. However, no such decrease was observed in the number of mCherry-Synapsin (26.17 ± 1.253 for Ab+/MG− vs. 26.18 ± 1.282 for Ab+/MG+, $p > .999$) (Figure 6a,c) or Synaptophysin-EGFP (26.25 ± 0.8186 for Ab+/MG− vs. 24.86 ± 1.128 for Ab+/MG+, $p = .7552$) (Figure 6d,f) puncta. Importantly, no change in any post- and pre-synaptic markers was detected in any of the other experimental groups: that is, untreated, no microglia (Ab+/MG−) and no hNR1-mAb (Ab−/MG$^+$). Thus, these results further indicate that hNR1-mAbs can selectively promote microglia-mediated removal of the post-synaptic material, but not necessarily the associated pre-synaptic proteins.

Furthermore, we utilized EM to test whether we see post-synaptic material within microglia after co-culture with hNR1-mAb bound hippocampal neurons. To this end, we utilized a lentivirus expressing Homer-EGFP to infect hippocampal neurons. Following hNR1-mAb addition to Homer-EGFP overexpressing neurons at (DIV 15–17), microglia were added for 90 min. The cells were then bleached, photo-converting EGFP in the presence of DAB, to a precipitate, before processing and EM imaging. EM micrographs revealed the presence of electron-dense material in membrane enclosed structures likely corresponding to multivesicular bodies or lysosomes containing photo-converted Homer-EGFP signal within microglia (Figures S5b and 5c). As in our antibody experiments (Figure S3) in the absence of the hNR1-mAb (Ab−/MG+), the photo-converted DAB was largely restricted to mitochondria due to photo-conversion of reactive oxygen species that are generated during the mitochondrial ATP generation process (Figure S5a). This is in concordance with the loss of Homer-EGFP fluorescent puncta along dendrites of hNR1-mAb bound neurons in the presence of microglia, further supporting the observation that microglia remove post-synaptic components in presence of hNR1-mAb bound to neurons.

3.6 | Mutations blocking FcγR and complement binding of hNR1-mAb prevent autoantibody-driven removal of NMDARs

Next, we wanted to study the downstream mechanisms by which hNR1-mAb promotes removal of NMDARs and synapses by microglia. As mentioned above, it is known that the Fc region of IgG1 can be recognized by at least two immune cell associated receptors (FcγRs and complement receptors), promoting both immune cell activation and the clearance of antibody/antigen complexes (Bournazos et al., 2017). Thus theoretically, it should be possible to test for the contribution of each, by introducing mutations into the Fc region of hNR1-mAb that block their binding. In this regard, it has been reported that Leu234Ala/Leu235Ala (LALA) mutations can block Fcγ receptor binding, while a Pro329Ala (PA) mutation dampens complement activation. Moreover, a combination of these mutations (Leu234Ala/Leu235Ala/Pro329Gly) (LALA-PG) is expected to block binding of both (Lo et al., 2017; Saunders, 2019). We thus created recombinant version of the hNR1-mAb containing the LALA, PA or LALA-PG mutations (Figure S6a) that could be expressed and purified. These purified mutant hNR1-mAbs were initially tested for their antigen, FcγR and complement binding properties. Importantly, none of the mutations in the Fc region of the hNR1-mAb affected antigen binding, as each stained cultured hippocampal neurons in a punctate pattern that co-localized with vGLUT1 puncta along MAP2 positive dendrites, similar to the un-mutated WT antibody (Figure S6b). Importantly, these mutations affected the FcγRI (CD64) and complement

FIGURE 5 hNR1-mAb promotes microglia-mediated loss of post-synaptic proteins and synapses from neuron: Microglia co-cultures. (a) Representative images of neurons either untreated (Ab−/MG−) or treated with Ab+/MG−, Ab+/MG+ and Ab−/MG+ before staining with MAP2 (gray), PSD95 or vGLUT1. Selected ROIs shows' staining's for PSD95 (magenta), vGLUT1 (green) and their merge (white) puncta along dendritic segments. Scale bar, 5 μm. (b) Quantification of synapse number (defined as vGLUT1+/PSD95+ double positive puncta) per unit length of dendrite. A significant decrease vGLUT1+/PSD95+ double positive puncta was only seen in the Ab+/MG+ condition, 6 h after co-culture. Each data point represents an ROI from three independent experiments ($n = 72$ for Ab−/MG−, $n = 78$ for Ab+/MG− $n = 82$ for Ab+/MG+ and $n = 76$ for Ab−/MG+). Error bars represent SEM. One-way ANOVA with Tukey's multiple comparison test was used to evaluate statistical significance (**$p = .0031$; ***$p = .0005$; ****$p < .0001$). (c) Quantification of PSD95 positive post-synaptic puncta per unit length of dendrite. A significant decrease was only seen in the Ab+/MG+ condition after 6 h of co-culture, while the number of vGLUT1 pre-synaptic puncta per unit length of dendrite remained unchanged (d). Each data point represents an ROI from three independent experiments ($n = 72$ for Ab−/MG−, $n = 78$ for Ab+/MG−, $n = 82$ for Ab+/MG+ and $n = 76$ for Ab−/MG+). Error bars represent SEM. One-way ANOVA with Tukey's multiple comparison test was used to evaluate statistical significance (****$p < .0001$). (e) CD11b positive microglia (gray) images from Ab−/MG+ and Ab+/MG+ conditions after co-culture, reveals the accumulation of PSD95 (magenta) but not vGLUT1 (green) in microglia. (f and g) Normalized intensity of PSD95 increased while that of vGLUT1 remained unchanged inside microglia in Ab+/MG+, respectively, compared to Ab−/MG+ condition. Each data point represents a microglia cell from three independent experiments ($n = 50$ for Ab−/MG+ and $n = 51$ for Ab+/MG+). Error bars represent SEM. Unpaired *t*-test with Welch correction was used to evaluate statistical significance (**$p = .0084$).

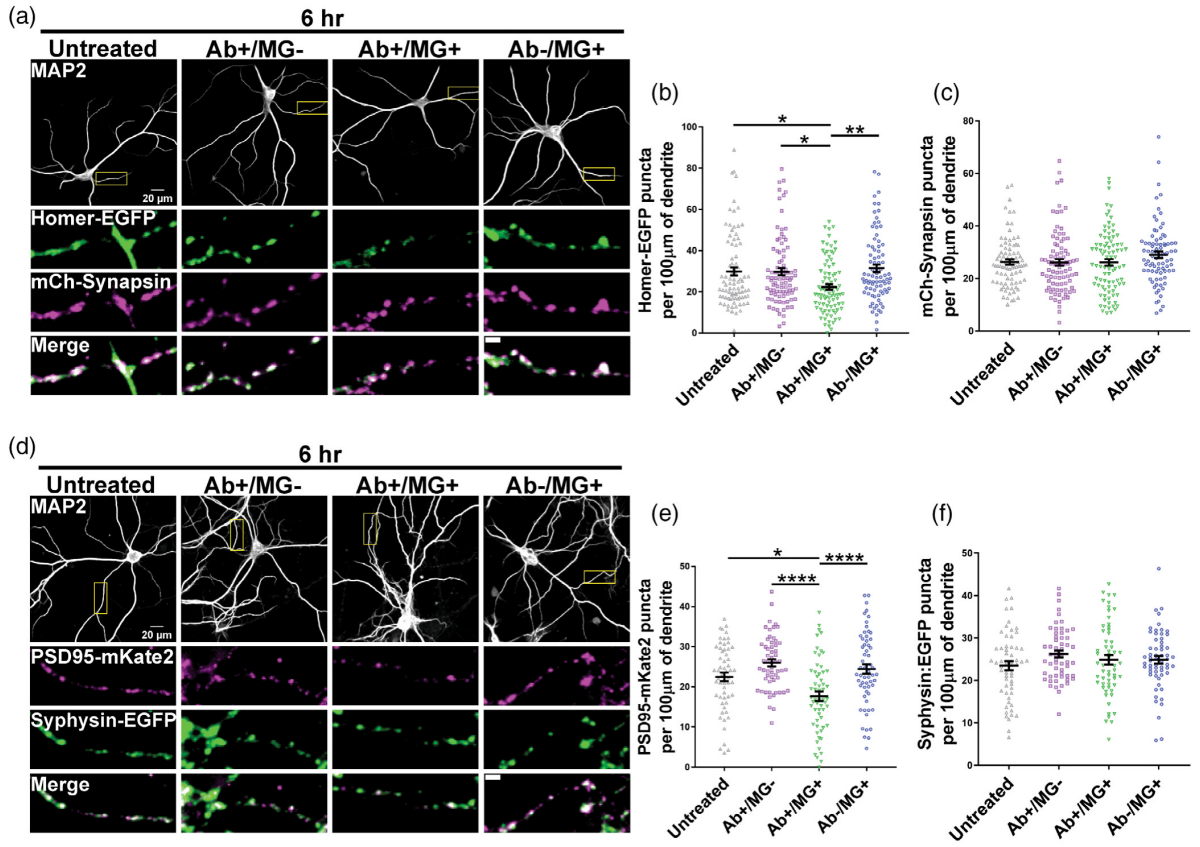

FIGURE 6 Microglia promotes hNR1-mAb mediated loss of excitatory post-synaptic but not pre-synaptic proteins. (a) Representative images of MAP2 (gray) stained neurons overexpressing mCherry(mCh)-Synapsin and Homer-EGFP from Ab−/MG−, Ab+/MG−, Ab+/MG+ and Ab−/MG+ experimental conditions after 6 h. Selected ROIs reveals distribution and overlap (merge, white) of Homer-EGFP (green) and mCh-Synapsin (magenta) positive puncta along dendritic segments. Scale bar, 5 µm. (b) Quantification of Homer-EGFP puncta number per unit length of dendrite, revealing a significant decrease only in the Ab+/MG+ condition, 6 h after co-culture. (c) Quantification of mCh-Synapsin puncta number per unit length of dendrite showed no change under any condition. Each data point represents an ROI from three independent experiments ($n = 86$ for Ab−/MG−, $n = 89$ for Ab+/MG− $n = 88$ for Ab+/MG+ and $n = 83$ for Ab−/MG+). Error bars represent SEM. One-way ANOVA with Tukey's multiple comparison test was used to evaluate statistical significance (*$p = .0118$; **$p = .0014$). (D) Representative images of MAP2 stained (gray) neurons overexpressing Synaptophysin-EGFP (Syphysin-EGFP) and PSD95-mKate2 from Ab−/MG−, Ab+/MG−, Ab+/MG+ and Ab−/MG+ experimental conditions, after 6 h. Selected ROIs show staining's for PSD95-mKate2 (magenta), Syphysin-EGFP (green) and their merge (white) puncta along dendritic segments. Scale bar, 5 µm (e) and (f) PSD95-mKate2 puncta along dendritic segments decreased only in Ab+/MG+ condition while that of Syphysin-EGFP remains unchanged, respectively. Each data point represents an ROI from two independent experiments ($n = 58$ for Ab−/MG−, $n = 57$ for Ab+/MG−, $n = 59$ for Ab+/MG+ and $n = 60$ for Ab−/MG+). Error bars represent SEM. One-way ANOVA with Tukey's multiple comparison test was used to evaluate statistical significance. (*$p = .0114$; ****$p < .0001$)

binding of the hNR1-mAb (Figure S6c,d). Surprisingly, all the mutants, that is, LALA, PA and LALA-PG had reduced FcγRI and C1q binding compared to the WT-hNR1-mAb in binding assays (Figure S6c,d). Of note the double mutant LALA-PG appeared to bind least well (Figure S6c,d). Unfortunately, these mutations reduced binding to both FcγRI and C1q, with little specificity over either receptor, an observation also reported by others (Schlothauer et al., 2016), precluding our ability to assess the individual contribution of each.

To assess the functional impact of the FcγRI and C1q binding mutations on microglia-mediated NMDAR removal, we utilized each in our neuron/microglia co-culture assay, during which each was added at 2 µg/mL, unlabeled to pre-labeled in 1:1 ratio, for 30 min before washing and adding microglia for 6 h. Here, we observed a significant decrease in the number of hNR1-mAb puncta along dendrites after 6 h only when WT hNR1-mAb* was used in co-culture (23.04 ± 1.245 for Ab+/MG− vs. 16.3 ± 0.9746 for Ab+/MG+, $p < .0001$) (Figure 7a,e). No such decrease was seen for LALA-PG (24.03 ± 0.9874 for Ab+/MG− vs. 22.51 ± 1.189 for Ab+/MG+, $p = .3281$) (Figure 7b,f), LALA (27.17 ± 0.7405 for Ab+/MG− vs. 26.69 ± 0.9778 for Ab+/MG+, $p = .6976$) (Figure 7c,g) or PA (25.56 ± 0.9195 for Ab+/MG− vs. 25.84 ± 0.9657 for Ab+/MG+, $p = .8358$) (Figure 7d,h) mutants of hNR1-mAb*. On analyzing

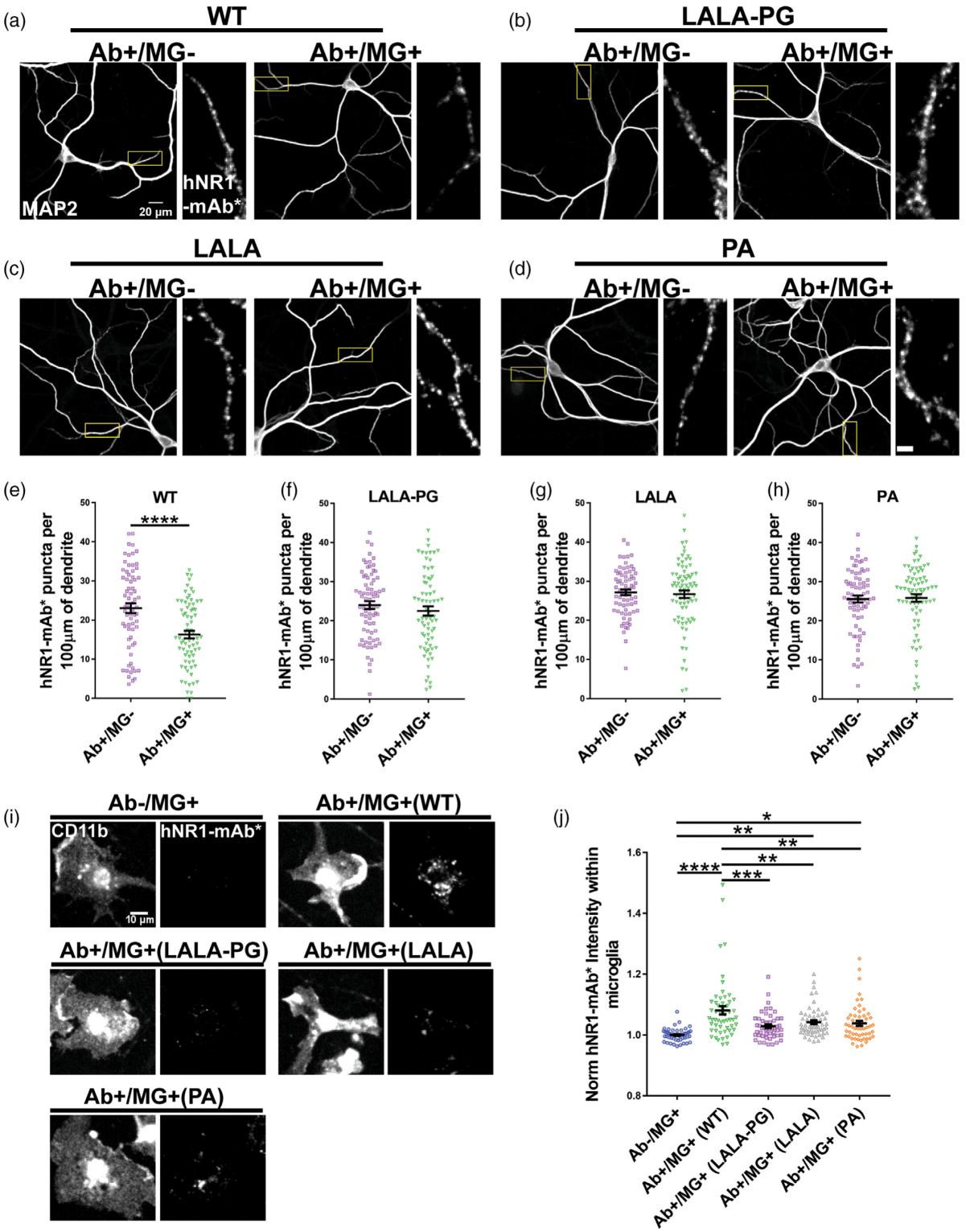

FIGURE 7 Legend on next page.

microglia from these co-culture experiments, significantly higher fluorescence intensities of antibody labeled puncta were found in CD11b positive microglia from co-cultures with WT hNR1-mAb*, while no appreciable increase was seen for the LALA-PG mutant (1 ± 0.0028 for Ab−/MG+, 1.081 ± 0.0137 for Ab+/MG+ (WT); $p < .0001$, 1.029 ± 0.0059 (LALA-PG); $p = .1255$) (Figure 7i,j). Even though less than WT, both LALA (1 ± 0.0028 for Ab−/MG+ vs. 1.042 ± 0.0.0064 for Ab+/MG+(LALA), $p = .0041$) and PA (1 ± 0.0028 for Ab−/MG+ vs. 1.038 ± 0.01028 for Ab+/MG+(PA), $p = .0127$) mutant antibodies exhibited detectable, yet low levels inside microglia (Figure 7i,j), suggesting some limited microglia receptor engagement, though without overt effects on hNR1-mAb* puncta number per unit length of dendrite (Figure 7g,h).

As the LALA and PA mutants did not allow us to cleanly separate FcγR from complement-mediated microglia engagement, we explored whether the stronger LALA-PG hNR1-mAb mutant (unlabeled) impairs microglia-mediated synapse loss in our co-culture system. This was initially accomplished by immuno-staining cultures with antibodies against vGLUT1 and PSD95 and then quantifying changes in puncta number and degree of co-localization. Here, we observed a decrease in the number of PSD95 positive puncta/unit length of dendrite (18.4 ± 0.9871 for Ab+/MG− vs. 13.32 ± 0.8324 for Ab+/MG+, $p = .0005$) (Figure 8c) and a similar decrease in the number of vGLUT1+/PSD95+ double positive puncta/unit length of dendrite (18.4 ± 0.9871 for Ab+/MG− vs. 13.32 ± 0.8324 for Ab+/MG+, $p < .0033$) (Figure 8b) 6 h after co-culturing microglia with neurons in presence of WT hNR1-mAb (Figure 8a). No such loss of synapses (vGLUT1+/PSD95+ double positive puncta) (19.65 ± 0.9473 for Ab+/MG− vs. 20.53 ± 0.9895 for Ab+/MG+, $p = .9846$) (Figure 8b) or post-synaptic PSD95 puncta (22.21 ± 0.9734 for Ab+/MG− vs. 23.62 ± 0.9876 for Ab+/MG+, $p = .8844$) (Figure 8c) was observed when the LALA-PGhNR1-mAb mutant was pre-bound to the neurons in our co-culture system (Figure 8c). The number of vGLUT1 positive puncta/unit length of dendrite remained the same for all experimental groups irrespective of whether WT or LALA-PG hNR1-mAb was present in the co-culture (Figure 8d). Consistent with this, immunostaining of PSD95 was found to be significantly higher inside microglia 6 h after co-culturing with neurons pre-bound with the WT hNR1-mAb (Figure 8e,f). Such an increase was not seen for vGLUT1 inside microglia with either WT or LALA-PG hNR1-mAb (Figure 8e,g). These data indicate that the stripping of NMDARs and post-synaptic entities by microglia requires the engagement of autoantibodies with FcγRs and/or complement receptors.

3.7 | Microglia-mediated removal of autoantibody-tagged receptors is selective

Conceptually, autoantibodies bound to neuronal receptors could either trigger microglia-mediated removal of specific receptors or through a general activation of microglia causing the unspecific upregulation of phagocytosis activity and indiscriminate removal of different receptors. To explore these options, we used another patient-derived monoclonal autoantibody that selectively binds α1 subunit of the $GABA_A$ receptor (α1-$GABA_A$R-mAb) in our co-culture setup. Initially, we investigated whether α1-$GABA_A$R-mAb, labeled with the Zenon-kit (Alexa 647) (α1-$GABA_A$R-mAb*), also induced microglia dependent removal of $GABA_A$Rs (Figure 9a). As above, labeled antibody was mixed 1:1 with unlabeled antibody (α1-$GABA_A$R-mAb*/α1-$GABA_A$R-mAb). Here, we observed a significant decrease in α1-$GABA_A$R-mAb* positive puncta along dendrites (21.88 ± 0.9537 for Ab+/MG− vs. 11.34 ± 1.001 for Ab+/MG+, $p < .0001$) (Figure 9b), 6 h after co-culture. Increased fluorescence from α1-$GABA_A$R-mAb* also seen within CD11b positive microglia (Figure 9c,d). Interestingly, we observed a higher intensity of α1-$GABA_A$R-mAb* puncta/fluorescence within microglia compared to NMDAR/NR1-mAb* (Figure S7a,b) even though the number of respective puncta/unit length of dendrite lost remained similar (Figure S7c). This is consistent with the high levels of expression of synaptic α1-$GABA_A$Rs compared to NR1/NMDARs in hippocampal cultures as reported previously (Behuet et al., 2019). Next, we utilized both the α1-$GABA_A$R-mAb and hNR1-mAb antibodies in the co-culture experiment to check for specificity of microglia-mediated removal of autoantibody tagged receptors. Initially, this was

FIGURE 7 FcRγ and C1q mutant hNR1-mAbs prevent microglia-mediated loss of NMDARs. (a–d) Representative images of neurons stained for MAP2 (gray) from Ab+/MG−, Ab+/MG+ experimental conditions after pre-labeling with either WT, LALA-PG, LALA or PA hNR1-mAb*. Selected ROIs shows hNR1-mAb* puncta (white) along dendritic segments for each of the Fc region mutant of hNR1-mAb. Scale bar, 5 μm. (e–h) Quantification of the number of hNR1-mAb* puncta per unit length of dendrite in the presence (Ab+/MG+) or absence (Ab+/MG−) of microglia. There was a significant decrease in the number of WT hNR1-mAb puncta, but not mutant antibodies (LALA-PG, LALA and PA) under Ab+/MG+ condition 6 h after co-culture. Each data point represents an ROI from three independent experiments ($n = 70$ for Ab+/MG− and $n = 74$ for Ab+/MG+) (WT hNR1-mAb, $n = 70$ for Ab+/MG− and $n = 74$ for Ab+/MG+) (LALA-PG hNR1-mAb, $n = 75$ for Ab+/MG− and $n = 72$ for Ab+/MG+) (LALA hNR1-mAb, $n = 70$ for Ab+/MG− and $n = 78$ for Ab+/MG+) (PA hNR1-mAb, $n = 73$ for Ab+/MG− and $n = 77$ for Ab+/MG+). Error bars represent SEM. Unpaired *t*-test was used to evaluate statistical significance (****$p < .0001$). For LALA hNR1-mAb* unpaired *t*-test with Welch correction was used to evaluate statistical significance as the variances were different within experimental groups. (i) Images of CD11b positive microglia with hNR1-mAb* immunoreactivity with or without different hNR1-mAb* (WT, LALA-PG, LALA or PA hNR1-mAb*) after co-culture for 6 h. Images presented in grayscale. (j) Normalized quantification of hNR1-mAb* intensity within microglia is significantly higher in Ab+/MG+ group for WT, LALA and PA hNR1-hAb* than Ab−/MG+ group. No such increase was seen in Ab+/MG+ group with LALA-PG hNR1-mAb bound to neurons after 6 h of co-culture. Each data point represents a microglia cell from three independent experiments ($n = 52–56$ for each experimental group). Error bars represent SEM. One-way ANOVA with Tukey's multiple comparison test was used to evaluate statistical significance (*$p = .0127$; **$p < .005$; ***$p = .0001$; ****$p < .0001$).

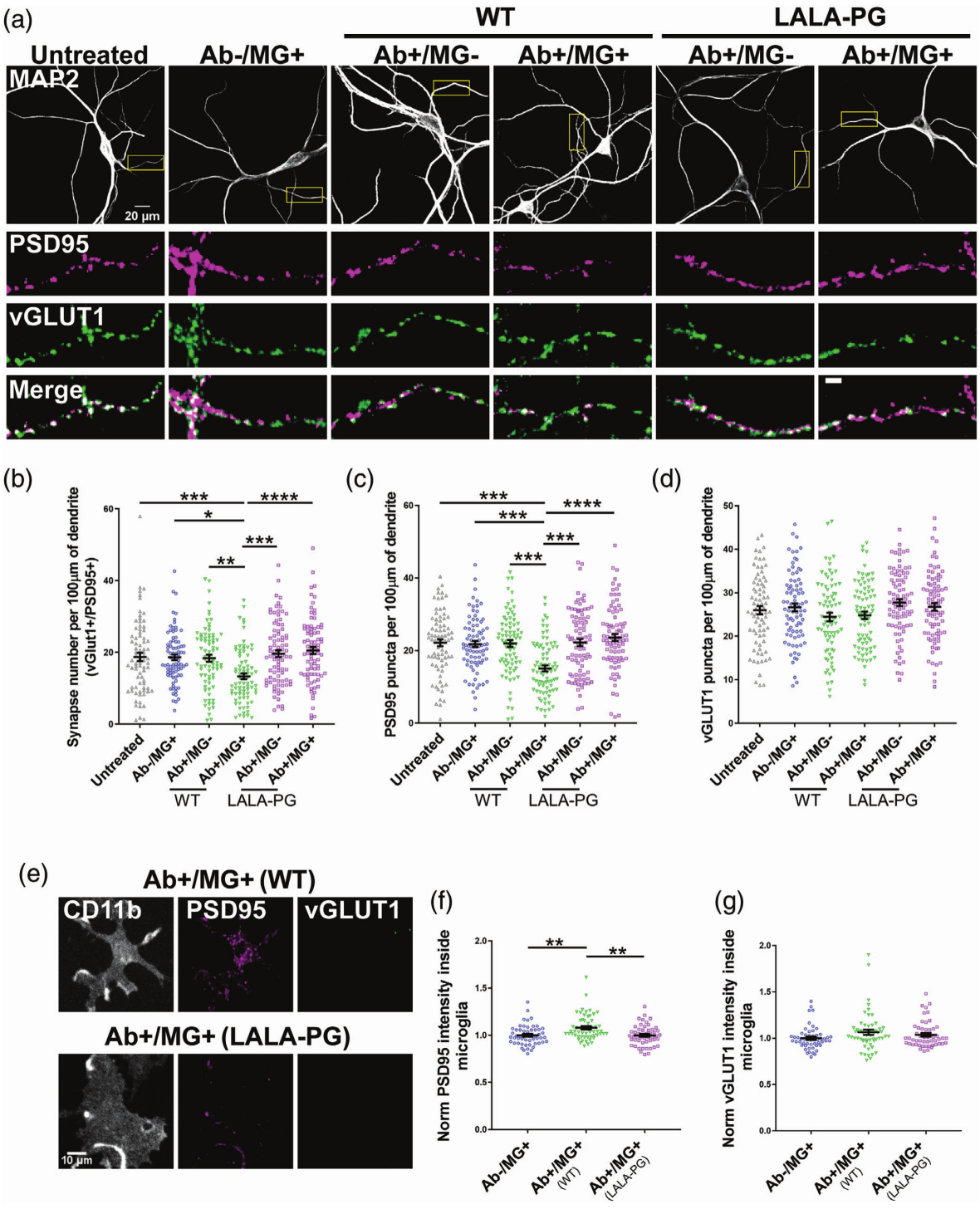

FIGURE 8 Legend on next page.

performed in a sequential labeling experiment, wherein microglia were added for 6 h to neurons pre-labeled with α1-GABA$_A$R-mAb* (Alexa 647)/α1-GABA$_A$R-mAb for 30 min (Figure 9e), followed by the addition of hNR1-mAb$^{\#}$ (Alexa 594) for 30 min before fixation. Here, we observed the expected decrease of number of α1-GABA$_A$R-mAb*/unit length of dendrite from the surface of neurons (25.63 ± 1.0190 for Ab+/MG− vs. 18.22 ± 0.8333 for Ab+/MG+, $p < .0001$) (Figure 9f), with no decrease in the number of hNR1-mAb$^{\#}$ positive puncta/unit length of dendrite (24.6 ± 0.8008 for Ab+/MG− vs. 24.7 ± 0.8437 for Ab+/MG+, $p = .9340$) (Figure 9g). To further validate this selective microglial action, we performed the converse experiment, wherein neuronal cultures were initially labeled with hNR1-mAb* (Alexa 647)/hNR1-mAb for 30 min before the addition of microglia for 6 h. Subsequently, co-cultures were labeled with α1-GABA$_A$R-mAb$^{\#}$ (Alexa 594) for 30 min fixed and imaged (Figure 9h). Again, we observed a significant decrease in hNR1-mAb* puncta (26.83 ± 1.006 for Ab+/MG− vs. 17.38 ± 0.8523 for Ab+/MG+, $p < .0001$) (Figure 9i), while the number of α1-GABA$_A$R-mAb$^{\#}$ puncta/unit length of dendrite remained unchanged (24.37 ± 1.032 for Ab+/MG− vs. 25.74 ± 0.9905 for Ab+/MG+, $p = .3397$) (Figure 9j). These data indicate that microglia can selectively remove autoantibody-tagged receptors and do not necessarily cause an unspecific removal of other neuronal receptors.

To explore this concept further, we examined whether microglia can distinguish between two antibodies added simultaneously. This allowed us to also compare the importance of the Fc region by pairing WT and LALA-PG mutant antibodies. This was accomplished by co-labeling neuronal culture for 30 min, with α1-GABA$_A$R-mAb$^{\#}$/α1-GABA$_A$R-mAb together with either the WT (Figure 10a) or LALA-PG mutant (Figure 10d) of the hNR1-mAb*/hNR1-mAb, before washing and adding microglia. When α1-GABA$_A$R-mAb$^{\#}$ and WT hNR1-mAb* were simultaneously bound to neurons and microglia then added for 6 h, we detected a significant reduction in the number of both α1-GABA$_A$R-mAb$^{\#}$ (22.06 ± 0.8494 for Ab+/MG− vs. 14.09 ± 0.9742 for Ab+/MG+, $p < .0001$) (Figure 10b) and hNR1-mAb* (23.9 ± 1.131 for Ab+/MG− vs. 14.42 ± 0.9521 for Ab+/MG+, $p < .0001$) (Figure 10c) puncta along dendrites. However, when α1-GABA$_A$R-mAb$^{\#}$ and LALA-PG hNR1-mAb* were present together in co-culture, there was a selective loss of α1-GABA$_A$R-mAb$^{\#}$ puncta (22.18 ± 1.248 for Ab+/MG− vs. 13.19 ± 1.013 for Ab+/MG+, $p < .0001$) (Figure 10e) from the surface of neurons, while the number of LALA-PG hNR1-mAb* puncta remained unchanged (25.68 ± 1.143 for Ab+/MG− vs. 27.37 ± 1.507 for Ab+/MG+, $p = .3719$) (Figure 10f). Taken together, these results indicate that microglia selectively remove autoantibody-tagged receptors via functional FcγRI and C1q binding sites within the Fc regions of these antibodies.

4 | DISCUSSION

Autoantibodies, implicated in autoimmune encephalitis, have been shown to employ different mechanisms leading to pathogenic outcomes. These include binding and blocking receptor function like GABA$_B$R (Dalmau & Graus, 2018) and GlyR (Rauschenberger et al., 2020), triggering receptor crosslinking driven internalization, like NMDAR (Hughes et al., 2010; Kreye et al., 2016) and inhibiting receptor ligand interaction like in leucine-rich glioma-inactivated 1 (LGI1) (Kornau et al., 2020; Ohkawa et al., 2013). Additionally, autoantibodies can also lead to inflammation and cell death via complement activation, for example, AQP4 (Sabater et al., 2009; Soltys et al., 2019). However, the role of encephalitis patient-derived autoantibodies in activating resident and infiltrating immune cells of the CNS through FcγR binding and non-classical pathway of complement mediated opsonisation of antigen remains largely unexplored.

In this study, using patient-derived recombinant hNR1-mAb in a neuron/microglia co-culture setup, we report that hNR1-mAb bound to NMDARs led to microglia engagement and loss of NMDAR/hNR1-mAb complexes from hippocampal neurons (Figure 3a–c). Concomitantly, these complexes appeared to accumulate within CD11b positive microglia (Figure 3c,d) inside Lamp2a+ and CD68+ lysosomal compartments (Figure 2e,f). The receptor removal was specific to the NR1 autoantibody-bound NMDARs, as we did not observe changes in

FIGURE 8 LALA-PG hNR1-mAb mutant prevents microglia-mediated synapse loss. (a) Representative images of neurons stained for MAP2 (gray) from untreated (Ab−/MG−), Ab+/MG−, Ab+/MG+ and Ab−/MG+ experimental groups for both WT and LALA-PG hNR1-mAb after 6 h. Selected ROIs shows immune-staining for PSD95 (magenta), vGLUT1 (green) and their merge (white) puncta along dendritic segments. Scale bar, 5 μm. (b) Quantification of the number of synapses (vGLUT1+/PSD95+ puncta) per unit length of dendrite. Data show a significant decrease only in synapse number with the WT hNR1-mAb containing Ab+/MG+ group 6 h after co-culture. Each data point represents an ROI from three independent experiments ($n = 78$ for Ab−/MG−, $n = 82$ Ab−/MG+, $n = 78$ for Ab+/MG−; $n = 80$ for Ab+/MG+ for WT hNR1-mAb, $n = 87$ for Ab+/MG−; $n = 85$ for Ab+/MG+ for LALA-PG hNR1-mAb). Error bars represent SEM. One-way ANOVA with Tukey's multiple comparison test was used to evaluate statistical significance (**$p < .003$; ***$p < .00001$). (C) Quantification of the number of PSD95 puncta per unit length of dendrite. Data reveal a decrease PSD95 puncta number in the WT hNR1-mAb containing Ab+/MG+ group after 6 h of co-culture, while the number of vGLUT1 pre-synaptic puncta remains unchanged in all experimental groups (d). Each data point represents an ROI from three independent experiments ($n = 78$ for Ab−/MG−, $n = 82$ Ab−/MG+, $n = 78$ for Ab+/MG−; $n = 80$ for Ab+/MG+ for WT hNR1-mAb, $n = 87$ for Ab+/MG−; $n = 85$ for Ab+/MG+ for LALA-PG hNR1-mAb). Error bars represent SEM. One-way ANOVA with Tukey's multiple comparison test was used to evaluate statistical significance (****$p < .00001$). (e) Images of microglia labeled with CD11b (gray) showing an increase PSD95 (magenta) staining inside microglia in WT hNR1-mAb treated group (Ab+/MG+) as compared to LALA-PG (Ab+/MG+) group. No significant staining for vGLUT1 (green) was observed inside microglia for any experimental group. Each data point represents a microglia cell from three independent experiments ($n = 53$ for Ab−/MG+, $n = 57$ for WT hNR1-mAb Ab+/MG+, $n = 51$ for LALA-PG hNR1-mAb Ab+/MG+). Error bars represent SEM. One-way ANOVA with Tukey's multiple comparison test was used to evaluate statistical significance (**$p < .005$).

$GABA_AR$ numbers after addition of microglia (Figure 9h–j). Similar results were obtained with a second patient-derived monoclonal against $GABA_ARs$. Here, again the α1-$GABA_AR$-mAb triggered a significant decrease in $GABA_AR$ puncta 6 h after microglia addition, without changes in the number of NMDARs (Figure 9e–g). Hence, we could show that antibody-dependent removal of receptors by microglia can be specific to the bound antibody and its target receptor.

Gestational transfer of patient-derived NR1-Abs was recently reported to cause a reduction in number of synapses as well as

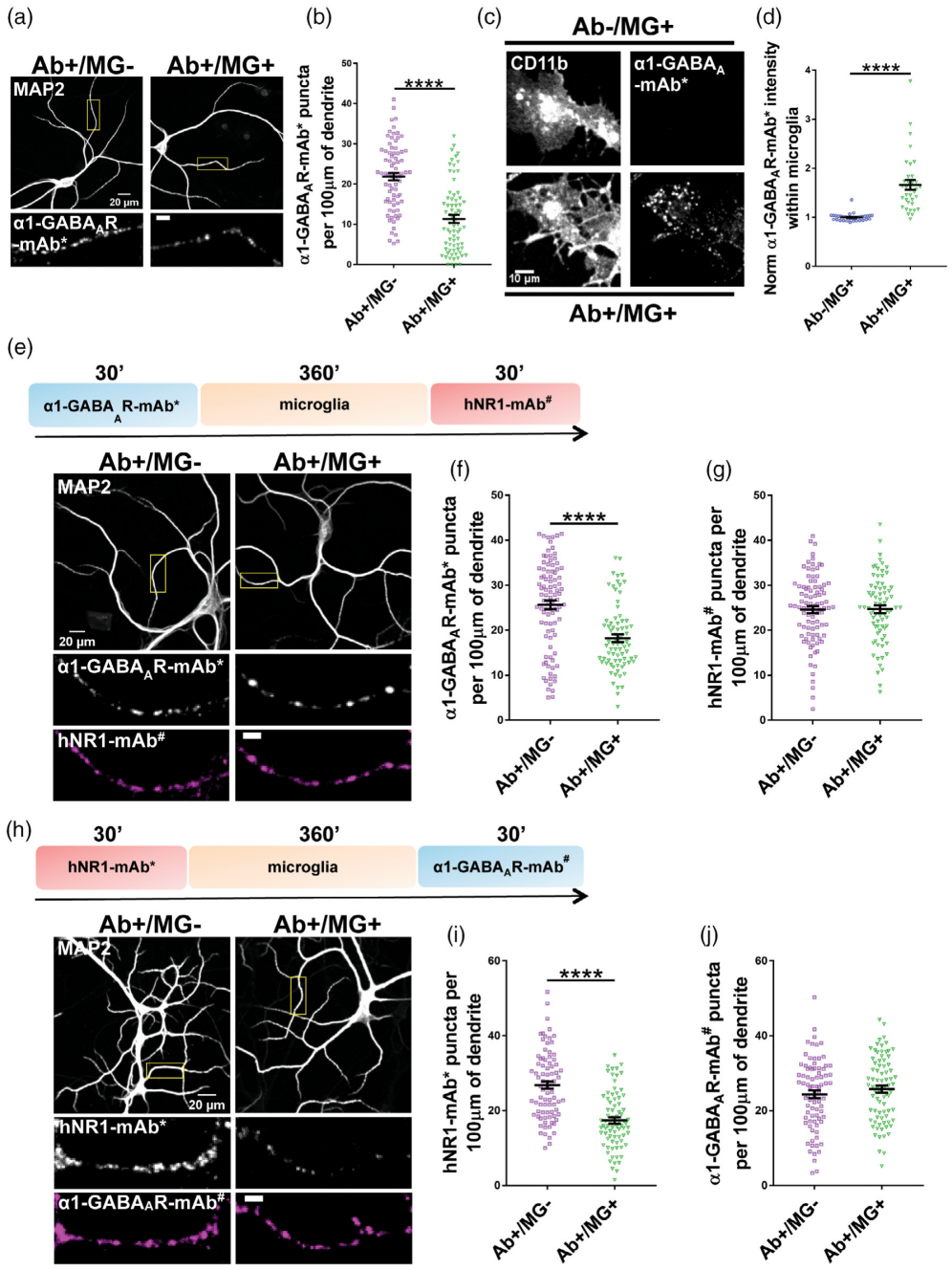

FIGURE 9 Legend on next page.

microglial activation in the hippocampus of postnatal mice following intrauterine exposure to patient IgGs (García-Serra et al., 2021). Consistent with a role of microglia in this clearance, we observed a significant decrease in the number of synapses 6 h after the addition of microglia to hNR1-mAb bound hippocampal neurons (Figure 5). Intriguingly, we observed a specific loss of post-synaptic markers like PSD95 and Homer1 without changes in markers of pre-synapse like vGLUT1, Synapsin1 and Synaptopysin, (Figures 5 and 6) which could be due to a majority of NMDARs being localized post-synaptically (Ehlers et al., 1995; Zhang et al., 2013). It should be noted that while significant changes in synaptic number was only detected after 6 h, microglia were capable in live-imaging and EM experiments of removing such complexes within the first hour. This delay would be related to the kinetics of synapse removal, migration rates of microglia and total number of labeled synapses.

Previous studies have reported the role of microglia in synapse pruning during development (Paolicelli et al., 2011; Schafer et al., 2012) and in neurodegenerative disorders like Alzheimer's disease (Hong et al., 2016; Rajendran & Paolicelli, 2018). Interestingly, others have shown that oligomeric amyloid beta (oAβ) localizes to post-synapses (Koffie et al., 2009; Lacor et al., 2004) and that such a post-synaptic localization requires NMDARs (Decker et al., 2010; Li et al., 2011). This oAβ localization at post-synapses has been reported to trigger microglia dependent removal of synapses, more intriguingly, only post-synapses, via post-synaptic complement deposition, in pre-plaque brains (3–4 months post-natal) of APP/PS1 mice (Hong et al., 2016). These studies add to our observation that hNR1-mAb bound NMDARs can cause microglia to selectively remove post-synaptic components. However, here we could not distinguish between whether microglia in the presence of bound hNR1-mAb removes only NMDAR associated post-synaptic proteins or the entire post-synaptic density (PSD), leaving behind previously reported orphan synapses with just the associated pre-synaptic bouton (Krueger et al., 2003; Liberman & Liberman, 2015). Another important unanswered question in our study is whether microglia can access the synaptic cleft to remove the whole post-synaptic density or whether hNR1-mAbs, or other pathogenic proteins like oAβ, first promote the lateral movement of receptors and different post-synaptic proteins into an extra synaptic space, from where they are more accessible for microglia-mediated clearance. Further work will be needed to address this important question.

Several studies have investigated the potential of antibody against self and non-self antigens to engage and activate immune cells. For example, monoclonal antibodies targeting specific cancer-associated proteins have been shown to bind FcγRs on macrophages leading to antibody-dependent cellular phagocytosis (ADCP), thereby killing tumor cells (Scott et al., 2012; Zhou et al., 2020). Similarly, autoantibodies involved in Inflammatory Rheumatoid Arthritis (IRA) have been reported to activate non-classical mode of complement activation (Ji et al., 2002), as well as engage FcγRs on macrophages leading to release of inflammatory cytokines like IL-6, IL-1β and TNFα (Ludwig et al., 2017) that increase osteoclast activity, ultimately reducing bone density (Zuo & Deng, 2021). Within CNS, antibodies against myelin oligodendrocyte glycoprotein (MOG) have been observed to promote the uptake and presentation of MOG via binding to FcγRs on myeloid antigen presenting cells (APCs), that is, macrophages and dendritic cells and resident phagocytes of the CNS, that is, microglia and astrocytes thereby leading to enhanced effector T cell engagement (Flach et al., 2016; Kinzel et al., 2016). In neuromyelitis optica (NMO), AQP4 reactive IgG resulted in microglia/macrophage reactivity in lesions along with complement activation (Lucchinetti et al., 2014). Furthermore, in microglia ablation studies wherein

FIGURE 9 Microglia selectively removes only autoantibody-bound receptors. (a) Images of MAP2 (gray) stained hippocampal neurons pre-labeled with α1-GABA$_A$R-mAb* (Alexa647) with or without microglia addition (i.e., Ab+/MG+ and Ab+/MG−) after 6 h. Selected ROIs shows immuno-staining for α1-GABA$_A$R-mAb* puncta (white) along dendritic segments. Scale bar, 5 μm. (b) Quantification of the number of α1-GABA$_A$R-mAb* puncta per unit length of dendrite reveals decrease in Ab+/MG+ group 6 h after co-culture. Each data point represents an ROI from three independent experiments ($n = 77$ for Ab+/MG−, $n = 73$ Ab+/MG+). Error bars represent SEM. Unpaired *t*-test was used to evaluate statistical significance (****$p < .00001$). (c) CD11b positive microglia with accumulated α1-GABA$_A$R-mAb* immunoreactivity in Ab+/MG + but not Ab−/MG+ condition. Images represented in grayscale. (d) Normalized intensity of α1-GABA$_A$R-mAb* fluorescence inside microglia was higher in Ab+/MG+ over Ab−/MG+ condition. Each data point represents a microglial cell over three independent experiments ($n = 35$ for Ab−/MG+, $n = 35$ Ab+/MG+). Error bars represent SEM. Unpaired *t*-test with Welch correction was used to evaluate statistical significance (****$p < .00001$). (e) Representative images of neurons with MAP2 staining (gray) with bound α1-GABA$_A$R-mAb* (Alexa647) with or without microglia addition for 6 h. Upper panel is a schematic of the experimental setup. Pre-labeled hNR1-mAb$^{\#}$ (Alexa 594) was added for 30 min after the 6 h microglia incubation. ROIs shows α1-GABA$_A$R-mAb*(white) and hNR1-mAb$^{\#}$ (magenta) puncta along dendritic segments. Scale bar, 5 μm. (f) Quantification of α1-GABA$_A$R-mAb* puncta number per unit length of dendrite reveals a significant reduction in puncta number in the presence of microglia Ab+/MG+. (g) The number of hNR1-mAb$^{\#}$ puncta per unit length of dendrite did not change. Each data point represents an ROI from three independent experiments ($n = 94$ for Ab+/MG−, $n = 78$ for Ab+/MG+). Error bars represent SEM. Unpaired *t*-test was used to evaluate statistical significance (****$p < .00001$). Unpaired *t*-test with Welch correction was used to evaluate statistical significance for hNR1-mAb$^{\#}$ puncta per unit length. (h) Representative images of MAP2 stained neurons (gray) with bound hNR1-mAb* (Alexa 647) with or without microglia addition for 6 h. Pre-labeled α1-GABA$_A$R-mAb$^{\#}$ (Alexa 594) was added for 30 min after 6 h. Upper panel is a schematic of the experimental setup. ROIs shows hNR1-mAb* (white) and α1-GABA$_A$R-mAb$^{\#}$ (magenta) puncta along dendritic segments. Scale bar, 5 μm. (i, j) Quantitation of hNR1-mAb* or α1-GABA$_A$R-mAb$^{\#}$ puncta per unit length of dendrite. hNR1-mAb* puncta number was significantly reduced in presence of microglia Ab+/MG+, while the number of α1-GABA$_A$R-mAb$^{\#}$ puncta per unit length of dendrite did not change. Each data point represents an ROI from three independent experiments ($n = 82$ for Ab+/MG−, $n = 78$ for Ab+/MG+). Error bars represent SEM. Unpaired *t*-test with Welch correction was used to evaluate statistical significance (****$p < .00001$).

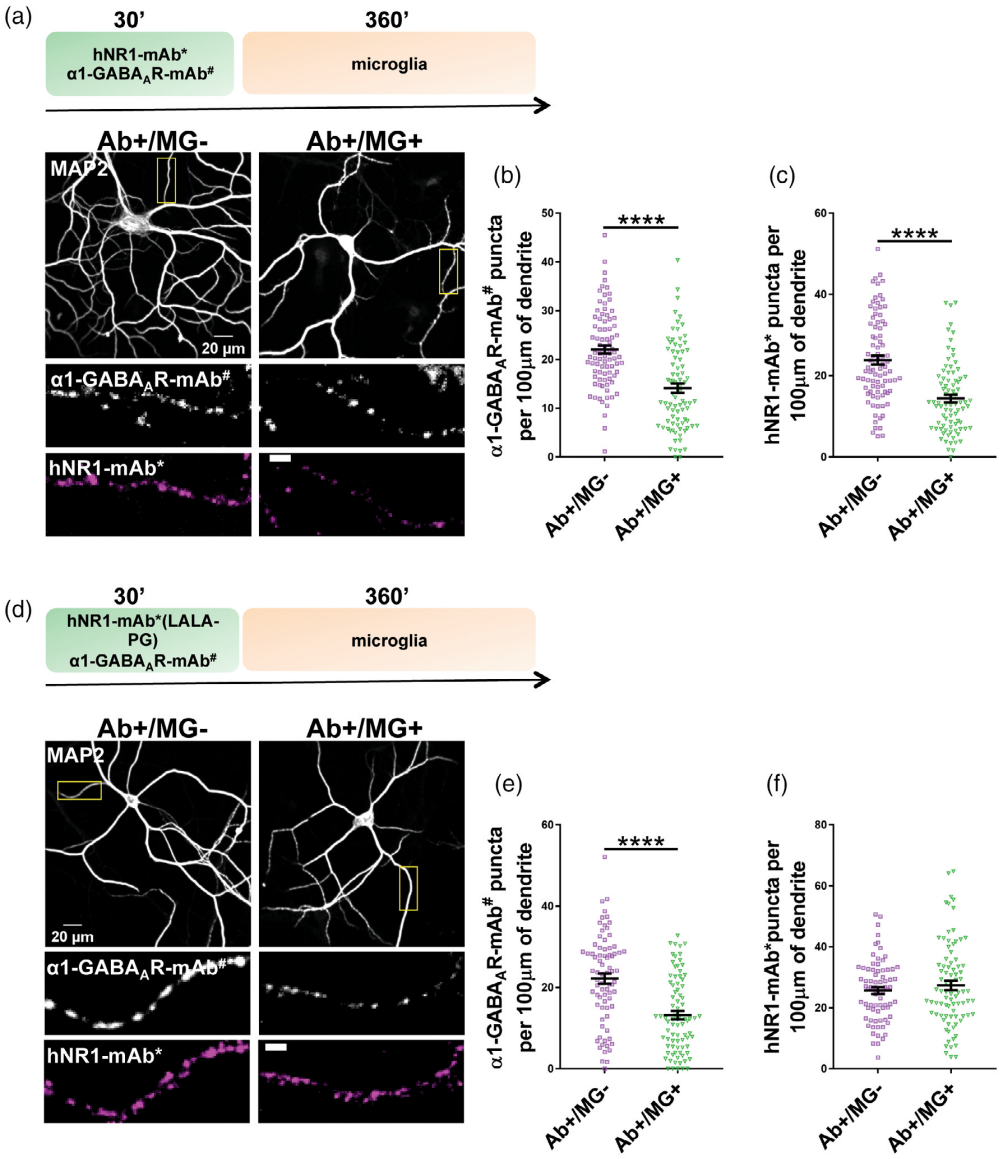

FIGURE 10 Microglia mediates the selective removal of receptors bound by WT but not LALA-PG mutated autoantibodies. (a) Schematic depicting the experimental setup (upper panel). Representative images of MAP2 stained neurons (gray) bound with α1-GABA$_A$R-mAb$^{\#}$ (Alexa 594) and hNR1-mAb* (Alexa 647) with (Ab+/MG+) or without (Ab+/MG−) microglia addition for 6 h. ROIs show α1-GABA$_A$R-mAb$^{\#}$ (white) and hNR1-mAb* (magenta) puncta along dendritic segments. Scale bar, 5 μm. (b and c) Quantification of α1-GABA$_A$R-mAb$^{\#}$ and hNR1-mAb* puncta number per unit length of dendrite, respectively. The number of both was significantly reduced in the presence of microglia Ab+/MG+. Each data point represents an ROI from three independent experiments ($n = 87$ for Ab+/MG−, $n = 83$ for Ab+/MG+). Error bars represent SEM. Unpaired t-test was used to evaluate statistical significance (****$p < .00001$). (d) Schematic depicting the experimental setup (upper panel). Representative images of neurons with MAP2 staining (gray) with bound α1-GABA$_A$R-mAb$^{\#}$ (Alexa 594) and LALA-PG hNR1-mAb* (Alexa 647) with or without microglia addition for 6 h. ROIs show α1-GABA$_A$R-mAb$^{\#}$ (white) and hNR1-mAb* (magenta) puncta along dendritic segments. Scale bar, 5 μm. (e and f) Quantitation of α1-GABAR-mAb$^{\#}$ and LALA-PG hNR1-mAb* puncta number per unit length of dendrite, respectively. α1-GABAR-mAb$^{\#}$ number was reduced significantly in presence of microglia Ab+/MG+, with no change in the number of LALA-PG hNR1-mAb* puncta along dendritic segments. Each data point represents an ROI from three independent experiments ($n = 77$ for Ab+/MG−, $n = 84$ for Ab+/MG+). Error bars represent SEM. Unpaired t-test was used to evaluate statistical significance (****$p < .00001$).

NMO-IgG was infused in to the spinal cord of mice, no motor impairment was observed when microglia were absent, but appeared around 5 days post ablation once microglia were allowed to replenish (T. Chen et al., 2020). Taken together, these studies highlight the relevance of autoantibody dependent FcγR and complement-driven activation of microglia and the associated downstream mechanisms in the etiology and pathology of specific autoimmune disorders.

At present it is less clear how and when such immune-mechanism manifest in patients with autoimmune encephalitis. Interestingly different antibody classes have been implicated, in for example, NMDAR autoimmune encephalitis, wherein IgG, IgA and IgM antibodies against NMDARs have all been isolated from sera of patients (Hara et al., 2018). Within the IgG subtype, IgG1 was reported to be the predominant subtype found in patients with NMDAR encephalitis (Tüzün et al., 2009). IgG1 and IgG3 subtypes have been shown to more efficiently trigger complement deposition as well as bind to different FcγRs expressed on the surface of myeloid cells and APCs (Dekkers et al., 2017; Vidarsson et al., 2014; Wang et al., 2018).

The recombinant hNR1-mAb used in this study belongs to the IgG1 subtype and can bind both to FcγRs and complement proteins like C1q (Figure S6c,d). By introducing point mutations described previously (LALA-PG, PA and LALA) (Lo et al., 2017; Saunders, 2019) into critical sites in the Fc region of hNR1-mAb, we could block its downstream interactions with FcγR1 and C1q complement protein. Surprisingly, we were unable to selectively dampen one interaction over the other as all three sets of mutations affected both FcγR1 and C1q binding (Figure S6c,d). This has been reported previously (Schlothauer et al., 2016) and could be due to partially overlapping binding regions of FcγRs and C1q (Vidarsson et al., 2014). Nonetheless, LALA-PG hNR1-mAb mutant was found to be highly effective in blocking both FcγR1 and C1q binding (Figure S6c,d). Importantly, blocking both FcγR1 and C1q binding and their subsequent downstream signaling, utilizing LALA-PG hNR1-mAb, prevented microglia-mediated loss of NMDAR puncta (Figure 7b,f) and synapses (Figure 8a–d) in our co-culture experiment. This suggests that NMDAR-bound hNR1-mAbs engage microglia using their Fc region either via FcγR and or complement binding leading to antibody dependent removal of NMDAR and synapses by microglia. Intriguingly, previous studies reported the lack of complement activation in patients with autoimmune encephalitis (Bien et al., 2012; Josep Dalmau et al., 2008; Tüzün et al., 2009). Although, these studies were performed on biopsied brain, one cannot rule out a role for complement at earlier phases of these diseases. Interestingly, all of these studies report prominent microgliosis in brains of these patients. Although there are obvious limitations of our *in-vitro* co-culture setup, as well as lack of specificity of our autoantibody Fc region mutants for complement vs FcγR, our data strongly indicate that engagement of autoantibodies via their Fc domains with complement and FcγR are critical interactions, promoting microglia-mediated removal of antibody labeled neurotransmitter receptors (e.g., NMDAR & $GABA_AR$), concepts worth further investigation *in-vivo*.

In conclusion, our results argue that NMDAR/$GABA_AR$ autoantibodies can cause engagement of microglia, in addition to previously reported receptor crosslinking and internalization (Hughes et al., 2010), promoting the loss of neurotransmitter receptors and synapses, thereby contributing to the etiology of autoantibody associated encephalitis symptoms and pathology. Further work is required to understand how autoantibody/receptor complexes lead to microglia activation and the associated release of inflammatory cytokines, which could in turn coordinate and recruit peripheral B cells, T cells and macrophages in sustaining and possibly worsening disease pathology. This study is an important step toward understanding this important yet poorly explored role of microglia in autoimmune encephalitis, as a common mechanism for disorders wherein pathogenic antibodies such as IgG1/ IgG3 subtypes are present, for example, in NMDAR and $GABA_AR$ encephalitis.

AUTHOR CONTRIBUTIONS

Kazi Atikur Rahman, Ayub Boulos, Ewa Andrzejak, Craig C. Garner, and Aleksandra Ichkova designed research; Kazi Atikur Rahman, Marta Orlando and Ayub Boulos performed research; Kazi Atikur Rahman, Marta Orlando and Aleksandra Ichkova analyzed data; Harald Prüss provided the antibodies; Noam E. Ziv provided constructs; Kazi Atikur Rahman wrote the first draft of the paper; Kazi Atikur Rahman, Marta Orlando, Ewa Andrzejak, Ayub Boulos, Dietmar Schmitz, Noam E. Ziv, Craig C. Garner, Aleksandra Ichkova and Harald Prüss edited the paper; Kazi Atikur Rahman, Craig C. Garner and Aleksandra Ichkova wrote the paper. Craig C. Garner and Dietmar Schmitz acquired funding. The authors declare no competing financial interest.

ACKNOWLEDGMENTS

This work was supported by the Einstein Foundation Berlin; by the German Center for Neurodegenerative Diseases; by the German Research Foundation Deutsche Forschungsgemeinschaft (DFG) (project 184695641—SFB 958 to C.C.G and D.S., project 327654276—SFB 1315 to D.S., project 415914819—FOR 3004 to. D.S., project 431572356 to D.S., under Germany's Excellence Strategy—Exc-2049-390688087 to D.S. and C.C.G., PR1274/3-1, PR1274/4-1, PR1274/5-1 to H.P.); by the Helmholtz Association (HIL-A03 to H.P.); by the German Federal Ministry of Education and Research (BMBF) (Connect-Generate 01GM1908D to H.P., SmartAge—project 01GQ1420B to D.S.); and by the European Research Council (ERC) under the European Union's Horizon 2020 research and innovation program (Grant agreement No. 810580 to D.S.). We thank Sabina Tahirovic for her intellectual inputs, Jakob Kreye for his inputs, Thorsten Trimbuch and the Viral Core Facility of the Charité-Universitätsmedizin Berlin for cloning and production of viral constructs; Anny Kretschmer, Chrsistine Bruns and Berit Söhl-Kielczynski for technical assistance; and the Advanced Medical Bioimaging Core Facility (AMBIO) of the Charité-Universitätsmedizin for support in acquisition of the light microscopy data and the Electron Microcroscopy Laboratory of the Institute of Integrative Neuroanatomy for granting us the access to their instruments.

DATA AVAILABILITY STATEMENT

The data that support the findings of this study are available from the corresponding authors upon reasonable request.

ORCID

Kazi Atikur Rahman https://orcid.org/0000-0001-8124-6026

REFERENCES

Andrzejak, E., Rabinovitch, E., Kreye, J., Prüss, H., Rosenmund, C., Ziv, N. E., Garner, C. C., & Ackermann, F. (2022). Patient-derived anti-NMDAR antibody disinhibits cortical neuronal networks through dysfunction of inhibitory neuron output. *The Journal of Neuroscience.*, *42* (15), 3253–3270. https://doi.org/10.1523/JNEUROSCI.1689-21.2022

Banker, G., & Goslin, K. (1988). Developments in neuronal cell culture. *Nature*, *336*(6195), 185–186. https://doi.org/10.1038/336185a0

Barry, H., Hardiman, O., Healy, D. G., Keogan, M., Moroney, J., Molnar, P. P., Cotter, D. R., & Murphy, K. C. (2011). Anti-NMDA receptor encephalitis: An important differential diagnosis in psychosis. *The British Journal of Psychiatry*, *199*(6), 508–509. https://doi.org/10.1192/bjp.bp.111.092197

Behuet, S., Cremer, J. N., Cremer, M., Palomero-Gallagher, N., Zilles, K., & Amunts, K. (2019). Developmental changes of glutamate and GABA receptor densities in Wistar rats. *Frontiers in Neuroanatomy*, *13*, 100. https://doi.org/10.3389/fnana.2019.00100

Bien, C. G., Vincent, A., Barnett, M. H., Becker, A. J., Blümcke, I., Graus, F., Jellinger, K. A., Reuss, D. E., Ribalta, T., Schlegel, J., Sutton, I., Lassmann, H., & Bauer, J. (2012). Immunopathology of autoantibody-associated encephalitides: Clues for pathogenesis. *Brain*, *135*(5), 1622–1638. https://doi.org/10.1093/brain/aws082

Bournazos, S., Wang, T. T., Dahan, R., Maamary, J., & Ravetch, J. V. (2017). Signaling by antibodies: Recent Progress. *Annual Review of Immunology*, *35*, 285–311. https://doi.org/10.1146/annurev-immunol-051116-052433

Camdessanché, J. P., Streichenberger, N., Cavillon, G., Rogemond, V., Jousserand, G., Honnorat, J., Convers, P., & Antoine, J. C. (2011). Brain immunohistopathological study in a patient with anti-NMDAR encephalitis. *European Journal of Neurology*, *18*(6), 929–931. https://doi.org/10.1111/j.1468-1331.2010.03180.x

Chen, A. K., Cheng, Z., Behlke, M. A., & Tsourkas, A. (2008). Assessing the sensitivity of commercially available fluorophores to the intracellular environment. *Analytical Chemistry*, *80*(19), 7437–7444. https://doi.org/10.1021/ac8011347

Chen, T., Lennon, V. A., Liu, Y. U., Bosco, D. B., Li, Y., Yi, M. H., Zhu, J., Wei, S., & Wu, L. J. (2020). Astrocyte-microglia interaction drives evolving neuromyelitis optica lesion. *The Journal of Clinical Investigation*, *130*(8), 4025–4038. https://doi.org/10.1172/jci134816

Coutinho, E., Menassa, D. A., Jacobson, L., West, S. J., Domingos, J., Moloney, T. C., Lang, B., Harrison, P. J., Bennett, D. L. H., Bannerman, D., & Vincent, A. (2017). Persistent microglial activation and synaptic loss with behavioral abnormalities in mouse offspring exposed to CASPR2-antibodies in utero. *Acta Neuropathologica*, *134*(4), 567–583. https://doi.org/10.1007/s00401-017-1751-5

Dalmau, J., Armangué, T., Planagumà, J., Radosevic, M., Mannara, F., Leypoldt, F., Geis, C., Lancaster, E., Titulaer, M. J., Rosenfeld, M. R., & Graus, F. (2019). An update on anti-NMDA receptor encephalitis for neurologists and psychiatrists: Mechanisms and models. *The Lancet Neurology*, *18*(11), 1045–1057. https://doi.org/10.1016/S1474-4422(19)30244-3

Dalmau, J., Gleichman, A. J., Hughes, E. G., Rossi, J. E., Peng, X., Lai, M., Dessain, S. K., Rosenfeld, M. R., Balice-Gordon, R., & Lynch, D. R. (2008). Anti-NMDA-receptor encephalitis: Case series and analysis of the effects of antibodies. *The Lancet Neurology*, *7*(12), 1091–1098. https://doi.org/10.1016/S1474-4422(08)70224-2

Dalmau, J., & Graus, F. (2018). Antibody-mediated encephalitis. *The New England Journal of Medicine*, *378*(9), 840–851. https://doi.org/10.1056/NEJMra1708712

Dalmau, J., Tüzün, E., Wu, H. Y., Masjuan, J., Rossi, J. E., Voloschin, A., Baehring, J. M., Shimazaki, H., Koide, R., King, D., Mason, W., Sansing, L. H., Dichter, M. A., Rosenfeld, M. R., & Lynch, D. R. (2007). Paraneoplastic anti–N-methyl-D-aspartate receptor encephalitis associated with ovarian teratoma. *Annals of Neurology*, *61*(1), 25–36. https://doi.org/10.1002/ana.21050

Day, G. S., High, S. M., Cot, B., & Tang-Wai, D. F. (2011). Anti-NMDA-receptor encephalitis: Case report and literature review of an under-recognized condition. *Journal of General Internal Medicine*, *26*(7), 811–816. https://doi.org/10.1007/s11606-011-1641-9

Decker, H., Jürgensen, S., Adrover, M. F., Brito-Moreira, J., Bomfim, T. R., Klein, W. L., Epstein, A. L., De Felice, F. G., Jerusalinsky, D., & Ferreira, S. T. (2010). N-Methyl-d-aspartate receptors are required for synaptic targeting of Alzheimer's toxic amyloid-β peptide oligomers. *Journal of Neurochemistry*, *115*(6), 1520–1529. https://doi.org/10.1111/j.1471-4159.2010.07058.x

Dekkers, G., Bentlage, A. E. H., Stegmann, T. C., Howie, H. L., Lissenberg-Thunnissen, S., Zimring, J., Rispens, T., & Vidarsson, G. (2017). Affinity of human IgG subclasses to mouse Fc gamma receptors. *MAbs*, *9*(5), 767–773. https://doi.org/10.1080/19420862.2017.1323159

Ehlers, M. D., Tingley, W. G., & Huganir, R. L. (1995). Regulated subcellular distribution of the NR1 subunit of the NMDA receptor. *Science*, *269*(5231), 1734–1737. https://doi.org/10.1126/science.7569904

Flach, A.-C., Litke, T., Strauss, J., Haberl, M., Gómez, C. C., Reindl, M., Saiz, A., Fehling, H.-J., Wienands, J., Odoardi, F., Lühder, F., & Flügel, A. (2016). Autoantibody-boosted T-cell reactivation in the target organ triggers manifestation of autoimmune CNS disease. *Proceedings of the National Academy of Sciences*, *113*(12), 3323–3328. https://doi.org/10.1073/pnas.1519608113

Fu, R., Shen, Q., Xu, P., Luo, J. J., & Tang, Y. (2014). Phagocytosis of microglia in the central nervous system diseases. *Molecular Neurobiology*, *49*(3), 1422–1434. https://doi.org/10.1007/s12035-013-8620-6

García-Serra, A., Radosevic, M., Pupak, A., Brito, V., Ríos, J., Aguilar, E., Maudes, E., Ariño, H., Spatola, M., Mannara, F., Pedreño, M., Joubert, B., Ginés, S., Planagumà, J., & Dalmau, J. (2021). Placental transfer of NMDAR antibodies causes reversible alterations in mice. *Neurology Neuroimmunology Neuroinflammation*, *8*(1), e915. https://doi.org/10.1212/nxi.0000000000000915

Hara, M., Martinez-Hernandez, E., Ariño, H., Armangué, T., Spatola, M., Petit-Pedrol, M., Saiz, A., Rosenfeld, M. R., Graus, F., & Dalmau, J. (2018). Clinical and pathogenic significance of IgG, IgA, and IgM antibodies against the NMDA receptor. *Neurology*, *90*(16), e1386–e1394. https://doi.org/10.1212/wnl.0000000000005329

Hinson, S. R., Clift, I. C., Luo, N., Kryzer, T. J., & Lennon, V. A. (2017). Autoantibody-induced internalization of CNS AQP4 water channel and EAAT2 glutamate transporter requires astrocytic Fc receptor. *Proceedings of the National Academy of Sciences of the United States of America*, *114*(21), 5491–5496. https://doi.org/10.1073/pnas.1701960114

Hong, S., Beja-Glasser, V. F., Nfonoyim, B. M., Frouin, A., Li, S., Ramakrishnan, S., Merry, K. M., Shi, Q., Rosenthal, A., Barres, B. A., Lemere, C. A., Selkoe, D. J., & Stevens, B. (2016). Complement and microglia mediate early synapse loss in Alzheimer mouse models. *Science*, *352*(6286), 712–716. https://doi.org/10.1126/science.aad8373

Hovens, I. B., Nyakas, C., & Schoemaker, R. G. (2014). A novel method for evaluating microglial activation using ionized calcium-binding adaptor protein-1 staining: cell body to cell size ratio. *Neuroimmunology and Neuroinflammation*, *1*, 82–88. https://doi.org/10.4103/2347-8659.139719

Hughes, E. G., Peng, X., Gleichman, A. J., Lai, M., Zhou, L., Tsou, R., Parsons, T. D., Lynch, D. R., Dalmau, J., & Balice-Gordon, R. J. (2010). Cellular and synaptic mechanisms of anti-NMDA receptor encephalitis. *The Journal of Neuroscience*, *30*(17), 5866–5875. https://doi.org/10.1523/JNEUROSCI.0167-10.2010

Jézéquel, J., Johansson, E. M., Dupuis, J. P., Rogemond, V., Gréa, H., Kellermayer, B., Hamdani, N., Le Guen, E., Rabu, C., Lepleux, M.,

Spatola, M., Mathias, E., Bouchet, D., Ramsey, A. J., Yolken, R. H., Tamouza, R., Dalmau, J., Honnorat, J., Leboyer, M., & Groc, L. (2017). Dynamic disorganization of synaptic NMDA receptors triggered by autoantibodies from psychotic patients. *Nature Communications*, *8*(1), 1791. https://doi.org/10.1038/s41467-017-01700-3

Ji, H., Ohmura, K., Mahmood, U., Lee, D. M., Hofhuis, F. M. A., Boackle, S. A., Takahashi, K., Holers, V. M., Walport, M., Gerard, C., Ezekowitz, A., Carroll, M. C., Brenner, M., Weissleder, R., Verbeek, J. S., Duchatelle, V., Degott, C., Benoist, C., & Mathis, D. (2002). Arthritis critically dependent on innate immune system players. *Immunity*, *16*(2), 157–168. https://doi.org/10.1016/S1074-7613(02)00275-3

Kinzel, S., Lehmann-Horn, K., Torke, S., Häusler, D., Winkler, A., Stadelmann, C., Payne, N., Feldmann, L., Saiz, A., Reindl, M., Lalive, P. H., Bernard, C. C., Brück, W., & Weber, M. S. (2016). Myelin-reactive antibodies initiate T cell-mediated CNS autoimmune disease by opsonization of endogenous antigen. *Acta Neuropathologica*, *132*(1), 43–58. https://doi.org/10.1007/s00401-016-1559-8

Koffie, R. M., Meyer-Luehmann, M., Hashimoto, T., Adams, K. W., Mielke, M. L., Garcia-Alloza, M., Micheva, K. D., Smith, S. J., Kim, M. L., Lee, V. M., Hyman, B. T., & Spires-Jones, T. L. (2009). Oligomeric amyloid beta associates with postsynaptic densities and correlates with excitatory synapse loss near senile plaques. *Proceedings of the National Academy of Sciences*, *106*(10), 4012–4017. https://doi.org/10.1073/pnas.0811698106

Kornau, H.-C., Kreye, J., Stumpf, A., Fukata, Y., Parthier, D., Sammons, R. P., Imbrosci, B., Kurpjuweit, S., Kowski, A. B., Fukata, M., Prüss, H., & Schmitz, D. (2020). Human cerebrospinal fluid monoclonal LGI1 autoantibodies increase neuronal excitability. *Annals of Neurology*, *87*(3), 405–418. https://doi.org/10.1002/ana.25666

Kreye, J., Wenke, N. K., Chayka, M., Leubner, J., Murugan, R., Maier, N., Jurek, B., Ly, L. T., Brandl, D., Rost, B. R., Stumpf, A., Schulz, P., Radbruch, H., Hauser, A. E., Pache, F., Meisel, A., Harms, L., Paul, F., Dirnagl, U., … Prüss, H. (2016). Human cerebrospinal fluid monoclonal N-methyl-D-aspartate receptor autoantibodies are sufficient for encephalitis pathogenesis. *Brain*, *139*(10), 2641–2652. https://doi.org/10.1093/brain/aww208

Kreye, J., Wright, S. K., van Casteren, A., Stöffler, L., Machule, M.-L., Reincke, S. M., Nikolaus, M., van Hoof, S., Sanchez-Sendin, E., Homeyer, M. A., Cordero Gómez, C., Kornau, H.-C., Schmitz, D., Kaindl, A. M., Boehm-Sturm, P., Mueller, S., Wilson, M. A., Upadhya, M. A., Dhangar, D. R., … Prüss, H. (2021). Encephalitis patient-derived monoclonal GABAA receptor antibodies cause epileptic seizures. *Journal of Experimental Medicine*, *218*(11), e20210012. https://doi.org/10.1084/jem.20210012

Krueger, S. R., Kolar, A., & Fitzsimonds, R. M. (2003). The presynaptic release apparatus is functional in the absence of dendritic contact and highly mobile within isolated axons. *Neuron*, *40*(5), 945–957. https://doi.org/10.1016/S0896-6273(03)00729-3

Lacor, P. N., Buniel, M. C., Chang, L., Fernandez, S. J., Gong, Y., Viola, K. L., Lambert, M. P., Velasco, P. T., Bigio, E. H., Finch, C. E., Krafft, G. A., & Klein, W. L. (2004). Synaptic targeting by alzheimer's-related amyloid β oligomers. *The Journal of Neuroscience*, *24*(45), 10191–10200. https://doi.org/10.1523/jneurosci.3432-04.2004

Lee, S. H., Le Pichon, C. E., Adolfsson, O., Gafner, V., Pihlgren, M., Lin, H., Solanoy, H., Brendza, R., Ngu, H., Foreman, O., Chan, R., Ernst, J. A., DiCara, D., Hotzel, I., Srinivasan, K., Hansen, D. V., Atwal, J., Lu, Y., Bumbaca, D., … Ayalon, G. (2016). Antibody-mediated targeting of tau in vivo does not require effector function and microglial engagement. *Cell Reports*, *16*(6), 1690–1700. https://doi.org/10.1016/j.celrep.2016.06.099

Li, S., Jin, M., Koeglsperger, T., Shepardson, N. E., Shankar, G. M., & Selkoe, D. J. (2011). Soluble Aβ oligomers inhibit long-term potentiation through a mechanism involving excessive activation of extrasynaptic NR2B-containing NMDA receptors. *The Journal of Neuroscience*, *31*(18), 6627–6638. https://doi.org/10.1523/jneurosci.0203-11.2011

Liberman, L. D., & Liberman, M. C. (2015). Dynamics of cochlear synaptopathy after acoustic overexposure. *Journal of the Association for Research in Otolaryngology*, *16*(2), 205–219. https://doi.org/10.1007/s10162-015-0510-3

Lo, M., Kim, H. S., Tong, R. K., Bainbridge, T. W., Vernes, J. M., Zhang, Y., Lin, Y. L., Chung, S., Dennis, M. S., Zuchero, Y. J., Watts, R. J., Couch, J. A., Meng, Y. G., Atwal, J. K., Brezski, R. J., Spiess, C., & Ernst, J. A. (2017). Effector-attenuating substitutions that maintain antibody stability and reduce toxicity in mice. *The Journal of Biological Chemistry*, *292*(9), 3900–3908. https://doi.org/10.1074/jbc.M116.767749

Lois, C., Hong, E. J., Pease, S., Brown, E. J., & Baltimore, D. (2002). Germline transmission and tissue-specific expression of transgenes delivered by lentiviral vectors. *Science*, *295*(5556), 868–872. https://doi.org/10.1126/science.1067081

Lucchinetti, C. F., Guo, Y., Popescu, B. F. G., Fujihara, K., Itoyama, Y., & Misu, T. (2014). The pathology of an autoimmune astrocytopathy: Lessons learned from neuromyelitis optica. *Brain Pathology*, *24*(1), 83–97. https://doi.org/10.1111/bpa.12099

Ludwig, R. J., Vanhoorelbeke, K., Leypoldt, F., Kaya, Z., Bieber, K., McLachlan, S. M., Komorowski, L., Luo, J., Cabral-Marques, O., Hammers, C. M., Lindstrom, J. M., Lamprecht, P., Fischer, A., Riemekasten, G., Tersteeg, C., Sondermann, P., Rapoport, B., Wandinger, K.-P., Probst, C., … Nimmerjahn, F. (2017). Mechanisms of autoantibody-induced pathology. *Frontiers in Immunology*, *8*. https://doi.org/10.3389/fimmu.2017.00603

Meberg, P. J., & Miller, M. W. (2003). Culturing hippocampal and cortical neurons. *Methods in Cell Biology*, *71*, 111–127. https://doi.org/10.1016/s0091-679x(03)01007-0

Meisslitzer-Ruppitsch, C., Röhrl, C., Ranftler, C., Stangl, H., Neumüller, J., Pavelka, M., & Ellinger, A. (2013). Photooxidation technology for correlative light and electron microscopy. In D. J. Taatjes & J. Roth (Eds.), *Cell imaging techniques: Methods and protocols* (pp. 423–436). Humana Press.

Moscato, E. H., Peng, X., Jain, A., Parsons, T. D., Dalmau, J., & Balice-Gordon, R. J. (2014). Acute mechanisms underlying antibody effects in anti-N-methyl-D-aspartate receptor encephalitis. *Annals of Neurology*, *76*(1), 108–119. https://doi.org/10.1002/ana.24195

Ohkawa, T., Fukata, Y., Yamasaki, M., Miyazaki, T., Yokoi, N., Takashima, H., Watanabe, M., Watanabe, O., & Fukata, M. (2013). Autoantibodies to epilepsy-related LGI1 in limbic encephalitis neutralize LGI1-ADAM22 interaction and reduce synaptic AMPA receptors. *The Journal of Neuroscience*, *33*(46), 18161–18174. https://doi.org/10.1523/jneurosci.3506-13.2013

Paolicelli, R. C., Bolasco, G., Pagani, F., Maggi, L., Scianni, M., Panzanelli, P., Giustetto, M., Ferreira, T. A., Guiducci, E., Dumas, L., Ragozzino, D., & Gross, C. T. (2011). Synaptic pruning by microglia is necessary for normal brain development. *Science*, *333*(6048), 1456–1458. https://doi.org/10.1126/science.1202529

Pozzo, E. D., Tremolanti, C., Costa, B., Giacomelli, C., Milenkovic, V. M., Bader, S., Wetzel, C. H., Rupprecht, R., Taliani, S., Settimo, F. D., & Martini, C. (2019). Microglial pro-inflammatory and anti-inflammatory phenotypes are modulated by translocator protein activation. *International Journal of Molecular Sciences*, *20*(18), 4467. https://doi.org/10.3390/ijms20184467

Prüss, H. (2021). Autoantibodies in neurological disease. *Nature Reviews Immunology*, *21*(12), 798–813. https://doi.org/10.1038/s41577-021-00543-w

Rajendran, L., & Paolicelli, R. C. (2018). Microglia-mediated synapse loss in Alzheimer's disease. *The Journal of Neuroscience*, *38*(12), 2911–2919. https://doi.org/10.1523/jneurosci.1136-17.2017

Rauschenberger, V., von Wardenburg, N., Schaefer, N., Ogino, K., Hirata, H., Lillesaar, C., Kluck, C. J., Meinck, H.-M., Borrmann, M.,

Weishaupt, A., Doppler, K., Wickel, J., Geis, C., Sommer, C., & Villmann, C. (2020). Glycine receptor autoantibodies impair receptor function and induce motor dysfunction. *Annals of Neurology*, *88*(3), 544–561. https://doi.org/10.1002/ana.25832

Sabater, L., Giralt, A., Boronat, A., Hankiewicz, K., Blanco, Y., Llufriu, S., Alberch, J., Graus, F., & Saiz, A. (2009). Cytotoxic effect of neuromyelitis optica antibody (NMO-IgG) to astrocytes: an in vitro study. *Journal of Neuroimmunology*, *215*(1-2), 31–35. https://doi.org/10.1016/j.jneuroim.2009.07.014

Saijo, K., & Glass, C. K. (2011). Microglial cell origin and phenotypes in health and disease. *Nature Reviews Immunology*, *11*(11), 775–787. https://doi.org/10.1038/nri3086

Saunders, K. O. (2019). Conceptual approaches to modulating antibody effector functions and circulation half-life. *Frontiers in Immunology*, *10*, 1296. https://doi.org/10.3389/fimmu.2019.01296

Schafer, D. P., Lehrman, E. K., Kautzman, A. G., Koyama, R., Mardinly, A. R., Yamasaki, R., Ransohoff, R. M., Greenberg, M. E., Barres, B. A., & Stevens, B. (2012). Microglia sculpt postnatal neural circuits in an activity and complement-dependent manner. *Neuron*, *74*(4), 691–705. https://doi.org/10.1016/j.neuron.2012.03.026

Schlothauer, T., Herter, S., Koller, C. F., Grau-Richards, S., Steinhart, V., Spick, C., Kubbies, M., Klein, C., Umaña, P., & Mössner, E. (2016). Novel human IgG1 and IgG4 Fc-engineered antibodies with completely abolished immune effector functions. *Protein Engineering, Design & Selection*, *29*(10), 457–466. https://doi.org/10.1093/protein/gzw040

Scott, A. M., Wolchok, J. D., & Old, L. J. (2012). Antibody therapy of cancer. *Nature Reviews Cancer*, *12*(4), 278–287. https://doi.org/10.1038/nrc3236

Smith, J. A., Das, A., Ray, S. K., & Banik, N. L. (2012). Role of pro-inflammatory cytokines released from microglia in neurodegenerative diseases. *Brain Research Bulletin*, *87*(1), 10–20. https://doi.org/10.1016/j.brainresbull.2011.10.004

Soltys, J., Liu, Y., Ritchie, A., Wemlinger, S., Schaller, K., Schumann, H., Owens, G. P., & Bennett, J. L. (2019). Membrane assembly of aquaporin-4 autoantibodies regulates classical complement activation in neuromyelitis optica. *The Journal of Clinical Investigation*, *129*(5), 2000–2013. https://doi.org/10.1172/jci122942

Tüzün, E., Zhou, L., Baehring, J. M., Bannykh, S., Rosenfeld, M. R., & Dalmau, J. (2009). Evidence for antibody-mediated pathogenesis in anti-NMDAR encephalitis associated with ovarian teratoma. *Acta Neuropathologica*, *118*(6), 737. https://doi.org/10.1007/s00401-009-0582-4

van Casteren, A. C. M., Ackermann, F., Rahman, K. A., Andrzejak, E., Rosenmund, C., Kreye, J., Prüss, H., Garner, C. C., & Ichkova, A. (2022). Differential modes of action of α1- and α1γ2-autoantibodies derived from patients with GABAAR encephalitis. *Eneuro*, *9*(6), 0369-22.2022. https://doi.org/10.1523/eneuro.0369-22.2022

Vidarsson, G., Dekkers, G., & Rispens, T. (2014). IgG subclasses and allotypes: From structure to effector functions. *Frontiers in Immunology*, *5*, 520. https://doi.org/10.3389/fimmu.2014.00520

Walker, D. G., Tang, T. M., Mendsaikhan, A., Tooyama, I., Serrano, G. E., Sue, L. I., Beach, T. G., & Lue, L.-F. (2020). Patterns of expression of purinergic receptor P2RY12, a putative marker for non-activated microglia, in aged and Alzheimer's disease brains. *International Journal of Molecular Sciences*, *21*(2), 678.

Wang, X., Mathieu, M., & Brezski, R. J. (2018). IgG Fc engineering to modulate antibody effector functions. *Protein & Cell*, *9*(1), 63–73. https://doi.org/10.1007/s13238-017-0473-8

Zhang, Z.-w., Peterson, M., & Liu, H. (2013). Essential role of postsynaptic NMDA receptors in developmental refinement of excitatory synapses. *Proceedings of the National Academy of Sciences*, *110*(3), 1095–1100. https://doi.org/10.1073/pnas.1212971110

Zhou, J., Tang, Z., Gao, S., Li, C., Feng, Y., & Zhou, X. (2020). Tumor-associated macrophages: Recent insights and therapies. *Frontiers in Oncology*, *10*, 81–92. https://doi.org/10.3389/fonc.2020.00188

Zuo, Y., & Deng, G.-M. (2021). Fc gamma receptors as regulators of bone destruction in inflammatory arthritis. *Frontiers in Immunology*, *12*, 2500. https://doi.org/10.3389/fimmu.2021.688201

SUPPORTING INFORMATION

Additional supporting information can be found online in the Supporting Information section at the end of this article.

How to cite this article: Rahman, K. A., Orlando, M., Boulos, A., Andrzejak, E., Schmitz, D., Ziv, N. E., Prüss, H., Garner, C. C., & Ichkova, A. (2023). Microglia actively remove NR1 autoantibody-bound NMDA receptors and associated post-synaptic proteins in neuron microglia co-cultures. *Glia*, 1–26. https://doi.org/10.1002/glia.24369

Curriculum Vitae

My curriculum vitae does not appear in the electronic version of my paper for reasons of data protection.

My curriculum vitae does not appear in the electronic version of my paper for reasons of data protection.

My curriculum vitae does not appear in the electronic version of my paper for reasons of data protection.

Publication list

- **Rahman KA**, Orlando M, Boulos A, Andrzejak E, Schmitz D, Ziv NE, Prüss H, Garner CC, Ichkova A. Microglia actively remove NR1 autoantibody-bound NMDA receptors and associated post-synaptic proteins in neuron microglia co-cultures. Glia. 2023. **Impact Factor – 8.073**

- van Casteren AC, Ackermann F, **Rahman KA**, Andrzejak E, Rosenmund C, Kreye J, Prüss H, Garner CC, Ichkova A. Differential modes of action of α1-and α1γ2-autoantibodies derived from patients with GABAAR encephalitis. Eneuro. 2022. **Impact Factor – 4.363**

- Hoffmann-Conaway S, Brockmann MM, Schneider K, Annamneedi A, **Rahman KA**, Bruns C, Textoris-Taube K, Trimbuch T, Smalla KH, Rosenmund C, Gundelfinger ED. Parkin contributes to synaptic vesicle autophagy in Bassoon-deficient mice. Elife. 2020;9:e56590. **Impact Factor – 8.713**

- Palchoudhuri S, Roy D, **Rahman KA**, Roy DS, Dasgupta P, Das S, Dastidar SG, Mukhopadhyay,D. Evaluation of Anti-oxidant and Free Radical Scavenging Potential of Withania Somnifera Water Extract. International Journal of Phytotherapy. 2016; 6:1-8. **Impact Factor – 0.675**

- Mukhopadhyay D, **Rahman KA**, Roy D, Dasgupta P. Evaluation of in vitro antioxidant activity and phytochemical constituents of Kulekhara (Hygrophilia spinosa). International Journal of Pharmacognosy and Phytochemical Research. 2015; 7:984-990. **Impact Factor – 1.129**

- Raybarman A, **Rahman KA**, Vincent RM, Chatterjee S, Sen U, Mitra AK, Choudhury SS, Majumder R. Isolation and Characterisation of Lignin- degrading fungus from coir. IOSR Journal of Environmental Science, Toxicology and Food Technology. 2014; 8:7-11. **Impact Factor – 6.612**

Acknowledgments

Alhamdulillah. All praise and thanks belong to Allah without Whom nothing would be possible.

I would like to thank Prof Craig Garner for being a wonderful mentor and giving me the opportunity to work on this exciting project. He has been a source of great support and guidance for me and all the members of AG Garner lab.

I am grateful to my ECN committee members, Prof Dietmar Schmitz, Prof Harald Prüss and Prof Karolina Krause for their valuable suggestions and guidance. I would also like to thank my examiners and thesis committee members for reading and evaluating my thesis.

Next, I would like to appreciate the help and support from all my lab members and colleagues. Their inputs and help in conducting my thesis work has been immense. A special thanks to Aleks, Kathy and Sheila for guiding me during my PhD and the technicians of our lab Anny and Christine for their assistance.

I would like to thank my friends both back home in India and in Berlin especially, Ashraf and Bilge, who have been by my side in this whole PhD journey. You guys are family.

Lastly, I would like to thank my family for supporting me and being there whenever I needed them. Mostly importantly I would like to thank my mother who is a rock in my life and a constant source of wisdom, love, and care. Nothing I achieved would be possible without her.